

Syracuse University

SURFACE

Dissertations - ALL

SURFACE

December 2018

Ecohydrology of Natural and Restored Wetlands in a Glacial Plain

Kyotaek Hwang
Syracuse University

Follow this and additional works at: <https://surface.syr.edu/etd>



Part of the [Engineering Commons](#)

Recommended Citation

Hwang, Kyotaek, "Ecohydrology of Natural and Restored Wetlands in a Glacial Plain" (2018). *Dissertations - ALL*. 990.

<https://surface.syr.edu/etd/990>

This Dissertation is brought to you for free and open access by the SURFACE at SURFACE. It has been accepted for inclusion in Dissertations - ALL by an authorized administrator of SURFACE. For more information, please contact surface@syr.edu.

Abstract

More than half of wetland area in the U.S. have been converted to other land use types for agricultural use and development. Limited understanding of ecological services provided to society by wetlands is another reason for the massive wetland loss in the past. Section 404 of the Clean Water Act and the 1989 federal mandate of “no net wetland loss” supported increased efforts for wetland restoration and creation to compensate for two centuries of ecosystem degradation. Hydrology is a critical driver for wetland formation and sustainability, yet few studies have investigated the ecosystem benefits of restored or constructed wetlands relative to natural wetlands. Considering that unexpected ecohydrologic behaviors such as drought have been reported as a main cause of unsuccessful restoration over the U.S., understanding and quantifying water movement within the local setting is imperative to future wetland restoration.

From an environmental engineering perspective, wetlands are regarded as complex environments controlled by regional geomorphology, atmosphere, geologic setting, and human activity. The U.S. Army Corps of Engineers was tasked with developing a hydrogeomorphic assessment approach for wetlands in the various regions throughout the U.S. to facilitate wetland restoration. This effort was redirected in the aftermath of Hurricane Katrina, but the need for assessment tools persists for several remaining regions including the southern coastlines.

The first part of the dissertation reports an investigation of impacts of geomorphic settings on hydrologic functions within the St. Lawrence River plain. Regional geomorphology links wetlands and surrounding areas by multiple pathways of water transfer such as groundwater exchange and surface water connections. However, recent U.S. Supreme Court rulings, including *Solid Waste Agency of Northern Cook County versus U.S. Army Corps-*

SWANCC (2001) and Rapanos versus U.S. (2006) overturned federal protection of wetlands by the Clean Water Act unless the wetlands are shown to be geographically connected with jurisdictional waters. These rulings jeopardize mitigation wetlands without federal protection because typical restoration practices often minimize surface water connection as a result of dredge-and-fill methods. Hydrologic behaviors and services of the geographically isolated wetlands (GIWs) were hypothesized to be identical to those of geographically connected wetlands in this study. Experimental evidence suggest that hydrologic connectivity is maintained between GIWs and downstream waters via subsurface flow exchange. Greater correlations for GIWs than the other connectivity types were found between variables including standard deviation of groundwater, geographic attributes (e.g., site elevation) and hydrologic attributes (e.g., duration of subsurface flow reversal). Mean groundwater table depended most strongly on wetland fraction within a drainage area.

Water temperature, particularly in summer, strongly influences the environmental suitability for wetland species such as a Blanding's turtle (*Emydoidea blandingii*) for nesting in northern New York. Although temperature dependency of wetland fauna has been investigated to determine the range of suitable environmental conditions, the hydrogeomorphic controls on seasonal thermal regimes of wetlands were not addressed in prior studies. In this study, temperature regimes at multiple sites under uniform climate and geologic settings were investigated to understand the controls on wetland temperature in several of hydrogeomorphic settings. Local geomorphology and alterations by wetland restoration affected wetland thermal regimes via various seasonal subsurface flow exchange patterns. Thermal sensitivity is defined as a response in surface water temperature to change in air temperature. Based on wetland temperature measurements, linear regression was used to estimate thermal sensitivity for each

site. Summer temperature values were shown as primary determinants by site comparison. In addition, the thermal sensitivity values were compared to site variables to seek for local controls. Results suggest that geographical and hydrologic variables including site elevation, duration of subsurface flow reversal, and standard deviation of wetland stage and groundwater table are significantly correlated with thermal sensitivity. Geomorphic settings are useful resources to characterize site hydrology and thermal functions of wetlands. Wetland restoration practitioners need to carefully choose class-appropriate hydrogeomorphic settings to promote establishment and conservation of temperature-sensitive species.

Finally, the impact of the land surface energy budget was measured to assess the patch level controls on evapotranspiration by various wetland species. Infrared thermometry was used within a standard meteorological measurement system to determine energy partitioning between sensible and latent heat fluxes in wetlands. A portable thermal infrared (TIR) camera was used to capture radiometric surface temperature of leaves, i.e., evapotranspiring surfaces, and then to estimate sensible and thus latent heat flux associated with a portable weather station. Two TIR-based methods including TIR temperature-based surface energy balance (SEB) and Bowen ratio (β) were compared to the well-known Priestley-Taylor (P-T) method for four species-level patches. For wetland plants including hardstem bulrush (*Scirpus Spp.*), reed canary grass (*Phalaris arundinacea*), cattail (*Typha Spp.*) and meadow willow (*Salix petiolaris*), results are similar for the TIR-based and P-T methods with mean absolute difference of 17.1-53.0 W m⁻² and root mean squared difference of 23.4-62.4 W m⁻² across sites. Greater differences were found from parameterization of aerodynamic resistance for flexible and tall vegetation structure and especially for greater wind speed. Finally, estimated crop coefficients will be useful for regional wetland restoration planning by providing major losses in local water budget.

Ecohydrology of Natural and Restored Wetlands in a Glacial Plain

by

Kyotaek Hwang

B.S., Hanyang University, Seoul, Korea, 2009

M.S., Hanyang University, Seoul, Korea, 2011

Dissertation

Submitted in partial fulfillment of the requirements for the degree of
Doctor of Philosophy in Civil Engineering

Syracuse University
December 2018

Copyright © Kyotaek Hwang 2018

All Rights Reserved

Acknowledgements

I was able to grow up academically with persistent support from Dr. David Chandler. As an advisor, he gave me valuable lessons on creative thinking about hydrologic field survey and use of cutting-edge technologies. He always encouraged me to participate in various field trips, workshops, and academic conferences. These activities had me learn things that I would not get from class as well as great opportunities for interacting with people from various backgrounds. Incessant discussion with him fertilized myself to become a better researcher.

I am sincerely grateful to my doctoral committee, Drs. Laura Lautz, Stephen Shaw, Christa Kelleher, and Teng Zeng. Their generous support with deep insight guided me to explore interesting topics in hydrology with brilliant ideas. I would also like to thank the committee chair, Dr. Jason Fridley for constructive discussion and feedback on this dissertation.

The dissertation studies were conducted by financial supports from the University of Michigan Water Center as an interdisciplinary project “Environmental and Socioeconomic Factors Associated with Public-Private Partnership Wetland Restoration Projects Benefiting Wildlife in the Great Lakes Watershed.” I thank Dr. Tom Langen and Brendan Carberry for their efforts to coordinate with the private land owners for my field work. Drs. Richard Welsh, Michael Twiss, and Martin Heintzelman also helped me understand the wetland sites with their knowledge and experiences. I am also grateful to the land owners of wetlands for accommodating me to work in their properties.

This work was also benefitted by multiple financial supports throughout the coursework. The University Water Fellowship and the Pathfinder Fellowship from Consortium of Universities for the Advancement of Hydrologic Science, Inc. (CUAHSI) allowed me to focus

on intensive field survey and data analysis. The Nelson L. Nemerow Memorial Scholarship from Department of Civil and Environmental Engineering, Syracuse University supported me to present these outcomes in the American Geophysical Union fall meeting. Travel grants from the Graduate Student Organization and the CUAHSI were also helpful to attend a conference and workshop, respectively.

Department faculties, staffs and colleagues always encouraged me to move forward by giving their advice. I was inspired by their persistent work with creative ideas. Particularly, they shared their knowledge with interesting topics from Environmental Group Seminar. I especially thank Babak, Ting, Javad, Komal, Nima, Kyle, Megan, Nick, James and Jing for their assistance for the field survey and data analysis.

Last but not least, I thank my family for their consistent care with love. It is my best luck to meet Kyungsun as a life companion. Sharing every moment with her was the best part of my life in Syracuse. My largest gratitude also goes to my parents, Wookhwan and Youngsook, and sister, Jihye, for their endless love and support.

Table of Contents

List of Tables	xi
List of Figures	xii
Chapter 1. Introduction.....	1
1.1 Motivation	1
1.1.1 Geographical and hydrological impacts on subsurface connectivity of restored wetlands	3
1.1.2 Hydrogeomorphic controls on thermal regime of wetlands in northern New York	5
1.1.3 Patch scale evapotranspiration of wetland plant species by ground-based infrared thermometry	7
1.2 Objectives and hypotheses	7
Chapter 2. Literature Review	10
2.1 Hydrogeomorphic (HGM) approach for mitigation wetlands.....	10
2.2 Ecohydrological functions and geomorphic characteristics of geographically isolated wetlands (GIWs)	12
2.3 Subsurface flow exchange between wetlands and adjacent uplands.....	14
2.4 Thermal sensitivity	15
2.5 Traditional meteorology-based methods for estimating evapotranspiration (ET).....	15
2.6 Ground-based thermal infrared temperature sensing	16
2.7 Crop coefficient method based on meteorological data	17
Chapter 3. Materials and methods	19
3.1 Study sites.....	19
3.1.1 Study region.....	19
3.1.2 Regional hydrology of wetlands.....	21
3.1.3 Site information.....	22
3.2 Data collection	26
3.2.1 Site information.....	26
3.2.2 Water level and temperature measurements.....	27

3.2.3 Atmospheric observation.....	28
3.2.4 Ground-based thermal infrared sensing.....	28
3.3 Methods	29
3.3.1 Hydrogeomorphic characterization and surface water connectivity.....	29
3.3.2 Thermal sensitivity.....	30
3.3.3 Sampling of the TIR measurement.....	31
3.3.3 TIR-based surface energy balance method (SEB).....	32
3.3.4 TIR-based Bowen ratio method (β).....	34
3.3.5 Priestley-Taylor method.....	35
3.3.6 Crop coefficient method.....	35
Chapter 4. Geographical and hydrological impacts on subsurface connectivity of natural and restored wetlands	37
4.1 Results	37
4.1.1 Categorization of wetlands by hydrogeomorphic settings and surface water connectivity	37
4.1.2 Seasonal variation of wetland stage and upland groundwater table	39
4.1.3 Relationships between geomorphic and hydrologic variables.....	42
4.1.4 Hydrologic functions of wetlands by downstream connectivity	45
4.2 Discussion.....	49
4.2.1 Impacts of landscape factors on groundwater regime at wetland restoration sites.....	49
4.2.2 Geographical impacts of GIWs on hydrologic functions	52
4.2.3 Experimental limitations and source of uncertainty.....	53
4.3 Summary and conclusions	54
Chapter 5. Hydrogeomorphic controls on thermal regime of wetlands in northern New York.....	56
5.1 Results	56
5.1.1 Seasonal variation of wetland stage and temperature.....	56
5.1.2 Water temperature trends by site.....	58
5.1.3 Thermal sensitivity.....	60

5.1.4 Hydrogeomorphic drivers of thermal sensitivity.....	61
5.2 Discussion.....	63
5.2.1 Hydrologic drivers on a thermal regime.....	63
5.2.2 Water temperature trends by site.....	64
5.2.3 Factors affecting thermal sensitivity	65
5.3 Summary and conclusions	66
Chapter 6. Patch scale evapotranspiration of wetland plant species by ground-based infrared thermometry	68
6.1 Results	68
6.1.1 Seasonal variation of atmosphere and radiation components.....	68
6.1.2 Comparison of TIR-based and P-T methods.....	77
6.1.3 Estimated crop coefficients of wetland species.....	81
6.2 Discussion.....	82
6.2.1 Impact of structures and input variables.....	82
6.2.2 Comparison of the TIR-based methods and P-T	85
6.2.3 Application of the crop coefficient method based on the TIR-based estimates.....	87
6.3 Summary and conclusions	89
Chapter 7. Conclusions and recommendations for future work.....	90
7.1 Conclusions.....	90
7.2 Recommendations for future work	91
References	94
Vita	110

List of Tables

Table 3.1 Site Profiles. Site naming code represents surface water connectivity as GI (geographically isolated), SC (seasonally connected), and GC (geographically connected) (see Section 4.1.1).	24
Table 4.1 Summary statistics of geomorphic settings and hydrologic variables. Surface water connectivity to downstream waters is indicated in part of site names as GI (geographically isolated), SC (seasonally connected), and GC (geographically connected). Note that abbreviations represent HGM (hydrogeomorphic), SDSW (standard deviation of wetland stage), MeanGW (mean groundwater depth), SDGW (standard deviation of groundwater depth), tr (accumulated duration of subsurface flow reversal), DEP (topographic depressions), RIV (riverine settings), SLO (slope settings), GW (groundwater from local groundwater table), and SW (surface water from upstream).	41
Table 4.2 Correlation and significance levels of site geomorphology and hydrologic variables by different site categories of surface water connection. (a) GIWs only (n=8), (b) GIWs and SCWs (n=13), and (c) all sites (n=17). An asterisk denotes significance at the 95% confidence levels. 44	
Table 5.1 Summary statistics of hydrologic variables and thermal sensitivity.....	62
Table 6.1 Estimation statistics of the TIR-based methods compared to P-T. SEB is the thermal infrared temperature-based surface energy balance method, β is the thermal infrared temperature-based Bowen ratio method, r^2 is the coefficient of determination calculated from a linear regression with P-T, MAD is the mean absolute difference with P-T, and RMSD is root mean squared difference with P-T.....	79
Table 6.2 Estimated daily crop coefficient (K_c) ranges by two TIR-based methods over wetland vegetation communities	82

List of Figures

Fig. 1.1 Conceptual diagram of wetland’s hydrologic services by linking surrounding ecosystems	2
Fig. 3.1 Geographic location of the study sites, shown in blue triangles, and the remaining sites in the larger study shown in red circles (ArcGIS online: http://www.arcgis.com/)	23
Fig. 3.2 Geographic locations and aerial imagery of three natural (Wetland 1-3) and one restored (Wetland 4) freshwater marshes nearby the St. Lawrence River. Blue triangles mark wetland sites and yellow triangles represent locations of the portable weather station during the study period (Aerial imagery via ArcGIS Online: http://www.arcgis.com/). Instrumentation setup for atmospheric observation is illustrated with a site photo.	26
Fig. 3.3 Sample visual (left) and TIR (right) images of reed canary grass at Wetland 2. The images were taken at 10:20 AM (GMT-5) on September 5, 2015.	32
Fig. 4.1 Seasonal variation of wetland stage (red) and depth of groundwater table (blue) at (a) GI8 (natural depressions), (b) GI5 (restored depressions), (c) SC1 (restored slope settings), and (d) GC2 (restored riverine settings). Datum of each site represents land surface elevation where groundwater well was installed.....	40
Fig. 4.2 Correlation and significance levels of site geomorphology and hydrologic variables of (a) GIWs only (n=8), (b) GIWs and SCWs (n=13), and (c) all sites (n=17). Color-filled correlations indicate significance at the 95% confidence levels where blue and red represents positive and negative correlation coefficient, respectively.....	43
Fig. 4.3 A relationship between fraction of wetland and mean groundwater table	46
Fig. 4.4 Relationships of standard deviation of daily groundwater table and (a) wetland elevation and (b) flow reversal days.....	47

Fig. 4.5 Relationship between upland groundwater fluctuation and land cover fraction of (a) forest, (b) open water/wetlands and (c) agriculture within a drainage area ranging 5-653 ha. Three sites presenting 0 of wetland fractions in (b) (GI3, GI4, GI5) are ones that are restored in vicinity of landowner’s residence and are not counted as wetland pixels from the NLCD 2011 land cover map providing pixel resolution of 30 m. 48

Fig. 4.6 Component scores and loadings from the principal component analysis. Sites are color-coded by surface water connectivity as red, green and blue for GIW, SCW and GCW, respectively. 49

Fig. 5.1 Wetland stage (red line) and water temperature (brown line) at (a) GI4 and (b) SC4. Data for wetland stage and groundwater table (blue line) measurements at each site are presented as elevation of the land surface where wetland stage was measured. 57

Fig. 5.2 Seasonal variation of wetland water temperature at seventeen sites. Three sites that represent highest (red lines) and lowest (blue lines) summer temperature are highlighted to show differences in summer response among sites. 59

Fig. 5.3 Estimation of thermal sensitivity as a linear regression slope between air and water temperature at (a) SC1 and (b) GI1. Red crosses were excluded from the linear regression (see Section 3.3.2). 61

Fig. 5.4 Thermal sensitivity of the wetland sites by (a) elevation, (b) accumulated duration of subsurface flow reversal, (c) standard deviation of groundwater level, and (d) standard deviation of wetland stage 63

Fig. 6.1 Ta and TS measurements. Ta and TS represent hourly average and instantaneous value within an hour frame, respectively. Note that the measurement data were acquired on different days by site. 70

Fig. 6.2 Hourly average VPD and u measurements. Note that VPD on 9/12/15 at Wetland 1 is zero throughout a day due to a rainfall event. VPD at 18:00 on 9/19/15 at Wetland 2 is zero due to a shower. 72

Fig. 6.3 Estimated H from SEB (a red circle), β (a blue cross), and P-T (a gray dot) at six vegetation communities 74

Fig. 6.4 ET estimations from SEB (a red circle), β (a blue cross), and P-T (a gray dot) at six vegetation communities 76

Fig. 6.5 Comparison of the TIR-based methods and P-T at selected vegetation communities. Note that measurement data during rainfall events are excluded. 78

Fig. 6.6 ET difference between the TIR-based methods and P-T by input variables. A red empty circle shows a difference between SEB and P-T plotted against u over meadow willow at Wetland 2. A blue cross shows a difference between β and P-T plotted against RH over hardstem bulrush at Wetland 1. 81

Chapter 1. Introduction

1.1 Motivation

More than half of the wetlands in the U.S. have been converted to other land use types due to the pressure of agricultural expansion, urban development, and a history of poor understanding of ecological value (Dahl, 1990). Section 404 of the Clean Water Act and the 1989 federal mandate of “no net wetland loss” provided the means to increase wetland restoration activity, especially to accelerate wetland creation recovery from centuries of wetland ecosystem degradation and loss. Mitigation wetlands are expected to perform similar ecosystem services as natural wetlands provide, such as promotion of groundwater recharge, water purification from nutrients and toxins, and maintenance of biodiversity. Implementation practices for mitigation wetlands include restoration, creation, and enhancement of wetlands intended to compensate for historic wetland losses. However, the ecohydrologic functions of individual wetlands are determined by the wide range of geographic factors which complicate standardization of mitigation procedures (Brinson, 1993). Furthermore, common tools and methods used for mitigation have mixed success in achieving design goals and can result in responses similar to other human disturbances. For example, mitigation banking is a popular method to impound water with structures that reduce surface discharge and groundwater outflow. The use of such manmade structures inevitably causes some degree of hydrologic alteration (Mitsch and Gosselink, 2015).

Regional and local hydrologic processes are major determinants of wetland function and provide the basis for establishment and persistence of ecosystem services such as water storage, groundwater recharge, and maintenance of biodiversity (Fig. 1.1). In wetland restoration and

creation perspectives, assessment of the local water budget is an important step to quantify wetland functions and guide hydrologic function to support ecosystem integrity (Hunt et al., 1999). The wetland flow regime depends primarily on site geomorphology, land use, and soil composition and appropriate characterization of associated hydrology is crucial for successful wetland mitigation.

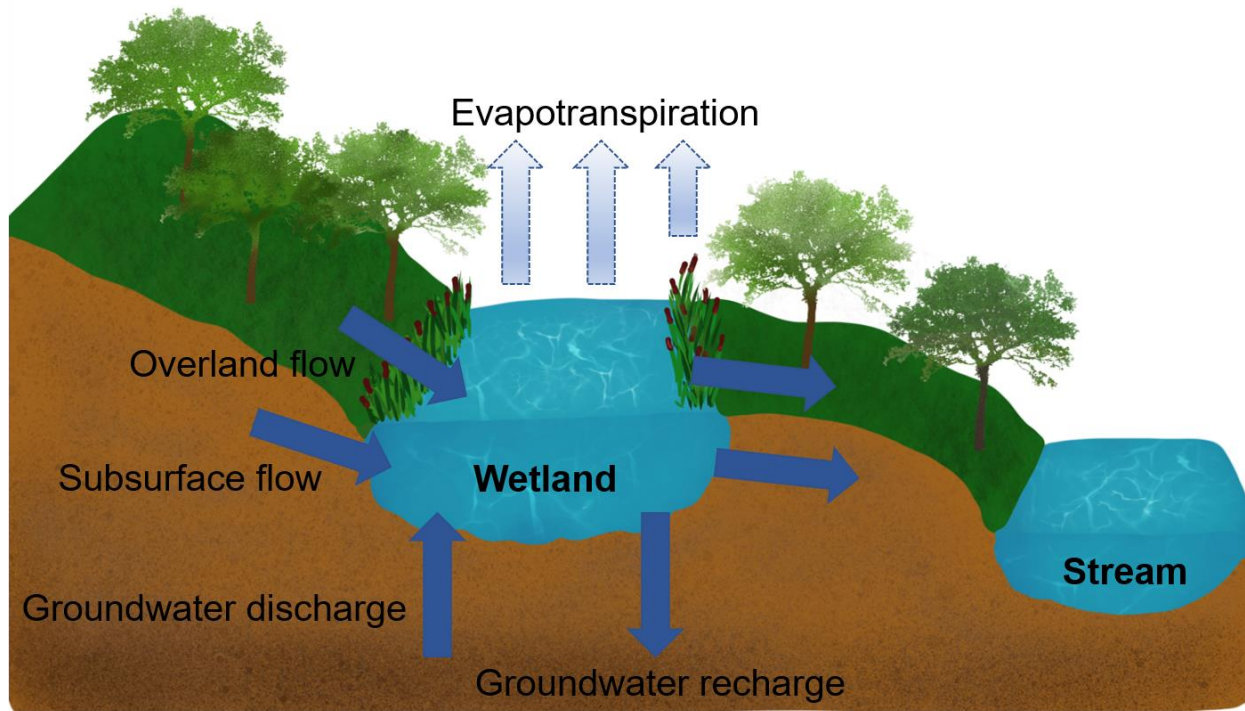


Fig. 1.1 Conceptual diagram of wetland's hydrologic services by linking surrounding ecosystems

Brinson (1993) and Smith et al. (1995) suggested that wetland functions were broadly determined by hydrogeomorphology and these functions could be assessed to evaluate wetland restoration and creation. Failures of wetland restoration projects are often related to weather and local ecosystem properties, such as immature plant development due to short hydroperiod (Galatowitsch and van der Valk, 1996) and problematic hydric soil formation (Stolt et al., 2000). Classification of wetlands by hydrogeomorphic features, including geomorphic setting, water

source, and hydrodynamics, provides valuable information for functional assessment and improves likelihood of successful restoration.

Despite some practical advantages of HGM assessment, especially the rapid assessment protocol with a limited set of hydrogeomorphic observations, prior studies recommend inclusion of complementary information for characterizing hydrological (Gwin et al., 1999; Shaffer et al., 1999) and biogeochemical (Azzolina et al., 2007; Stander and Ehrenfeld, 2009) processes in various regions (Findlay et al., 2002). In particular, hydrologic modification and thermal alteration act as ecohydrological stressors that are imposed on mitigation wetlands (Gebo and Brooks, 2012). Therefore, regional assessment of these controls is essential to promote suitable habitats, especially for endangered species such as a Blanding's turtle (*Emydoidea blandingii*) (Stryszowska et al., 2016).

In the dissertation, ecohydrological controls including subsurface flow exchange (Section 1.1.1), wetland stage records and temperature regimes (Section 1.1.2), and energy partitioning (Section 1.1.3) were estimated from the in-situ survey and compared to geomorphic variables to better inform these impacts on hydrogeomorphic settings for providing a guidance of wetland mitigation projects.

1.1.1 Geographical and hydrological impacts on subsurface connectivity of restored wetlands

Wetland mitigation often results in hydrologic alteration due to a lack of congruence between geomorphic context and regional landscape setting (Gwin et al., 1999). For example, mitigation banking is typically implemented by dredge-and-fill methods, which are soil excavations below the local groundwater table, construction of berms and water control

structures, and removal of tile drains. These actions are often used to increase hydroperiod by delaying surface outflow from wetlands. This promotes greater residence time in the pool and promotes subsurface flow. Reducing the period of surface connectivity from such artificial depressions to a stream is intended to abate geomorphic impacts of regional hydrologic controls at local scales (Gwin et al., 1999; Shaffer et al., 1999). However, the absence of visible surface flow can be interpreted as a disconnection in flow paths between a wetland and stream and an indication that such wetlands are not geographically connected.

Geographically isolated wetlands (GIWs) are defined as wetlands that are fully surrounded by uplands. This term has been developed to promote understanding of the importance of downstream connectivity of wetlands for ecosystem protection purposes rather than a description of functional isolation which has negative connotations (Tiner, 2003). Recent U.S. Supreme Court rulings, including *Solid Waste Agency of Northern Cook County versus U.S. Army Corps-SWANCC* (2001) and *Rapanos versus U.S.* (2006) overturned Clean Water Act protection of wetlands not geographically connected with jurisdictional waters (EPA and U.S. Army Corps of Engineers, 2008). Compliance with Federal rules requires demonstration of hydrologic connectivity between GIWs and downstream waters, which has increased attention to investigating of hydrological (Evenson et al., 2015; Golden et al., 2016, 2014; McLaughlin et al., 2014; Park et al., 2014) and biogeochemical (Lane et al., 2015; Marton et al., 2015) connectivity and documentation of the unique ecosystem services provided by GIWs (Cohen et al., 2016; Rains et al., 2016). For example, GIWs were recently simulated in a hydrological model as small reservoirs to understand GIW influence on streamflow and baseflow of a watershed (Evenson et al., 2015; Golden et al., 2016; Park et al., 2014).

1.1.2 Hydrogeomorphic controls on thermal regime of wetlands in northern New York

Regional and local hydrologic processes are major determinants of wetland function and provide the bases for establishment and persistence of ecosystem services such as water storage, groundwater recharge, thermal habitat, and maintenance of biodiversity. From the perspective of wetland restoration and creation, assessment of the local water budget is an important step to quantify wetland functions and guide hydrologic function in a way that best supports ecosystem integrity (Hunt et al., 1999). The wetland flow regime depends primarily on site attributes, including climate, geomorphology, soil properties, and land use and cover. The various interactions among site attributes and hydrology can determine the suitability of a site for successful wetland establishment, restoration, or mitigation. Thus, the success of wetland restoration efforts is likely to depend, in part, on knowledge of wetland-upland interactions for both local and regional hydrologic flow paths.

Establishment of a suitable thermal regime is important for successful restoration efforts with a goal of developing appropriate habitat for temperature-sensitive species. The site-wide thermal regime of wetlands is also an important factor to characterize suitability of certain species in an ecosystem. For example, reptiles (Telemeco et al., 2017), amphibians (Richter-Boix et al., 2015) and fish (Elliott, 2000) breed or survive at particular temperature ranges. Similarly, seed germination of vegetation species is largely affected by temperature and moisture availability (Budelsky and Galatowitsch, 1999). The thermal refugia within wetlands are important to the lifecycle of many species, and are likely to become increasingly important in a changing climate (Erwin, 2009). Prior studies indicate that many aquatic species adapt to such temperature change by changing their behaviors (Elliott, 2000; Kaya, 1977; Torgersen et al.,

1999). At a landscape level, wetlands interact with various hydrographic features in the surrounding environment including floodplains, streams and lake margins. Therefore, an understanding of the typical thermal regimes for both natural and restored wetlands, as affected by hydrologic setting, is important to guide successful wetland restoration design and creation. One goal of this dissertation is to better understand thermal interactions between wetlands and the surrounding ecosystems.

Thermal sensitivity is a useful metric to represent the thermal response of a body of water to weather. It is determined as a correlation between daily stream or pool water temperature and air temperature (Chang and Psaris, 2013; Kelleher et al., 2012). Previous studies have often focused on investigating the tolerance of individual species of interest to air or soil temperature (Richter-Boix et al., 2015; Telemeco et al., 2017). These studies were often limited in dry seasons by ephemeral or intermittent surface water supply, consumptive use, and groundwater recharge. Most often, thermal sensitivity analysis has been conducted at larger scales such as lakes (Ekström et al., 2017; Fey and Cottingham, 2012; Kraemer et al., 2017) and streams (Caissie, 2006; Chang and Psaris, 2013; Lisi et al., 2015; Shaw, 2017). Although many wetlands are found at lake margins or floodplains, small isolated wetlands have gained attention due to the increasing number of small wetland restoration projects. The primary water source is also important because thermal sensitivity varies widely, according to climate and local geomorphology. Where wetland area depends on groundwater contribution as a primary source, local geomorphology often controls groundwater cooling. Therefore, characterization of geomorphic setting and associated hydrology is important to understand seasonal temperature patterns of a wetland pool.

1.1.3 Patch scale evapotranspiration of wetland plant species by ground-based infrared thermometry

Accurate estimation of local water budgets is essential for understanding the contribution of various biotic communities to nutrient circulation and landscape function. Water loss by evapotranspiration (ET) from wetlands has been estimated to account for up to 100% of annual precipitation (Lafleur, 1990; Shoemaker et al., 2008), and is therefore considered a critical factor for successful wetland restoration and design. Despite the importance of wetland ET to local water budgets and ecosystems, quantification of this flux is challenged by the complex surface characteristics (Drexler et al., 2004), diverse plant species and density (Souch et al., 1998), and various scales and forms of wetlands (e.g., the clothes line effect) (Borin et al., 2011; Drexler et al., 2004). Wetland ET is particularly important to understanding contaminant and nutrient transport (Drexler et al., 1999), consumptive use (Pauliukonis and Schneider, 2001) and hydrologic regimes (Rosenberry and Winter, 1997). Many wetland biota rely on periodic inundation of the land surface or soil saturation. Such conditions should be quantified to provide guidance to hydrologic alteration or remediation strategies to support these ecosystem functions (Souch et al., 1998). However, current techniques for estimation of ET are limited by the typical scales of spatial and temporal variability, and sensitivity to dramatic differences in vegetation composition between wetlands and the surrounding environment.

1.2 Objectives and hypotheses

This dissertation aims to identify functional attributes of natural and restored wetlands. Multiple wetlands under uniform climate and geologic conditions are analyzed to reveal

principal controls on hydrologic functions (Chapter 4), thermal regimes (Chapter 5), and energy partitioning (Chapter 6). The overarching research question is: How do geomorphic modifications from wetland restoration affect site hydrologic and thermal processes? The documentation of functional attributes from the dissertation are expected to contribute to further development of analyses and approaches that extend the use of hydrogeomorphic assessment for wetland protection and development.

Specific objectives are:

- 1) To identify geographical and hydrologic variables that represent the dominant ecohydrological attributes of natural and mitigation wetlands. Relationships between geographical and hydrological variables were investigated by surface water connectivity.
- 2) To identify temperature regimes of wetlands using wetland stage and groundwater table measurement. Temperature behaviors at multiple sites under uniform climate and geologic settings were investigated to understand spatial differences. Thermal sensitivity was then estimated and compared with geographical and hydrologic variables to find local controls.
- 3) To compare traditional and small scale-based thermal infrared temperature methods to estimate ET over species-level patches of wetland plant cover in natural and restored wetlands.

Hypothesis 1: Hydrologic services of wetlands, such as excessive water storage and groundwater regulation, are persistent over a range of surface water connectivity due to subsurface flow exchange.

Hypothesis 2: The thermal regimes of wetlands are controlled by hydrogeomorphic settings via groundwater moderation.

Hypothesis 3: Estimation of actual ET within wetlands by thermal infrared temperature-based methods compares reasonably with traditional methods.

Chapter 2. Literature Review

This chapter reviews contemporary findings of the research literature. Section 2.1 reviews background and prior studies of hydrogeomorphic (HGM) approach and hydrogeomorphic impacts on wetland functions associated with wetland mitigation. This leads to the introduction of differences in wetland classification approach by surface water connectivity and implied ecohydrological functions of wetlands the same HGM class (Section 2.2). Thermal sensitivity as a proxy of temperature regime is introduced in Section 2.3. Finally the performance of widely used evapotranspiration (ET) estimation methods over wetlands (Section 2.4 and 2.6) and use of a state-of-the-art device for energy partitioning (Section 2.5) are reviewed.

2.1 Hydrogeomorphic (HGM) approach for mitigation wetlands

Alteration of geomorphology from dredge or fill, and of hydrology from use of a berm or water control structure often causes degradation of wetland functions compared to pre-disturbance status (Smith et al., 1995). Although there is general consensus that wetland mitigation is useful for recovering ecosystem functions lost in development, the extent of beneficial ecological impact is controversial. On one hand, problems associated with altered hydrology and water chemistry were found subsequent to mitigation (Shaffer et al., 1999; Whittecar and Daniels, 1999) and were identified to result from insufficient policy and implementation (National Research Council, 2001). On the other hand, wetland restoration and creation were proven to be positive interventions in terms of amphibian (Baker and Halliday, 1999; Benson et al., 2017; Dixon et al., 2011; Petranka et al., 2007) and bird species richness and diversity (Armitage et al., 2007; Balcombe et al., 2005; Benson, 2017; Ratti et al., 2001). To

resolve the difference in outcomes, a functional classification and assessment method should be accompanied to fulfill a goal of mitigation within the complexity functions and impacts arising from multidisciplinary planning and implementation (Brinson, 1993).

The hydrogeomorphic (HGM) classification scheme, originally introduced by Brinson (1993), was developed to cover shortcomings of the existing classification methods and to comply with federal legislation for wetland conservation and mitigation. The approach is based on an assumption that ecosystem function is determined by site-wide hydrogeomorphic characteristics: geomorphic setting, water source, and hydrodynamics. Regional wetland types are classified by a hierarchical decision model with physical and landscape features, which supports application over various environments (Bedford, 1996). Inland freshwater wetlands are generally categorized as flat, depressional, slope, riverine, and lacustrine fringe classes where different degrees of environmental feedback over them are present. Previous studies agreed with validity of the regional classification in terms of hydrology and water quality (Cole et al., 1997; Shaffer et al., 1999), and plant community composition (Magee et al., 1999; Peterson-Smith et al., 2008). However, some wetland characteristics were found to be inconsistent over regional HGM classes by surface water geochemistry (Azzolina et al., 2007) and overall wetland functions (Hruby, 2001). Some characteristic discrepancies arose from human intervention during restoration or construction processes (Hruby, 2001; Shaffer et al., 1999). Although HGM classification is widely regarded as a useful tool for functional assessment of wetlands, it is less reliable for assessment of mitigated wetlands due to the inconsistencies between the local setting and the surrounding landscape (Gwin et al., 1999; Shaffer et al., 1999).

The 2008 update of the mitigation rule under the Clean Water Act stresses reflection of landscape into the mitigation design and management (Bedford, 1996; U.S. Environmental

Protection Agency, 2008). Gwin et al. (1999) pointed out that mitigation wetlands may not reflect the landscape context. Many wetlands have generally been turned into palustrine open water wetlands such as typical dredged ponds because of cost, ease of construction, and aesthetic purposes (Dahl et al., 1991; Tiner, 1984). Such site-wide “mitigation” can alter hydrologic function and lead to ecological degradation. Gwin et al. (1999) identified mitigated wetlands with a discordance between a local and regional landscape as “atypical” classes. Where local depressions occurred as a result of mitigation within the area of a slope or riverine landscape the site showed a loss of seasons natural variability in pool stage (Shaffer et al., 1999). Given that wetland functions rely heavily on pool hydroperiod (Smith et al., 1995), it follows that wetland functions, including biotic species composition and nutrient supply, may be affected by human intervention in hydrology.

2.2 Ecohydrological functions and geomorphic characteristics of geographically isolated wetlands (GIWs)

Geographically isolated wetlands (GIWs) are currently of great interest, as they provide valuable hydrologic functions such as flood buffering and climate regulation. The current literature has few case studies of GIW influence on ecosystem function. Hydrologic functions of GIWs are categorized broadly in terms of local water budgets and fluxes of subsurface exchange (Rains et al., 2016). McLaughlin et al. (2014) specified that the primary ecohydrological function of a GIW is to moderate shallow aquifer depth and baseflow in associated streams. Evenson et al. (2015) showed that GIWs play an important role on baseflow control, peak flow mitigation, and watershed water balance. Several hydrologic functions related to hydrological connectivity were

suggested by Cohen et al. (2016) and are differentiated by processes; stormwater generation, refugia, and flow and solute regulation. These processes are commonly controlled by the degree of surface connection with downstream waters. Furthermore, these processes are often assumed to range by geographical characteristics, including geomorphic settings (McLaughlin and Cohen, 2013; Mushet et al., 2015), distribution density (McLaughlin et al., 2014), and disturbance and land use gradient (McKinney and Charpentier, 2009; McLaughlin and Cohen, 2013).

An overview of recent studies shows comprehensive analysis of natural wetlands by modeling approaches. McLaughlin et al. (2014) argued that subsurface flow reversals between GIWs and uplands is evidence of significant interaction between GIWs and downstream waters. Since GIWs are typically located on topographic depressions, site hydrodynamics rely exclusively on precipitation, evapotranspiration, and subsurface exchange. Regional characterizations of such wetlands are available for diverse sites including south Atlantic coastal plain (Evenson et al., 2015; Golden et al., 2016, 2014), prairie potholes (Ameli and Creed, 2017; Cohen et al., 2016; Evenson et al., 2016), and cypress domes (McLaughlin and Cohen, 2013; Min et al., 2010; Nilsson et al., 2013; Park et al., 2014). In these studies, wetlands with the least disturbance were ordinarily selected to minimize the influence of human intervention. In the context of contemporary restoration projects, mitigation wetlands are designed to perform similar hydrologic functions on various land use compositions within a drainage area but have received less attention. Considering that most mitigation projects are conducted at relatively small (< 5 ha) wetland parcels (Benson et al., 2017), they are often not considered in regional analyses, wetland inventories and finer scale geographic (and of remotely sensed) data. As hydrologic assessment is essential for successful wetland mitigation, understanding and representing the different hydrologic behaviors for the large number of small watersheds is imperative.

2.3 Subsurface flow exchange between wetlands and adjacent uplands

Upland contribution of water by both surface and subsurface pathways are the primary controls on the local behavior of wetland water budgets, which vary through space and time (Fitzgerald et al., 2003; Jolly et al., 2008; Min et al., 2010; Nilsson et al., 2013; Rains, 2011; Roulet, 1990; Siegel, 1988; Woods et al., 2006). Many studies also point to the regional control of hydrogeology and climate on wetland water sources (e.g., Devito et al., 1996; Winter et al., 2001). Similarly, local studies have documented the flow regime dependence of wetlands on an adjacent uplands over a range of geomorphic settings (Rains, 2011; Stein et al., 2004; Woods et al., 2006). Efforts to characterize wetland water budgets by traditional wetland types (e.g., fen, bog, and marsh) found inconsistent hydrologic function over wetland classes (Devito et al., 1996; Winter et al., 2001). Other studies indicate that hydrogeomorphology-based classification and assessment approaches may be suitable for characterizing wetland-upland interactions (Smith et al., 1995).

Groundwater exchange links wetlands and surrounding areas by water and solute transfer (Dahl et al., 2007; Hayashi and Rosenberry, 2002; Jolly et al., 2008; Kalbus et al., 2006; Winter, 1995). From a water quantity perspective, groundwater discharge and recharge are major sources and sinks of solutes (Cohen et al., 2016). For instance, spring snowmelt and summer evapotranspiration play important roles on the timing and amount of groundwater recharge into, and discharge from a wetland. As a result, groundwater discharge is closely related to wetland stage and soil properties such as specific yield (Hunt et al., 2006, 1999; Min et al., 2010).

2.4 Thermal sensitivity

Thermal sensitivity is widely used as a proxy for quantification of biogeochemical processes (Davidson and Janssens, 2006; Dowrick et al., 2015; Inglett et al., 2012), characterization of biological processes (Hester and Doyle, 2011), and determination of thermal refugia for temperature-sensitive species (Caissie, 2006). Prior studies generally focused on relationships of these biogeochemical and ecological indicators with air or soil temperature. However, seasonal inundation often limits monitoring to less than a full annual cycle (Davidson and Janssens, 2006; Inglett et al., 2012; Seabloom et al., 1998) which may be important when species of interest depend heavily on air or soil temperature.

2.5 Traditional meteorology-based methods for estimating evapotranspiration (ET)

Among various approaches applied over different wetland type and climate regime (Drexler et al., 2004), the Priestley-Taylor (P-T) method (Priestley and Taylor, 1972) has been presented as a reliable approach for energy-limited conditions (Rosenberry et al., 2004). This simplified version of the Penman-Monteith (Monteith, 1965) method is radiation-based with elimination of the mass transfer terms. Only a few atmospheric measurements are required, and parameterization of the vegetation canopy cover is not necessary. Therefore, like other field-based meteorological methods, P-T is primarily driven by atmospheric conditions near the land surface and does not reflect vegetative characteristics by species and spatial heterogeneity of different vegetation patches. As mixed vegetation distribution is fairly common in an unmanaged ecosystem, monitoring local variations of vegetation cover at a finer scale is expected to better quantify the consumptive use by species and thereby represent the roles mixed vegetation play in

wetland water balances.

Micrometeorological approaches, such as the Bowen ratio (β) and eddy covariance methods, are commonly used to measure vertical vapor flux. β is routinely estimated from a pair of atmospheric measurements at different heights above the canopy and assumes a linear relationship of vertical heat transfer. This approach allows simple instrumentation and robust results (Gavilán and Berengena, 2007; Todd et al., 2000). Where temperature measurement at the height of the evaporating surface is available, more accurate vertical heat transfer to the near-surface atmosphere can be defined for disaggregated areas (Brutsaert, 1982). The more recently developed eddy covariance method depends on coupled measurements of water vapor content and eddy direction and requires complex instrumentation and specialized statistical analyses. For either method, a statistically defined representative area of land surface is generally considered as the area of upwind fetch for 50 times the measurement height (Drexler et al., 2004; Monteith and Unsworth, 1990). Land surface heterogeneity within this window is often regarded as a potential source of error due to variability in prevailing wind direction and velocity (Masoner and Stannard, 2010). Similarly, parametrization of wind by a fixed aerodynamic resistance value introduces uncertainty in the Penman-Monteith method. Although remote sensing of land surface characteristics by satellites coupled with ground-based atmospheric observations has been utilized for a several decades to estimate ET, hyperspectral observations remain limited by the coarse spatio-temporal resolution of land surface characteristics (Hwang and Choi, 2013; Schmugge et al., 2002).

2.6 Ground-based thermal infrared temperature sensing

Ground-based thermal infrared (TIR) thermometry is a relatively new technology that enables measurement of surface skin temperature in agricultural and hydrologic research (Alves and Pereira, 2000; Cardenas et al., 2008; Maes and Steppe, 2012). Compared to airborne or satellite remote sensing, ground-based TIR sensors and cameras have several advantages, including low cost, high spatial resolution, high sample rates, real-time imaging, constant viewing geometry, and no need for atmosphere attenuation and cloud cover corrections (Cardenas et al., 2008; Harris et al., 2003). The scale of the land surface window is often much greater than the length scale of variability in wetland vegetation and results in an aggregate measurement over complex plant community. The TIR-based approach supports direct calculation of actual sensible heat flux and smaller scale measurements to disaggregate the various contributions to ET. The opportunity to evaluate discrete areas of mixed cover such as ponds or vegetation patches is important to understanding the variability in ET contributions by various plant communities that are lumped by traditional methods. Despite these potential areas of application, few studies have been published on the use of TIR devices to estimate ET and drought stress (Ahrends et al., 2014; Maes and Steppe, 2012).

2.7 Crop coefficient method based on meteorological data

Plant community monitoring is a potentially useful approach for guiding plant selection and design of wetland restoration and creation projects. The effect of wetland plant community composition on consumptive use is often estimated by the crop coefficients method, a practical approach for estimating ET over plants (Allen et al., 1994; Drexler et al., 2004). In this approach, the standard reference ET is estimated by the parameterized FAO Penman-Monteith equation

(Allen et al., 1998). This approach relies on a minimal set of measurements to develop an estimate of potential ET (PET) that is multiplied by a crop coefficient to represent ET. This, and many similar methods, such as P-T, assume a uniformly vegetated surface for parameterization of surface and aerodynamic resistance. Prior studies found various crop coefficient values for wetland plants (Borin et al., 2011; Drexler et al., 2004; Peacock and Hess, 2004) due to differences in vegetation, density and climate, and determined that local calibration was necessary. This indicates that the assumption of a uniformly distributed dominant plant species common to large areas, is often violated by the patchy structure of small wetlands.

Chapter 3. Materials and methods

In this chapter, study sites, data collection, and methods are introduced. Based on site information acquired from visual observation and the public database (Section 3.1.1, 3.1.3 and 3.2.1), selected sites were classified by hydrogeomorphic approach (Section 3.3.1). Surface water connectivity to downstream waters was determined primarily by repeated site visits. Hydrologic data were acquired by the field survey where stage and water temperature (deployment of automated sensors; Section 3.2.2), and atmospheric (intensive measurement on particular days; Section 3.2.3 and 3.2.4) measurements were conducted independently to each other. These two different sets of data were processed to analyze the thermal regimes (Section 3.3.2) and to estimate evapotranspiration (Section 3.3.3-3.3.6). Regional hydrology of wetlands is also illustrated for contextual background to better understand results and discussion (Chapters 4-6).

3.1 Study sites

3.1.1 Study region

There are more than 300 wetlands located in the St. Lawrence River valley region in northern New York. The land cover is mainly agricultural crops, pasture, and forest (Fig. 3.1). Study sites lie between 44.0–45.0°N and 74.4–76.3°W. Most area of the region is generally classified as the Lake Ontario and St. Lawrence Lowlands where linear, rock walled valleys and striae are broadly developed along with St. Lawrence River by differential erosion of the

Precambrian bedrock from glacier retreat (Pair, 1997). U.S. Environmental Protection Agency's (EPA) hierarchical ecoregion framework (Omernik, 1987) identifies the most study sites into three Level 4 ecoregions: St. Lawrence Lowlands (43 sites), Ontario Lowlands (12 sites), and Upper St. Lawrence Valley (10 sites). Most of the study area is classified into the Eastern Temperate Forests (Ecoregion Level 1) and more specifically into the Mixed Wood Plains (Level 2) and Eastern Great Lakes Lowlands (Level 3) by a top-down hierarchy. The ecoregion map data were provided by EPA (<https://catalog.data.gov/dataset/level-iv-ecoregions-of-new-york>). Soil texture varies from clay to sandy loam by sites where silty clay is the most common followed by silty clay loam and silt loam.

The study area is classified as humid continental climate by Köppen climate classification system (Peel et al., 2007) with an annual normal temperature range of 6.1 to 7.3°C at five regional weather stations. Seasonal temperature ranges are -7.7 to -5.4°C in winter and 18.7 to 19.9°C in summer. Annual normal precipitation ranges from 888 to 955 mm, with slightly less precipitation during winter and spring. However, streamflow is greatest during spring, due to the timing of the annual snowmelt freshet. The historic weather data were provided by the Climate Data Online of the National Oceanic and Atmospheric Administration (NOAA) National Centers for Environmental Information (<http://www.ncdc.noaa.gov/cdo-web/>).

Private landowners were encouraged to participate in mitigation banking programs by the U.S. Army Corps of Engineers Section 404 permitting program, as voluntary public-private partnership programs are an important driver in development of restored wetlands (Fishburn et al., 2009; Kiesecker and Blaustein, 1997). Two federal programs, the Wetlands Reserve Program (Natural Resources Conservation Service) and the Partners for Fish and Wildlife Program (U.S. Fish and Wildlife Service), have conserved more than 1.5 million ha of wetlands across the U.S.

(Benson et al., 2017). Non-profit agencies (e.g., Ducks Unlimited) or local land trusts are also regional restoration partners. Although more than 400 private landowners have participated in these programs, the legally mandated assessment of these programs is little seen in the academic literature.

3.1.2 Regional hydrology of wetlands

Here, the typical hydrologic seasonality over a water year beginning October 1 is presented for the study area: Substantial water supply from frequent precipitation events and near complete cessation of plant water use raise wetland stage and expand inundation area from October to April (see Fig. 4.1 and 5.1 for detailed information). During this period wetland storage is maximized and excess water is discharged either through a flooded stream channels or spillways. When air temperature retains below 0°C from November to March, surface layer of wetland water body forms a few centimeters of ice. The ice cover affects accuracy of water pressure measurements and some differences with barometric pressure. During periods when the groundwater surface remains higher than wetland stage the wetland is consistently fed by groundwater. During winter months, wetland temperature is controlled by groundwater discharge that varies by geomorphic settings.

After a peak in stage associated with the snowmelt freshet in March and April, the ecosystem turns into a transitional period from May to early June. Wetland stage gradually decreases over time but often sharply increases for several days due to rainfall events. As considerable amount of water is still present in wetlands and persistent groundwater contribution is made, anaerobic conditions are dominant in this period. Wetland temperature increase from 7°C to higher than 20°C yet largely affected by fluctuation of air temperature.

In the dry season, typically from mid-June to September, wetland stage declines over time by reduced groundwater supply, lack of rainfall, and maximized evapotranspiration from high solar insolation and vapor pressure deficit. Although wetlands receive subsurface discharge from the surrounding area throughout summer, the input rate decreases due to less frequent precipitation and greater evaporative demand use by vegetation. Accordingly, upland groundwater table temporarily soars with precipitation events while consistently decreasing, resulting in higher seasonal fluctuation. When the upland groundwater store is depleted from middle to end of dry season, the wetland water balance switches from gaining to losing to the surrounding groundwater. This is referred to as subsurface flow reversal and is accompanied by generally dry and aerobic conditions out of the inundated until it recovers in October. Average wetland temperature in this period is around 20°C but varies due to the seasonal trend and local fluctuations in solar insolation, rainfall events and associated surface and groundwater contributions.

3.1.3 Site information

Seventeen wetlands were selected from the Saint Lawrence Valley region of upstate New York (Fig. 3.1). Twelve wetland sites are restored or created, and five are natural wetlands. The sites are distributed over a large area of 44.0–45.0°N and 74.4–76.3°W. Most sites are in the St. Lawrence River watershed (HUC 041503) (Table 3.1). The regional land cover is primarily row crops, pasture, and forest: pasture and forest dominate the uplands for the study wetlands. Regional soils range from silty clay to loam with silty clay predominant (Table 3.1).

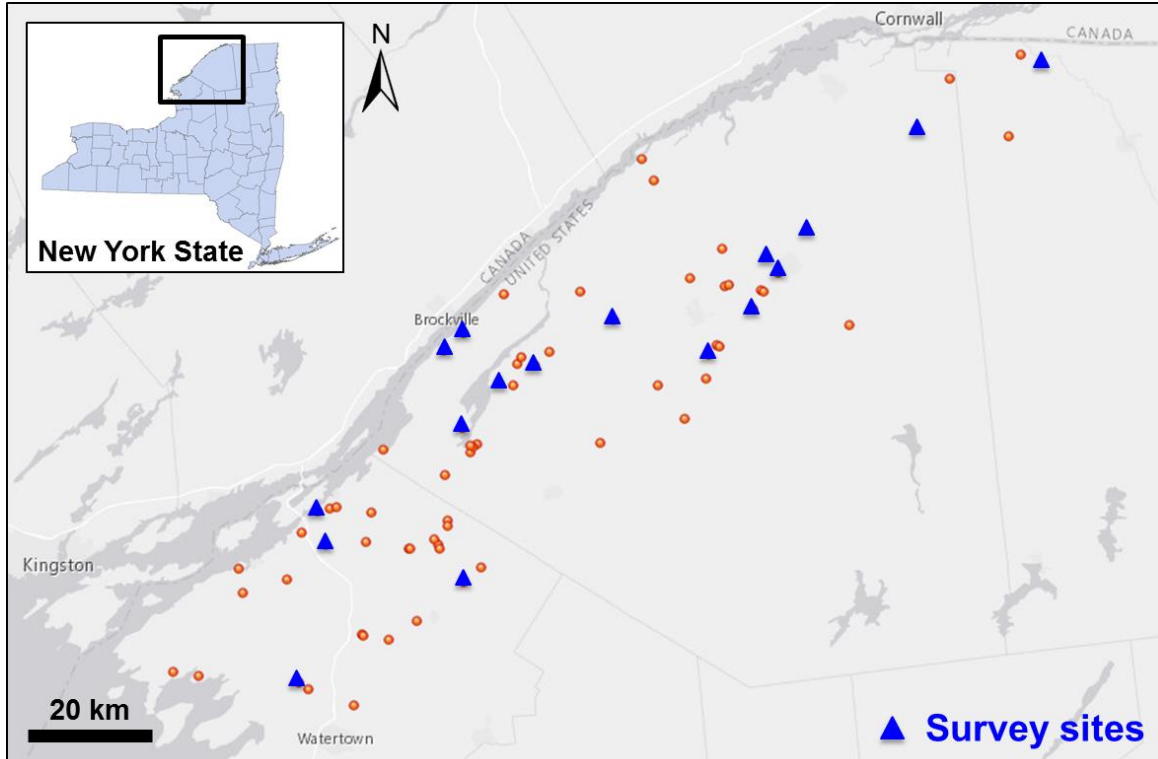


Fig. 3.1 Geographic location of the study sites, shown in blue triangles, and the remaining sites in the larger study shown in red circles (ArcGIS online: <http://www.arcgis.com/>)

Table 3.1 Site Profiles. Site naming code represents surface water connectivity as GI (geographically isolated), SC (seasonally connected), and GC (geographically connected) (see Section 4.1.1).

Site Name	Latitude (°N)	Longitude (°W)	Elevation (m)	Soil texture	Surrounding land cover	Watershed	Area (ha)	Wetland type
GI1	44.9642	74.4641	58	Silty clay loam	Shrub-scrub-grass	Salmon	0.07	Restored
GI2	44.5910	75.3368	87-90	Silt loam	Forest	Oswegatchie	0.17	Restored
GI3	44.5696	75.6483	93-96	Silty clay	Pasture, Shrub-scrub-grass	Headwaters St. Lawrence River	0.21	Restored
GI4	44.5437	75.6905	105-108	Silty clay	Pasture	Headwaters St. Lawrence River	0.44	Restored
GI5	44.0723	75.9700	99-102	Silty clay	Pasture, Forest	Chaumont-Perch	0.91	Restored
GI6	44.6819	75.0256	120-123	Muck	Pasture, Forest	Raquette	2.73	Restored
GI7	44.3099	75.9494	81-84	Silty clay	Pasture, Forest	Headwaters St. Lawrence River	3.45	Restored
GI8	44.5382	75.1403	126-132	Silty clay	Forest	Grass	3.58	Natural
SC1	44.2613	75.9297	90-93	Silty clay	Pasture, Forest	Headwaters St. Lawrence River	3.09	Restored
SC2	44.6056	75.0526	127-130	Silty clay	Pasture, Forest	Grass	3.14	Restored
SC3	44.2059	75.6519	138-144	Silt loam	Pasture, Forest, Shrub-scrub-grass	Indian	3.33	Restored
SC4	44.4969	75.5778	87-90	Silty clay loam	Forest, Shrub-scrub-grass	Indian	3.99	Natural
SC5	44.4299	75.6535	84-90	Silty clay loam	Forest	Indian	4.05	Natural
GC1	44.8561	74.5282	97	Loam	Pasture, Forest	Salmon	0.24	Restored
GC2	44.7214	74.9438	113-116	Silty clay	Forest	Raquette	3.46	Restored
GC3	44.6575	75.0014	123-126	Muck	Forest	Raquette	3.61	Natural
GC4	44.8648	74.7181	76	Silty clay	Forest	St. Regis	4.18	Natural

Four of the seventeen monitored sites were selected for intensive measurement of infrared temperature and atmospheric variables. These sites were selected for differences in size, HGM classes, surface water connectivity, dominant vegetation species, and surrounding land cover. Wetland 1 (GC4 from Table 3.1) surrounds a second order stream and is dominated by hardstem bulrush (*Scirpus Spp.*) in the south and by cattail (*Typha Spp.*) in the north (Fig. 3.2). The measurement station was established on a soil berm and elevated 2 m above the surrounding wetland. The periphery of the wetland is surrounded by mixed forest. Wetland 2 (SC4 from Table 3.1) is a wet meadow dominated by reed canary grass (*Phalaris arundinacea*). The weather station was located within a patch of 1.2 m mixed grass nearby a shallow pond. The area is surrounded by forest. Wetland 3 (SC5 from Table 3.1) is dominated by reed canary grass (*Phalaris arundinacea*) and is inundated from April to June by groundwater drainage from an upland forest. Wetland 4 (GI5 from Table 3.1) is a small restored wetland dominated by cattail (*Typha Spp.*) and located in a sloping pasture (Fig. 3.2). The weather station was set up on the pasture (vegetation height < 0.3 m) approximately 10 m from the pond. The wetland sites were classified as open (1 and 4) and sheltered (2 and 3) in terms of landscape settings.

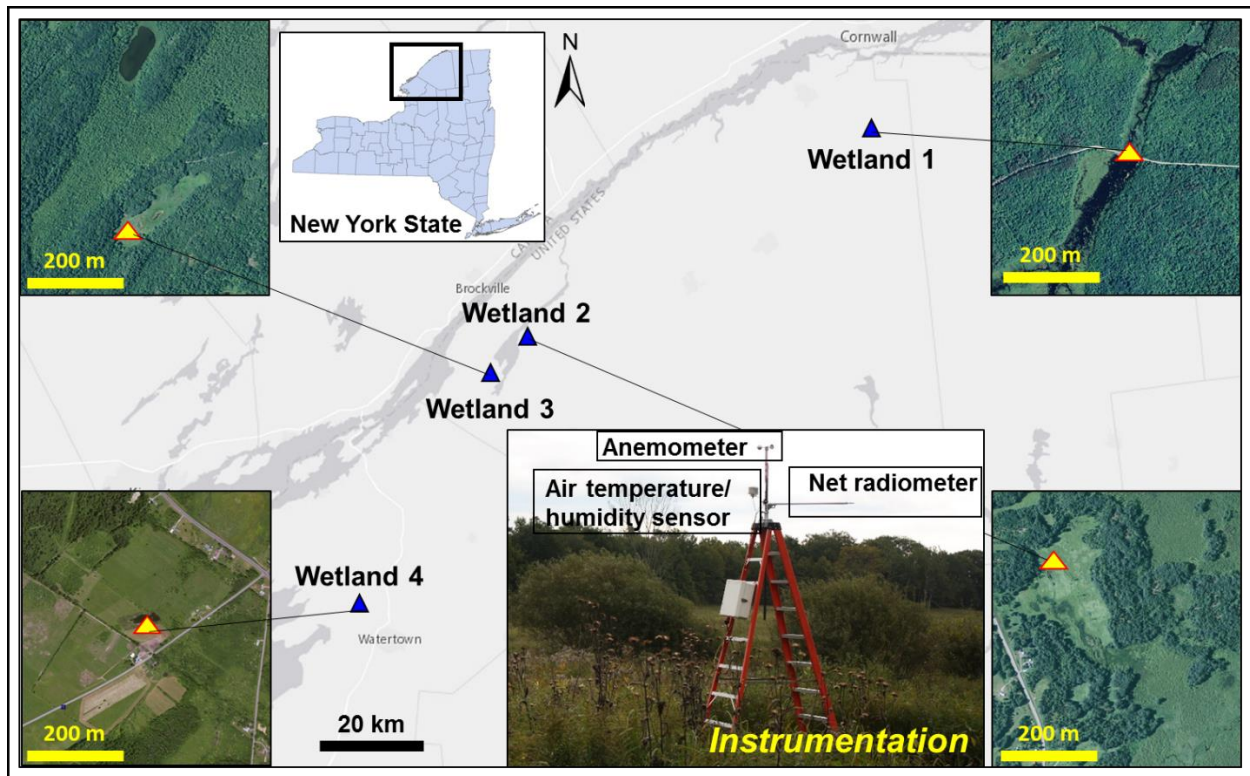


Fig. 3.2 Geographic locations and aerial imagery of three natural (Wetland 1-3) and one restored (Wetland 4) freshwater marshes nearby the St. Lawrence River. Blue triangles mark wetland sites and yellow triangles represent locations of the portable weather station during the study period (Aerial imagery via ArcGIS Online: <http://www.arcgis.com/>). Instrumentation setup for atmospheric observation is illustrated with a site photo.

3.2 Data collection

3.2.1 Site information

Site information was acquired from various sources (Table 3.1). Wetlands were manually delineated on ArcGIS 10 (ESRI, Redlands, CA, USA) using aerial imageries, site pictures and multiple site observations. Drainage areas of wetlands were estimated via USGS StreamStats (<https://water.usgs.gov/osw/streamstats/>). Site elevations were taken from the USGS topographic maps (<http://ngmdb.usgs.gov/maps/TopoView/>). Microtopography within the wetlands ranged generally less

than 3 m. A land use map was acquired from the National Land Cover Database 2011, provided by the Multi-Resolution Land Characteristics Consortium (<http://www.mrlc.gov/nlcd2011.php>). Its subset map by drainage area was used to estimate land use distributions within the drainage areas at 30-m resolution. The major land use classes were agriculture (0-89.3% of drainage area), forest (0.5-84.7%), wetlands (0-41.8%), with smaller areas of grassland (0-18.3%) and residential property (0-19.4%).

3.2.2 Water level and temperature measurements

Surface water level and temperature of each study wetland, and groundwater level and temperature from an adjacent upland borehole were monitored on an hourly basis using gage pressure sensors (U20 HOBO water loggers, Onset Computer Corporation, Bourne, MA, USA) for the 2015 water year. The wetland measurement was sited at the deepest practical location. The upland well site was selected in the direction of the greatest contributing areas, based on topographic analysis of the site in GIS. The well was installed by hand auguring to a depth of 0.67-2.01 m depending on the groundwater level or impediment by stone. The well consisted of a 5-cm diameter PVC pipe with a 15-cm well screen attached at the bottom end and covered by a vented PVC cap. In each well, one pressure sensor was placed at the bottom of the well and tethered to the cap with a nylon cord, and a second sensor was suspended above the water level within the piezometer tube to monitor the reference atmospheric pressure. Reference atmospheric pressure measurements were used provide a common datum for the submerged sensors. When upland well placement was not practical due to private property restrictions, the groundwater wells were installed either in transitional zones or edge of wetlands.

Hydraulic head between the groundwater wells and the wetland surface were calculated

by difference. The datum for each site is arbitrary: the elevation of the land surface where upland groundwater well was installed was set as a local datum. An elevation difference between the observation points was measured by a total station (DR200+, Trimble Navigation Limited, Sunnyvale, CA, USA) at each site.

3.2.3 Atmospheric observation

A portable weather station was constructed by fitting instruments and a data logger to a 3-m stepladder. Measurements included net radiation (NR-LITE2, Kipp and Zonen, Bohemia, NY, USA), air temperature and humidity (CS500, Campbell Scientific Inc., Logan, UT, USA), and wind speed from a 3-cup anemometer (014A, Met One Instruments, Grants Pass, OR, USA). These instruments were positioned at 3.0 m, 3.2 m, and 3.6 m from the land surface, respectively (Fig. 3.2). The radiometer was gimballed for simple adjustment to level. Measurements were made at 5-minute intervals and hourly average values were recorded with a data logger (CR1000, Campbell Scientific Inc., Logan, UT, USA) from 8:00 to 18:00 local time (GMT-5). Biweekly replicate measurements were made from mid-July to early October, 2015.

3.2.4 Ground-based thermal infrared sensing

Complementary TIR images of the local plant community were obtained manually every two hours during the measurement time frame with a portable TIR camera (E4, FLIR Systems Inc., Wilsonville, OR, USA). The temperature range of the device is -20–250°C, estimated accuracy is 2°C, field of view is 45°×34° and native TIR resolution is 80×60 pixels. Resolution was increased to 320×240 pixels using a corresponding image captured from the onboard visible light camera and the thermal multispectral dynamic imaging technique within the supporting

software (FLIR Tools). Hourly averages of atmospheric variables were matched to instantaneous TIR photographs for each site and plant species. For example, the TIR images of two selected plant communities at Wetland 1 were individually taken every two hours from 8:00 to 18:00 on six days (i.e., August 1, 14, 29, September 12, 26, and October 11, 2015). Field days were selected by weather forecast of little rain, but cloud cover and precipitation are common in the study area throughout the year. Emissivity was set to 0.95 for vegetated surfaces (Jones, 2004; Voortman *et al.*, 2016; Kormos *et al.*, 2017).

3.3 Methods

3.3.1 Hydrogeomorphic characterization and surface water connectivity

Regional hydrogeomorphology was defined in terms of geomorphic setting, water source, and hydrodynamics, following Brinson (1993) and Smith *et al.* (1995). Local geomorphology of each site was identified by the National Wetlands Inventory maps from the U.S. Fish and Wildlife Service (<http://www.fws.gov/wetlands/data/mapper.html>) and the U.S. Geologic Survey topographic maps (<http://ngmdb.usgs.gov/maps/TopoView/>). Aerial images were used to understand site landscape attributes and evidence of human disturbance or restoration activities, especially the existence and construction of artificial berms, ditches, and spillways. Image analysis (Google Earth software) was used to identify historical changes in the wetlands over 23 years (1994-2016). Hydrogeomorphic settings, including probable water sources, existence of artificial structures, surface water connectivity, and landscape context were characterized for each site. Flow direction of streams in or through a wetland were determined by topographic evaluation. Surrounding land cover was verified using the National Land Cover Database 2011 (Multi-

Resolution Land Characteristics Consortium; <http://www.mrlc.gov/nlcd2011.php>).

Site visits were conducted to confirm the estimated HGM classes. Surficial structures, including beaver dams, berms, other water control structures and spillways, and local flow characteristics were noted. Surficial contributing areas were also confirmed by visual observation during repeated field visits in May 2014-October 2015.

Three traditional HGM classes were represented in the natural wetlands: depression, slope, and riverine (Smith et al., 1995). Restored wetlands were categorized similarly but slope and riverine classes were amended to depression-in-slope-setting and in-stream-depression, respectively, to emphasize the presence of artificial depressions by excavation or impoundment on the landscape (Gwin et al., 1999). Although the dominant contributing sources are altered little by mitigation, seasonal hydrodynamics may differ by geomorphic settings. Typically dry period hydrodynamics are radial from the pool to the surrounding soil, with little or no outflow from local depressions. Conversely, wet period hydrodynamics are dominated by overland flow toward the outlet, is similar to slope and riverine classes.

3.3.2 Thermal sensitivity

Thermal sensitivity was estimated as the slope of a linear regression between surface water temperature and air temperature:

$$T_w = ET_a + b \quad (1)$$

where T_w and T_a is surface water and air temperature ($^{\circ}\text{C}$), respectively, E the thermal sensitivity as the slope of the first-order relationship between the temperature pairs, and b the y-intercept of the regression line (Chang and Psaris, 2013; Kelleher et al., 2012). Prior studies found limited predictability for T_a below 0°C (Kelleher et al., 2012; Morrill et al., 2005).

Additionally, T_w at the bottom of a wetland (where pressure transducer is located) below 4°C were excluded from the linear regression analysis. This restriction was imposed to address the complications arising from settlement of water at 4°C (which is the maximum density of water). When daily water temperature is around or below 4°C, the ice sheet forming at the water surface precluded internal circulation of water beneath and the surface water eventually became stratified. Thermal sensitivity value for each site was calculated from daily water and air temperature values over a one-year study period. Hourly water temperature measurements from the deployed pressure transducers were averaged to daily values. Daily air temperature data were obtained by measurements from the nearest weather stations. The weather station data were downloaded from the Climate Data Online of the National Oceanic and Atmospheric Administration (NOAA) National Centers for Environmental Information (<http://www.ncdc.noaa.gov/cdo-web/>). Missing daily air temperature data were filled with the mean of daily maximum and minimum data.

3.3.3 Sampling of the TIR measurement

TIR temperature data representing the canopy leaf surface of the plant community were sampled individually by the FLIR Tools software (Fig. 3.3). Intact areas of the vegetation patches in the scene were identified visually from field observation and site pictures. Within a box area presented in Fig. 3.3, for example, all pixel values were averaged to determine the instantaneous surface temperature in the software.

The IR pictures of vegetation communities were taken with nearly constant geometry over a study period. The pictures were generally oriented to south, when practically available, to minimize the shadow area. Local high and low extremes represent damaged or inactive surfaces

for ET and shadows, respectively (Fig. 3.3).

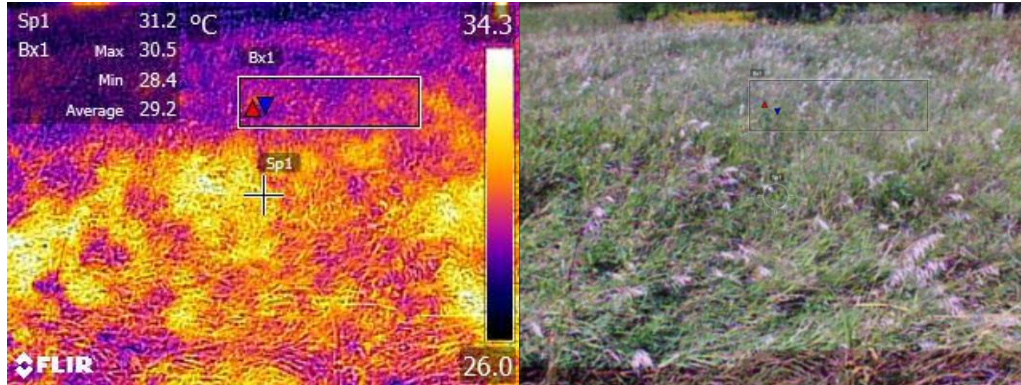


Fig. 3.3 Sample visual (left) and TIR (right) images of reed canary grass at Wetland 2. The images were taken at 10:20 AM (GMT-5) on September 5, 2015.

3.3.3 TIR-based surface energy balance method (SEB)

Observation of leaf surface temperature by TIR thermography can be used to quantify heat transfer at a lateral scale down to a few centimeters. Once a heat transfer profile is accurately established, ET can be estimated directly by energy balance calculations. Heat transfer is quantified based on the theoretical vertical temperature gradient near the leaf surface. The larger scale temperature gradient at for traditional Bowen ratio measurements can be used to partition large scale turbulent heat fluxes (Ahrends et al., 2014; Triggs et al., 2004).

Actual ET can be estimated as a residual from the energy balance equation:

$$\lambda E = R_n - G - H \quad (2)$$

where

λE is the latent heat flux (W m^{-2}),

R_n is the net radiation (W m^{-2}),

G is the soil heat flux (W m^{-2}), and

H is the sensible heat flux (W m^{-2}).

G has a strong relationship with R_n in general conditions (Santanello et al., 2007; Wang et

al., 1998). In this study, G was calculated by $0.3R_n$ as empirically suggested for an open water marsh (Mohamed et al., 2012). H is calculated as a ratio of the difference between ambient air temperature measurements by the relative humidity/temperature sensor and leaf surface temperature measurements by the TIR camera to the aerodynamic resistance:

$$H = \rho_a c_p \frac{T_s - T_a}{r_a} \quad (3)$$

where

ρ_a is the air density assumed as a constant of 1.225 kg m^{-3} ,

c_p is the heat capacity of air ($1013 \text{ J kg}^{-1} \text{ }^\circ\text{C}^{-1}$),

T_s is the surface temperature ($^\circ\text{C}$),

T_a is the air temperature ($^\circ\text{C}$), and

r_a is the aerodynamic resistance (s m^{-1}).

For study sites subject to local advection, Richardson number (Ri) is used for the stability correction of the aerodynamic resistance (Tolk et al., 1995):

$$r_a = 5Ri + 1 \text{ if } Ri < -0.008 \text{ or } Ri > 0.008 \quad (4)$$

$$Ri = g(T_a - T_s) \frac{z-d}{T_{av} u_z^2} \quad (5)$$

$$T_{av} = \frac{T_a + T_s}{2} \quad (6)$$

where

g is the acceleration due to gravity (9.81 m s^{-2}),

z is the measurement height (m),

d is the zero plane displacement height (m) parameterized as $1/3$ times vegetation canopy height,

T_{av} is the average temperature of the air and surface temperature ($^\circ\text{C}$), and

u_z is the wind speed at height z (m s^{-1}).

To determine d , average canopy height of vegetation community was measured manually

at each visit. Vegetation height varied little over the study period.

3.3.4 TIR-based Bowen ratio method (β)

The Bowen ratio (β) was used to estimate ET from the vertical gradients of temperature and humidity between observation height of the weather station and the leaf surface. β is defined as $H/\lambda E$ and thus λE can be obtained without measuring turbulent heat fluxes by substituting β for H in the energy budget equation (Eq. 2):

$$\lambda E = \frac{R_n - G}{1 + \beta} \quad (7)$$

Parameterization of β by measurable atmospheric variables can be made using sensible and latent heat flux density:

$$\beta = \frac{H}{LE} = \frac{\frac{(T_2 - T_1)}{r_a}}{\frac{1}{\gamma} \left(\frac{e_2 - e_1}{r_a} \right)} = \gamma \left(\frac{T_2 - T_1}{e_2 - e_1} \right) \quad (8)$$

where

γ is the psychrometric constant (0.0667 kPa °C⁻¹),

T is the temperature (°C)

e is the vapor pressure (kPa), and

subscripts 1 and 2 indicate two different heights of observation.

Therefore, β can be simply determined if pairs of matched temperature and humidity measurements data are made. This approach is commonly used to estimate β from a micrometeorological station. In this study, β was determined directly from measurements at the heights of the atmospheric instruments and at leaf surface level. If the lower measurement height is set to the vegetation leaf level, the ambient air parcel there can be regarded as saturated and measured TIR temperature represents the temperature of the leaf surface:

$$\beta = \gamma \left(\frac{T_{leaf} - T_a}{e_{leaf} - e_a} \right) = \gamma \left(\frac{T_s - T_a}{e_s - e_a} \right) \quad (9)$$

where

T_{leaf} and e_{leaf} are the air temperature (°C) and vapor pressure (kPa) at the leaf surface level, respectively,

T_a and e_a are the air temperature (°C) and actual vapor pressure (kPa) in the atmosphere, respectively, and

T_s and e_s are the surface temperature (°C) and saturated vapor pressure (kPa) at the leaf, respectively.

3.3.5 Priestley-Taylor method

Priestley and Taylor (1972) empirically simplified the combination equation, so called Penman (Penman, 1948), for wet surface with minimal advection:

$$\lambda E = \alpha \frac{\Delta}{\Delta + \gamma} (R_n - G) \quad (10)$$

where

α is the Priestley-Taylor multiplier (often referred as a constant of 1.26 as used in this study) (Priestley and Taylor, 1972), and

Δ is the slope of the saturation vapor pressure curve (kPa °C⁻¹).

3.3.6 Crop coefficient method

The crop coefficient (K_c) is defined as a multiplier that links reference to crop ET under standard conditions and was developed for use in irrigation planning for agricultural crops.

Estimating actual ET generally requires supporting data to characterize the land surface, vegetation distribution and meteorology, which often challenges accurate prediction. In this

approach, actual ET from a crop surface can be simply acquired once land surface properties are quantified into K_c :

$$ET = K_c ET_0 \quad (11)$$

where

ET_0 is the reference ET (mm d^{-1}).

The FAO Penman-Monteith reference ET method (Allen et al., 1998) is the most widely used parameterized version of the original Penman-Monteith equation (Monteith, 1965) particularly for the reference surface:

$$ET_0 = \frac{0.408\Delta(R_n - G) + \gamma \frac{900}{T_a + 273} u_2 (e_s - e_a)}{\Delta + \gamma(1 + 0.34u_2)} \quad (12)$$

where

u_2 is wind speed at 2-m height (m s^{-1}).

The reference surface is defined as hypothetical 0.12 m grass in which a surface resistance and an albedo are assumed to be fixed as 70 s m^{-1} and 0.23, respectively.

In order to apply K_c information in any area of interest, a sufficient number of studies should be used to represent a range of vegetation species under various climate and land surface conditions. For wetlands, reported studies have mostly focused on a few species such as common reed, cattail, and bulrush (Allen, 1995; Drexler et al., 2004; Wu and Shukla, 2014). In this study, daily K_c from four crop surfaces was calculated as the linear regression slope of two TIR-based ET versus FAO Penman-Monteith standard reference ET (Allen et al., 1998; Beebe et al., 2014; Mao et al., 2002). The estimated K_c sets were then compared with the ranges suggested in other papers to understand how crop ET is different by regional climate and geography.

Chapter 4. Geographical and hydrological impacts on subsurface connectivity of natural and restored wetlands

This chapter provides results of experiments conducted to demonstrate support for the first hypothesis; Hydrologic services of wetlands, such as excessive water storage and groundwater regulation, are persistent over a range of surface water connectivity due to subsurface flow exchange. Seasonal stage patterns associated with adjacent groundwater table were analyzed (Section 4.1.2) by surface water connectivity types (Section 4.1.1). Geographical and hydrological variables were selected to find any significant correlations (Section 4.1.3). Based on these results, hydrological functions at a range of surface water connectivity were discussed (Section 4.1.4 and 4.2.2).

4.1 Results

4.1.1 Categorization of wetlands by hydrogeomorphic settings and surface water connectivity

Depressional wetlands occur as both natural and restored wetlands. Although local topographic depressions with closed contours are uncommon in the study area, some example sites were identified to study. Most of the observed depressional wetlands were constructed. Construction of wetlands is relatively common and typically consists of excavation and banking at a local depression in rolling topography. Thus, depressional topography of both natural and mitigated wetlands are hereafter regarded as having similar geomorphic features despite the different level of ecosystem disturbance.

Riverine wetlands are defined as floodplain wetlands adjacent to a stream channel and

primarily fed by overbank flow from the stream (Smith et al., 1995). In-stream-depression is defined here as a floodplain local depression following excavation (mitigation), resulting in a mixture of riverine and depressional hydrogeomorphology. Both riverine and in-stream-depressions sites are located within first and second order streams where streamflow is shallow and slow. These stream-associated classes in this area are often associated with beaver activity, which is to regulate outflow from a stream.

Slope wetlands are predominantly fed by groundwater and usually have explicit outflow on sloping land (Stein et al., 2004; Woods et al., 2006). With a same way that the in-stream-depression occurs, the depression-in-slope-setting is formed as local depression within the slope wetlands by the mitigation. Both classes of wetlands in the study area are located at the base of a slope (toe-of-slope).

All depressional wetlands were classified as GIWs because they are wetland areas in topographic depressions entirely surrounded by uplands, with no apparent surface connection to other water bodies. Riverine and slope wetlands were grouped regardless of whether perennially or seasonally connected to downstream waters. Only difference between classes was the dominant input source of water: riverine wetlands were fed from upstream and slope wetlands by groundwater discharge. Seasonal connection was determined by seasonal presence of flow and observation of a channel in dry conditions. If discharge type, i.e., surface outflow, alternates seasonally, sites were considered as seasonally connected wetlands (SCWs). Restored wetlands typically fell in this category due to activities related to impounding water, e.g., excavation, berm construction. These activities promote seasonal connection due to excessive outflow by spring snowmelt during wet seasonal conditions. Hereafter, surface connectivity of wetlands is classified by three types: geographically isolated, seasonally connected, and geographically (or

perennially) connected.

4.1.2 Seasonal variation of wetland stage and upland groundwater table

Fig. 4.1 shows example data for seasonal trends precipitation, surface pool depth at the point of measurement and depth of water in surface wells for two of the seventeen sites. Wetland stage and upland groundwater surface often show similar response to precipitation over all seasons. Evapotranspiration results in reductions to pond storage from May to September. Surface runoff and overland sheet flow from a wetland is a dominant water loss in a wet period where it can be observed from seasonally or fully connected wetlands. Wetland stage curves are more dependent to groundwater fluctuation at GIWs than the other types due to lack of surface inflow or outflow as other primary drivers (Fig. 4.1).

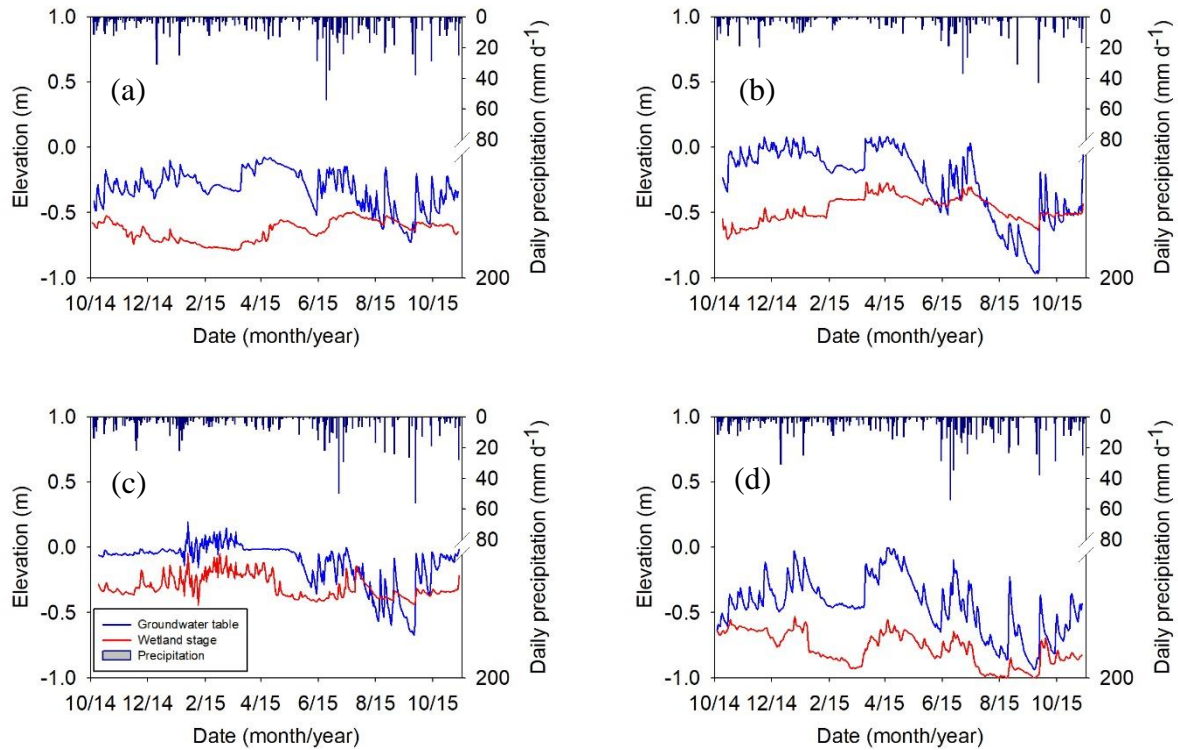


Fig. 4.1 Seasonal variation of wetland stage (red) and depth of groundwater table (blue) at (a) GI8 (natural depressions), (b) GI5 (restored depressions), (c) SC1 (restored slope settings), and (d) GC2 (restored riverine settings). Datum of each site represents land surface elevation where groundwater well was installed.

Drainage area is predominantly related to site hydrogeomorphology (Table 4.1). The largest drainage areas were the riverine settings (33-653 ha), and depressional (6-48 ha) and slope (7-42 ha) settings had similar contributing areas. Nevertheless, ranges of hydrologic variables such as standard deviation of wetland stage (SD_{sw}), upland groundwater table (SD_{GW}) and mean groundwater table ($mean_{GW}$) did not differ by hydrogeomorphic setting. Surface water connectivity of wetlands did not distinguish these summary variables (Table 4.1). Mean wetland stage was highly variable due to the side range in measurement datum and site bathymetry across sites.

Table 4.1 Summary statistics of geomorphic settings and hydrologic variables. Surface water connectivity to downstream waters is indicated in part of site names as GI (geographically isolated), SC (seasonally connected), and GC (geographically connected). Note that abbreviations represent HGM (hydrogeomorphic), SD_{SW} (standard deviation of wetland stage), $Mean_{GW}$ (mean groundwater depth), SD_{GW} (standard deviation of groundwater depth), t_r (accumulated duration of subsurface flow reversal), DEP (topographic depressions), RIV (riverine settings), SLO (slope settings), GW (groundwater from local groundwater table), and SW (surface water from upstream).

Site Name	HGM Class	Input Source	Area (ha)	Perimeter (km)	Drainage area (ha)	SD_{SW} (m)	$Mean_{GW}$ (m)	SD_{GW} (m)	t_r / total observation period (d)
GI1	DEP	GW	0.07	0.05	5.54	0.14	0.30	0.38	309/375
GI2	DEP	GW	0.17	0.17	16.26	0.13	0.70	0.22	55/314
GI3	RIV	SW	0.21	0.30	32.75	0.13	0.86	0.15	5/357
GI4	SLO	GW	0.44	0.51	7.19	0.19	1.01	0.16	1/366
GI5	DEP	GW	0.91	0.35	7.80	0.09	0.74	0.27	91/381
GI6	SLO	GW	2.73	0.93	8.72	0.11	0.66	0.17	34/341
GI7	DEP	GW	3.45	1.15	6.54	0.10	0.45	0.25	201/382
GI8	DEP	GW	3.58	1.38	48.03	0.08	0.63	0.14	24/380
SC1	RIV	SW	3.09	1.36	653.31	0.09	0.57	0.17	50/385
SC2	RIV	SW	3.14	1.99	126.79	0.05	0.71	0.15	25/371
SC3	RIV	SW	3.33	1.37	65.76	0.06	0.62	0.09	107/378
SC4	SLO	GW	3.99	1.72	13.86	0.14	0.61	0.15	0/360
SC5	SLO	GW	4.05	1.23	35.90	0.13	0.98	0.20	15/320
GC1	RIV	SW	0.24	0.36	82.89	0.12	1.14	0.16	0/293
GC2	RIV	SW	3.46	1.31	512.44	0.13	0.76	0.21	0/384
GC3	SLO	GW	3.61	1.33	42.17	0.11	0.54	0.10	0/335
GC4	RIV	SW	4.18	1.44	578.54	0.14	1.73	0.15	0/281

During dry periods, periodic subsurface flow reversal from filling to exfiltration is observed (Fig. 4.1). Such subsurface interaction is largely driven by persistent evapotranspiration loss and temporary input from sporadic rainfall events. Differences in surface water loss across the land cover mosaic resulted in different stage recession rates in wetland stage and upland groundwater table. All GIWs and SCWs except SC4 experienced the flow reversal over the study period (Table 4.1). GCs did not experience flow reversal.

Duration of the flow reversal event varied by up to days (e.g., GI2, GI3, GI8, SC5), weeks (e.g., GI6, SC1, SC2, SC3), or months (e.g., GI1, GI5, GI7). Exfiltration periods at the

most sites range within 60 days where up to 309 days were observed.

4.1.3 Relationships between geomorphic and hydrologic variables

To better understand likely relationships between local and regional controls on site hydrology, correlation analysis was performed between a targeted set of geographic and hydrologic variables. These include wetland size, site elevation, and land use composition of a drainage, and mean groundwater table ($mean_{GW}$), standard deviation of groundwater table (SD_{GW}) and surface water stage of a wetland (SD_{sw}). Mean wetland stage was not used in the analysis because the absolute measure of wetland stage was not consistent to represent site hydrology due to different geometry and bathymetry across the region. Correlation coefficients (r) and significance levels were estimated by three groups with different sample numbers, i.e., (a) GIWs only ($n=8$), (b) GIWs and SCWs ($n=13$), and (c) GIWs, SCWs, and GCWs (all sites, $n=17$), to determine if there was any relationship that was only found from GIWs (Fig. 4.2).

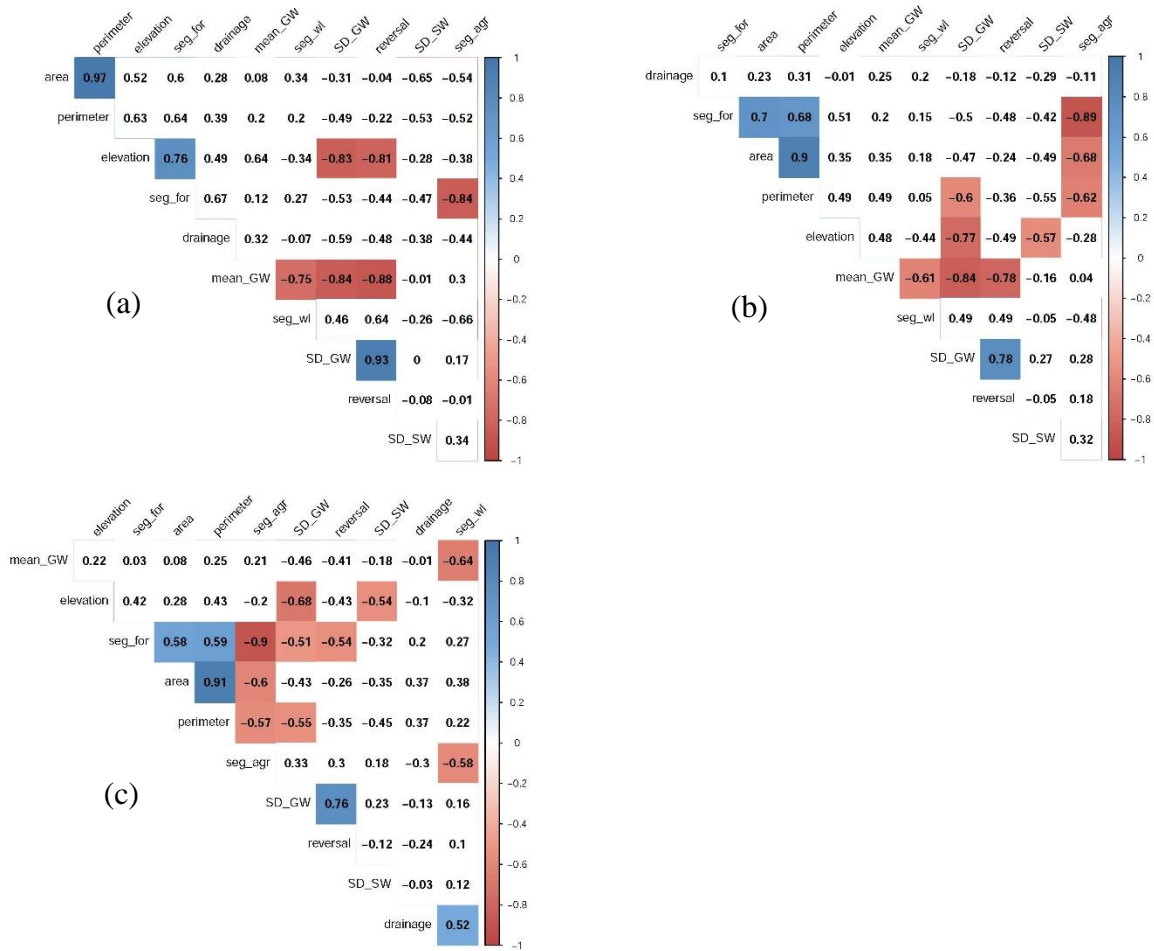


Fig. 4.2 Correlation and significance levels of site geomorphology and hydrologic variables of (a) GIWs only (n=8), (b) GIWs and SCWs (n=13), and (c) all sites (n=17). Color-filled correlations indicate significance at the 95% confidence levels where blue and red represents positive and negative correlation coefficient, respectively.

Meaningful correlations are selected from Fig. 4.2 and moved to the separate table (Table 4.2) for better presentation. Wetland area and perimeter show similar or relatively strong correlations ($r=-0.65$ and -0.53 , respectively) for GIWs than the other site groups while not statistically significant (Table 4.2). However, standard deviation of wetland stage (SD_{sw}) is not significantly correlated with any of the tested geographical variables (Fig. 4.2). Higher SD_{sw} is found at smaller wetlands and it decreases for larger wetlands. This trend is obvious at GIWs but this geometric signal became weaker when SCWs or GCWs are included. Attenuation of such

signal over expanding sample group is found for wetland area (Table 4.2). Impact of wetland perimeter on SD_{sw} was relatively consistent over a range of surface water connectivity.

Table 4.2 Correlation and significance levels of site geomorphology and hydrologic variables by different site categories of surface water connection. (a) GIWs only (n=8), (b) GIWs and SCWs (n=13), and (c) all sites (n=17). An asterisk denotes significance at the 95% confidence levels.

Variable pairs	correlation coefficient		
	GIW (n=8)	GIW+SCW (n=13)	GIW+SCW+GCW (n=17)
Wetland area (ha) and SD_{sw} (m)	-0.65	-0.49	-0.35
Wetland perimeter (km) and SD_{sw} (m)	-0.53	-0.55	-0.45
Fraction of wetland (%) and $mean_{GW}$ (m)	-0.75*	-0.61*	-0.64*
Elevation (m) and SD_{GW} (m)	-0.83*	-0.77*	-0.68*
Flow reversal period (d) and SD_{GW} (m)	0.93*	0.78*	0.76*
Wetland perimeter (km) and SD_{GW} (m)	-0.49	-0.60*	-0.55*
Fraction of forest (%) and SD_{GW} (m)	-0.53	-0.50	-0.51*
Fraction of wetland (%) and SD_{GW} (m)	0.46	0.49	0.16
Fraction of agriculture (%) and SD_{GW} (m)	0.17	0.28	0.33

The fraction of wetlands within a drainage area is the only significant geographical driver that negatively affects mean groundwater table (Fig. 4.2). Deeper mean groundwater table from the land surface is found in a drainage area that wetlands dominate. This relationship is strong for GIWs and slightly decreases when SCWs and GCWs are added.

SD_{GW} is significantly correlated with multiple variables such as site elevation, an accumulated flow reversal, wetland perimeter, and fraction of forest for all groups (Fig. 4.2). Elevation and wetland perimeter present strong correlations with SD_{GW} ($r=-0.83$ and 0.93 , respectively) for GIWs where correlation coefficients decrease when SCWs and GCWs are included. On the other hand, the other two variables show opposite patterns that significant correlations are observed only from mixed groups. The strongest negative relationship between wetland perimeter and SD_{GW} is found from GIWs and SCWs ($r=-0.60$). Impacts of wetland perimeter and fraction of forest on SD_{GW} are relatively little to GIWs with no significance while

a negative relationship is present (Table 4.2).

Land use composition within a drainage area suggests less impact on SD_{GW} with low r values with no statistical significance (Fig. 4.2). Forest has a negative impact on SD_{GW} with similar correlation coefficients across surface water connectivity types where statistical significance is not observed from GIWs and SCWs. Correlations between fraction of forest and SD_{GW} are not crucially affected by surface water connectivity types (Table 4.2). Wetland and agriculture show positive relationships with SD_{GW} despite no significance. Agricultural impacts on SD_{GW} are very low particularly for GIWs (Table 4.2). Despite similar patterns, impact of fraction of wetland shows far less agreement when GCWs are included.

4.1.4 Hydrologic functions of wetlands by downstream connectivity

To explore hydrologic impacts that geographical variables impose, selected sets of variables were compared by geographical connectivity with downstream waters. Mean groundwater level is only significantly correlated with occupancy of wetland within a drainage (Fig. 4.2). A relationship between such variables by surface water connectivity is presented in Fig. 4.3. Groundwater table tends to fluctuate at a root zone for wetlands occupying approximately less than 20% within a drainage area. $mean_{GW}$ is at shallow depths (0-0.3 m from the land surface) where less than 10% of wetlands are only present in a drainage area. With elevated wetland ratio, $mean_{GW}$ tends to decrease. Since most of restored wetlands are located on private properties, their spatial occupancy ratio is relatively low with mostly less than 20%.

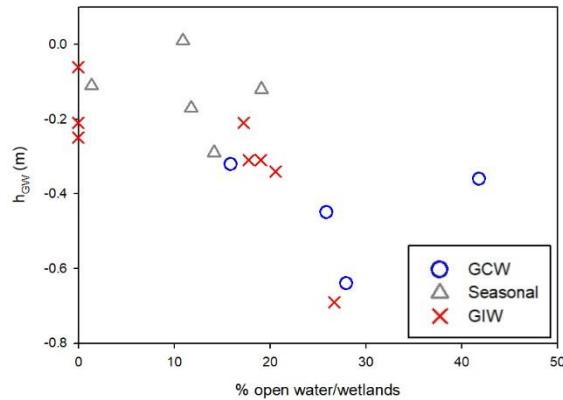


Fig. 4.3 A relationship between fraction of wetland and mean groundwater table

Impact of landscape and hydrologic drivers on seasonal fluctuation of groundwater table depends on surface water connectivity (Fig. 4.4). Site elevation and an accumulated period of subsurface flow reversal show consistent trends over GIWs (Fig. 4.4a, b). SD_{GW} decreases with higher site elevation for GIWs (Fig. 4.4a). The similar patterns are observed while less decreasing slope and locally inconclusive distribution are featured for SCWs and GCWs, respectively. Distribution patterns of flow reversal periods against SD_{GW} are different (Fig. 4.4b). The longer period of subsurface flow reversal leads higher SD_{GW} for GIWs, whereas discrete patterns are observed from SCWs and GCWs. All SCWs did not experience the flow reversal, i.e., persistent groundwater discharge (Table 4.1). On the other hand, the less consistent relationship was observed for wetland perimeter (Fig. 4.4c). Although data points of three connectivity types form significant relationship with SD_{GW} in combination, individual data sets do not seem to be conclusive. Nevertheless, all four variables form significant relationships with SD_{GW} for all surface connectivity types (Table 4.2).

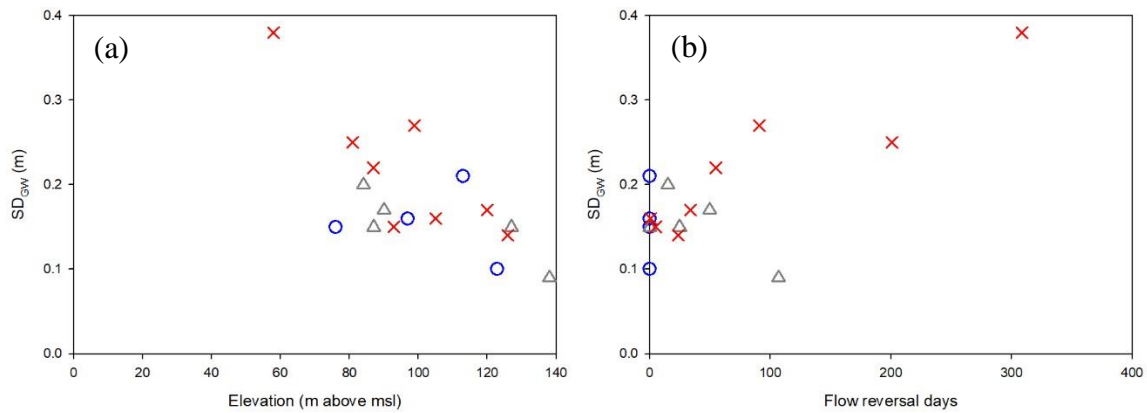
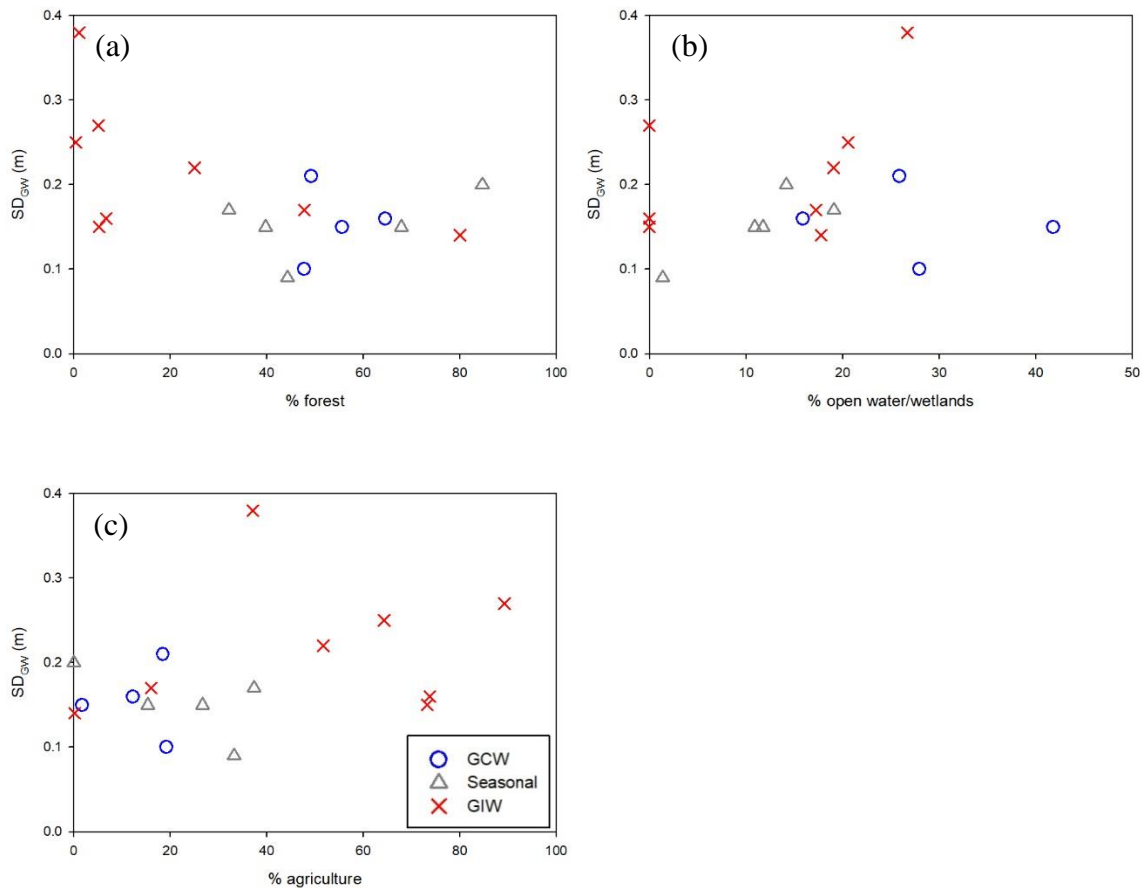


Fig. 4.4 Relationships of standard deviation of daily groundwater table and (a) wetland elevation and (b) flow reversal days

Land cover composition within a drainage area also influences SD_{GW} . Fractions of forest and wetlands regulate SD_{GW} supposedly via persistent consumption of surface runoff and shallow groundwater by evapotranspiration (Fig. 4.5). In contrary, greater groundwater fluctuation is observed at drainage areas that are composed of larger agricultural land use. SD_{GW} is significantly correlated only with fraction of forest for all sites (Table 4.2).



characteristics.

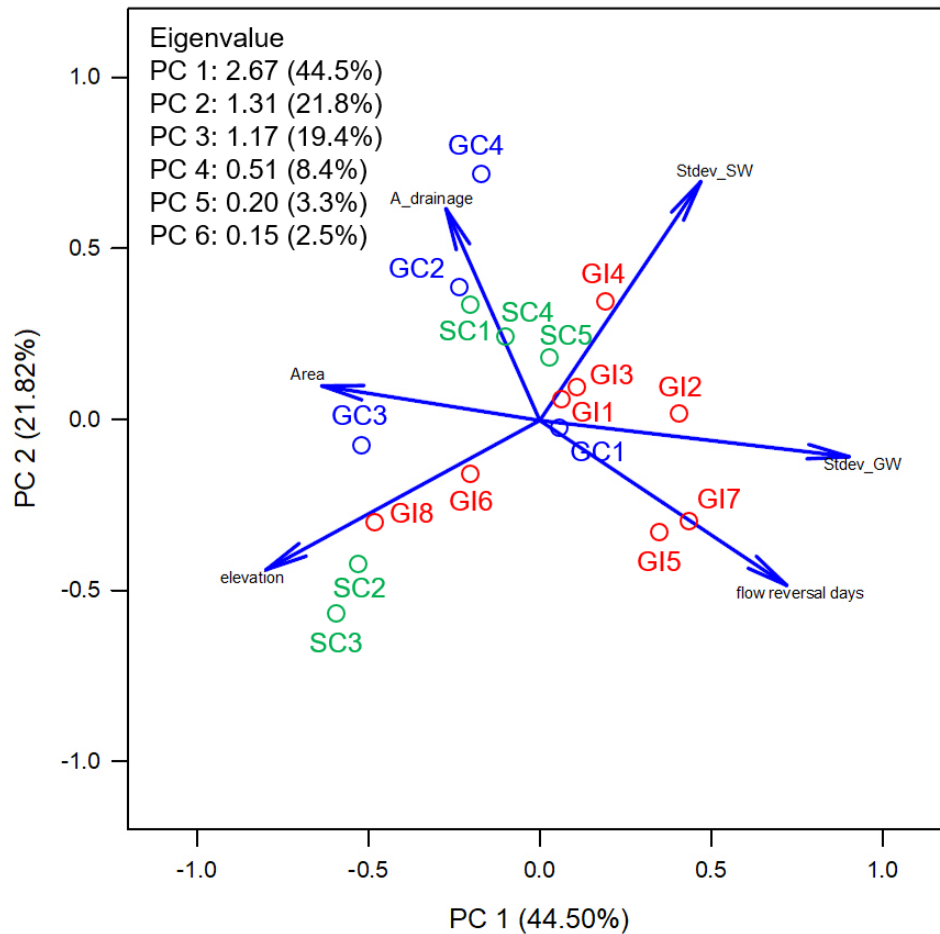


Fig. 4.6 Component scores and loadings from the principal component analysis. Sites are color-coded by surface water connectivity as red, green and blue for GIW, SCW and GCW, respectively.

4.2 Discussion

4.2.1 Impacts of landscape factors on groundwater regime at wetland restoration sites

sites

Changes to the land surface topography from restoration activities dominated site surface hydrology and subsurface flow variation. Hydrogeomorphic settings exerted a secondary

influence on flow variation (Mushet et al., 2015). Modification of the land surface during wetland restoration abated geomorphic controls on site hydrology. Mitigation banking and associated activities for water impoundment resulted in greater frequency or duration of subsurface flow reversal between wetlands and surrounding uplands (Table 4.1, Fig. 4.1). Where the sites are hydrogeomorphically categorized in three groups, i.e., riverine, slope, and depression, riverine and slope wetlands typically have obvious surface connections for outflow. From the natural wetlands, flow reversal was observed only from one out of four GCWs (i.e., SC5). From the restored riverine and slope wetlands, however, at least a day of flow reversal were observed (Table 4.1). Once geographical connectivity is characterized, impact of dominant input source, such as groundwater discharge from slope wetlands and upstream runoff from riverine wetlands, on site hydrology was minimized for restored wetlands.

The impacts on hydrologic behavior of wetlands from mitigation than natural wetlands with least disturbance (Cole and Brooks, 2000; Ehrenfeld et al., 2003), sometimes in combination with land use composition of a drainage area resulting in losing consistency on similar geomorphology (McLaughlin and Cohen, 2013). Mitigation banking also resulted in modifying surface connectivity of wetlands and downstream waters. Subsurface connectivity between wetlands and downstream waters was explored by various approaches (Hunt et al., 2006, 1999; Min et al., 2010; Rains, 2011; Woods et al., 2006). For GIWs, hydrologic connectivity is controlled primarily by interactions between wetland stage and upland groundwater table via periodic subsurface flow reversals. Subsurface flow reversals have been reported only with respect to particular regional geomorphic settings (Devito et al., 1997; McLaughlin et al., 2014; Winter, 1999). Experimental evidence that current restoration methods also promote such subsurface exchange was found. Investigation of subsequent hydrological and

biogeochemical interactions will contribute to reveal unique ecosystem functions that GIWs or restored wetlands provide.

Subsurface flow reversal essentially occurred by balancing wetland stage and upland groundwater table. Flow reversal was commonly found from wetlands that are located on topographic depressions (Hunt et al., 2006; Mclaughlin and Cohen, 2014). Relatively slow groundwater transport where surface water connection was absent caused flow reversal in a growing season by different vegetation uptake and groundwater evaporation rates. Ultimately, GIWs (and SCWs restrictedly in a dry period) experienced such groundwater exchange more frequently than GCWs. Where surface water input was persistently supplied to wetlands, flow reversal did not happen. Intermittent surface connection at SCWs allowed wetlands to experience shorter period (0-107 days) of flow reversal than GIWs (1-309 days) (Table 4.1). Sites having frequent flow reversal are typically attributed to local geomorphology that sufficient groundwater supply is prohibited due to shallow bedrock (e.g., GI7) or relatively deep groundwater table from the land surface (e.g., GI1). Consistent water supply was attributed to surface water flow either from upstream or back swamp (GC1, GC2, GC4) or from groundwater discharge from steep downslope (GC3).

Following human modification, effect of land use within a drainage area controlled both mean and standard variation of groundwater table as a secondary driver (Table 4.2, Fig. 4.5). The drainage-scale approach was used to characterize ecosystem functions that wetlands provide. With an assumption that geomorphic settings are uniform across the region, greater wetland area per unit drainage resulted in lower groundwater table. As groundwater regulation is major hydrologic function that wetlands provide, GIWs show similar functional capacity (Table 4.2, Fig. 4.3). If areas and number of wetland entities within a drainage area are all identified in the

analysis, functional capacity that GIWs provide will be better quantified. Along with wetlands, fraction of forest had a direct impact on SD_{GW} . The greater groundwater contribution at the higher forest occupancy is unexpected because of more water loss by evapotranspiration and canopy interception would diminish groundwater discharge toward wetlands by less infiltration for local storage.

4.2.2 Geographical impacts of GIWs on hydrologic functions

GIWs maintained hydrologic functions even if surface water connectivity was not present. Fraction of wetlands within a drainage area also had a significant impact on mean groundwater table. Modelling results from the previous study showed that groundwater table stayed nearly constant along with increasing number or total area of GIWs within an unit area (McLaughlin et al., 2014). Although not strictly limited to GIWs, our results suggest that presence of wetlands has significant impact on groundwater regulation (Table 4.2, Fig. 4.4). Most of the survey sites had relatively small drainage areas particularly for the groundwater-fed wetlands ranging 5-48 ha (Table 4.1). Although results restrictedly partition impacts of GIWs from other types due to limited sample number, they indicate that GIWs potentially perform at least similar degree of the groundwater regulation function that other types of wetlands provide. Considering that most of drainage areas consist of many relatively small wetlands (typically less than 5 ha) in the study region (Benson et al., 2017), results verify that occupying rate of wetlands within their drainage area effectively regulates groundwater table as a local sink. Groups of relatively small wetlands contribute to regulate groundwater table more effectively.

Geographical and hydrological variables affected seasonal variation of groundwater table despite little association of soil texture as a direct medium. Four variables including wetland

perimeter and elevation, accumulated flow reversal period, and a ratio of forest within a drainage area significantly affected SD_{GW} across a range of direct surface water connection (Fig. 4.3). Increase of wetland perimeters for representing for larger amount of water storage raised hydrologic capacitance despite an insignificant relationship of wetland areas as another surrogate. GIWs showed consistent responses to these four variables whereas SCWs and GCWs did not follow the overall trend in the same point cloud (Fig. 4.4). Such alternation of flow direction enhances suppressing seasonal fluctuation of groundwater table although surface water connection is absent. Such buffer effect within an unit area was controlled both by number and individual sizes of wetland entities (McLaughlin et al., 2014). Although this study did not partition impacts of abundance and size of individual wetlands per unit area, their combined effect was presented using relative landscape composition as a proxy from the analysis.

4.2.3 Experimental limitations and source of uncertainty

This chapter demonstrates the impacts of geographical factors on groundwater regime and associated ecosystem functions in the study region. Specifically, stronger correlations were found for GIWs than were found between mean groundwater table and fraction of wetland area, and standard deviation of groundwater table and site elevation and cumulative duration of subsurface flow reversal (Table 4.2). Relationships of these variable pairs are also inconsistent with those suggested from prior findings. For example, increasing area of individual wetland was suggested to result in greater groundwater table and baseflow variation from hypothetical GIWs (McLaughlin et al., 2014), while the area was not significantly correlated with any hydrologic variables in this study (Table 4.2, Fig. 4.2). This is likely due to a range of natural variability and human disturbance (Ehrenfeld et al., 2003). Particularly, altered hydrology from restoration

processes often resulted in great uncertainty in the quantification of ecological impacts (Hruby, 2001; Stander and Ehrenfeld, 2009).

This study was conducted over seventeen wetlands representing individual geomorphic and hydrologic connectivity in terms of categorizing standards. Although selection of wetlands that fall into same categories in the similar geographic region is hard, this may be necessary to assess geophysical controls on site hydrology and subsurface interaction with landscape for ecosystem services. Further investigations should be conducted at various climate and wetland types.

4.3 Summary and conclusions

Most mitigation wetlands experienced hydrologic alteration due to a loss of surface water connection either temporarily or permanently to downstream waters. This alteration would remove them from blanket federal protection from development. Despite the absence of obvious connectivity, this study clearly demonstrates subsurface connectivity through relationships that represent ecosystem functions of wetlands. Although the degrees of feedback differed with range of surface water connectivity, mitigation wetlands did regulate the local groundwater system. GIWs, depressional wetlands without surface water connectivity that often attributed to wetland mitigation, had a similar impact to other wetland types on groundwater regulation in landscape composition within a drainage. The presented results demonstrate that geomorphic alteration due to human activities was the primary driver of hydrologic functions including groundwater regulation (Fig. 4.3) and water storage (Fig. 4.4b) and that landscape composition within a drainage area as the secondary driver. For mitigation wetlands, hydrogeomorphic settings should

be used supplementary to alteration of wetland structure.

This study presented experimental evidence of hydrologic connectivity between GIWs and downstream waters through the local groundwater regime. Connection of GIWs and groundwater were identified by correlation of several geographical and hydrologic variables, including site elevation, accumulated flow reversal period, wetland perimeter, and land use composition. Significant correlations were only found between a few geographical and hydrological variables, i.e., wetland fraction and mean groundwater table, and site elevation and groundwater variation (Table 4.2). Hydrologic characteristics resulted in more condition-dependent in variation rather than in scale.

Chapter 5. Hydrogeomorphic controls on thermal regime of wetlands in northern New York

The hypothesis that the thermal regimes of wetlands are moderated by summer groundwater abundance associated with hydrogeomorphic settings is tested in this chapter. Seasonal trends of wetland stage and temperature are compared by site (Section 5.1.1-5.1.2 and 5.2.1-5.2.2). In addition, estimated thermal sensitivity (Section 5.1.3), a proxy of the wetland thermal regime, is compared to wetland elevation, cumulative period of subsurface loss, standard deviation of wetland stage and groundwater surface depth to identify any significant correlations (Section 5.1.4 and 5.2.3).

5.1 Results

5.1.1 Seasonal variation of wetland stage and temperature

Stage records at the seventeen monitored wetlands differ occasionally by site but show similar overall temporal patterns in stage and temperature (Fig. 5.1). The two sites presented here are a geographically isolated wetland in a depression setting and a seasonally connected floodplain of a headwater stream. These types of wetlands are primarily fed by groundwater (GI4; Fig. 5.1a) and streamflow (SC4; Fig. 5.1b) from surrounding uplands. Overland flow is occasional following substantial rainfall or snowmelt during periods of soil saturation.

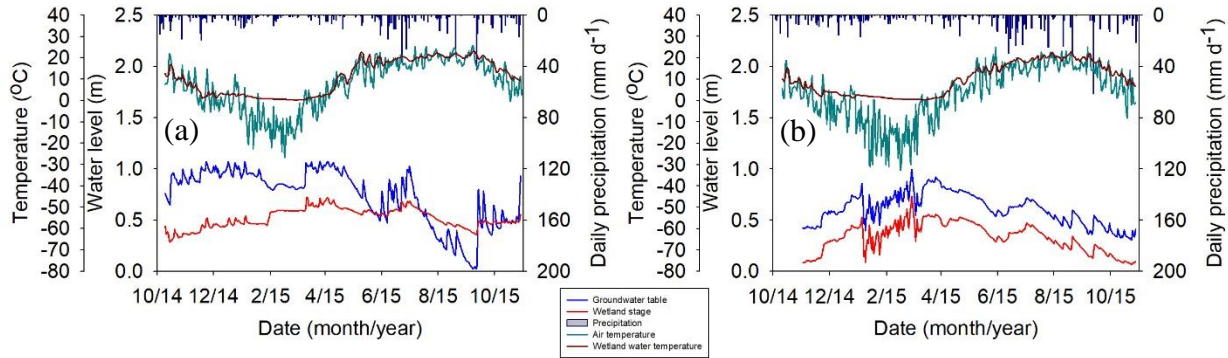


Fig. 5.1 Wetland stage (red line) and water temperature (brown line) at (a) GI4 and (b) SC4. Data for wetland stage and groundwater table (blue line) measurements at each site are presented as elevation of the land surface where wetland stage was measured.

Within the annual trends, wetland stage and variation in stage differ by hydrogeomorphic setting and are most affected by loss to groundwater. Groundwater-surface water stage coupling was tightest at depressional and slope wetlands due to the dominance of groundwater source, relative to surface water inputs. Nevertheless, stage recession rates at depressional wetlands are generally less than those of the corresponding groundwater records. It is important to note that the difference in datum for wetland surface and groundwater measurements often results in an offset in records for slope wetlands, but not for the other more level sites. Seasonal stage patterns of riverine wetlands near the groundwater surface are confounded by unsteady flow conditions and response lag between headwater and groundwater.

The construction of restoration practices intensify the influence of topographic depressions, therefore wetland stage is commonly tied to groundwater surface elevation across the restored wetlands. Consequently, dry-period stage in restored slope wetlands (Fig. 5.1b), becomes similar to natural depressions, which are primarily fed by upslope groundwater discharge (Fig. 5.1a). Whereas seasonal trends and fluctuations in stage are similar for both natural and restored wetlands throughout winter and spring, the upland groundwater depth is

nearly constant during dry conditions at the natural wetlands but often variable the restored wetlands.

Restoration practices also affect dry season wetland hydrology. Fig. 5.1a shows an example of the shift from wetland stage increase (gaining) to decrease (losing) by subsurface flow reversal. This pattern is found at most sites where timing and duration of flow reversal vary and is associated with site geomorphology and class (natural or restored). Natural wetlands show flow reversal only for depressional wetlands such as GI8.

Relatively uniform daily air temperatures across the region influence wetland water temperatures (Fig. 5.1) along with solar irradiance. Wetland water temperature ranges 0.1-29.1°C across sites, with maximum and minimum temperatures observed in July and March, respectively. Winter daily air temperature is typically below 0°C, and varies widely, whereas water temperature stays within 5°C above melting point (0°C). During summer, water temperature fluctuates with precipitation events and is mostly greater than air temperature. (Fig. 5.1).

5.1.2 Water temperature trends by site

Daily water temperature is compared to air temperature for seventeen sites to understand thermal sensitivity of wetlands (Fig. 5.2) which correspond to phases of the solar cycle. Among sites, three sites that represent highest and lowest summer temperature are shown as red and blue lines, respectively. Geographical proximity primarily drives similar temperature trends where offsets at local peaks are observed (Fig. 5.2).

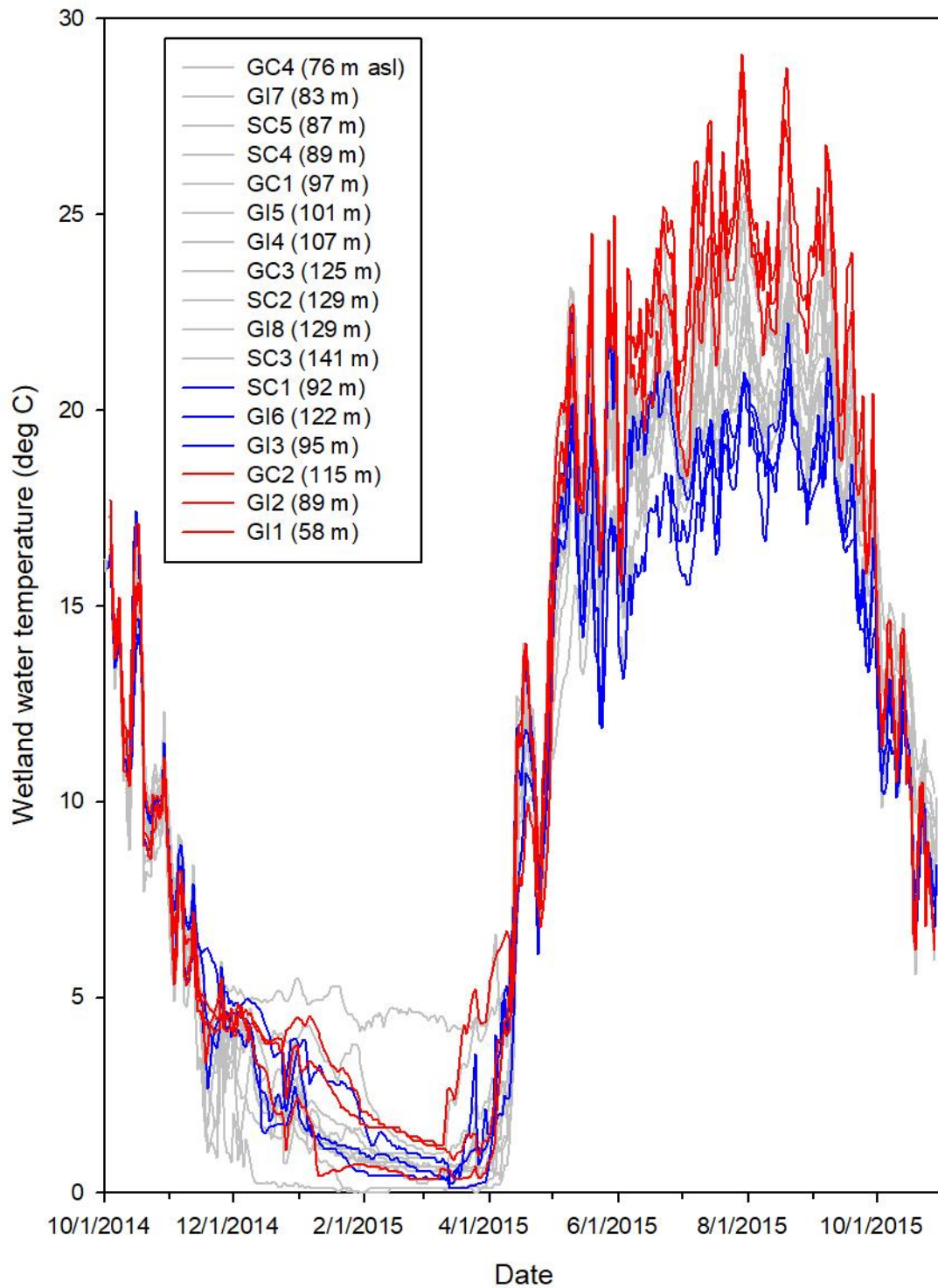


Fig. 5.2 Seasonal variation of wetland water temperature at seventeen sites. Three sites that represent highest (red lines) and lowest (blue lines) summer temperature are highlighted to show differences in summer response among sites.

The start of this study corresponds to the start of the water year, which is delayed by approximately one month from the start of the autumnal equinox, in September. From the Autumnal Equinox to late November, temperatures decline systematically among sites over the range 15°C to 5°C. A similar period of systematic increase in water temperature follows the Vernal Equinox in late March. The intervening winter (November to late May) and summer (late May to September), daily temperatures are typically less than 5°C and greater than 15°C, respectively (Fig. 5.2). Within the summer period water temperatures across sites generally maintain a consistent rank order and can vary by more than 5°C among sites (Fig. 5.2). Early winter water temperatures fluctuate with the cold rain and snow additions, then decline regularly during the period of ice cover. These changes are gradual due to the buffer presented by ice cover. Water temperature tends to gradually decrease from beginning of winter to early March and then sharply increase from late March. Summer temperatures are not ordinated by elevation (Fig. 5.2).

Wetland water temperature ranges across the sites differ by season (Fig. 5.1). The greatest discrepancy (greater than 5°C) is observed in summer months (June-September). Otherwise, wetlands maintain similar temperatures. Site water temperatures do not maintain the same rank orders across seasons. This is demonstrated in Fig. 5.2 with example summer temperature ranks sites at the three highest (red lines) and three lowest (blue lines) summer temperature sites.

5.1.3 Thermal sensitivity

Thermal sensitivity was calculated from air and water temperature pairs. Thermal

sensitivity values are distinguished by point clouds in summer while similar distributions were observed in other seasons (Fig. 5.3).

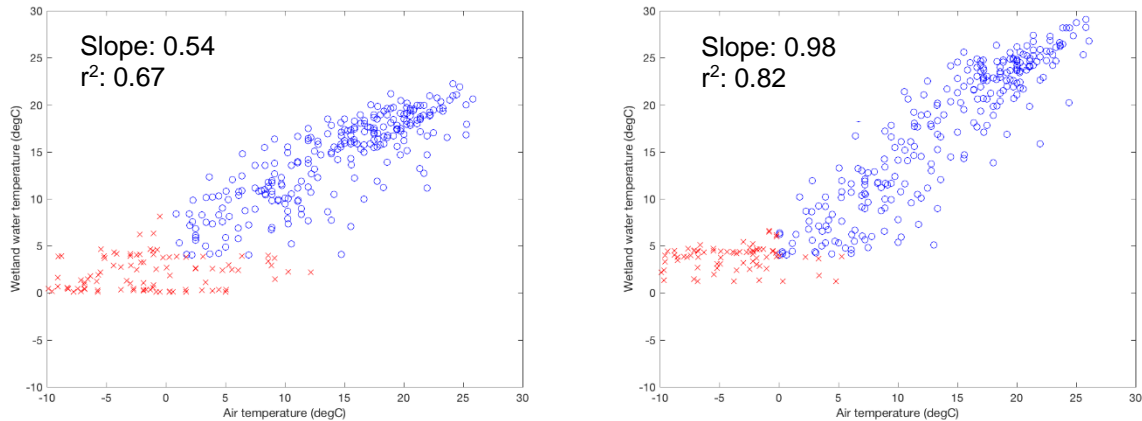


Fig. 5.3 Estimation of thermal sensitivity as a linear regression slope between air and water temperature at (a) SC1 and (b) GI1. Red crosses were excluded from the linear regression (see Section 3.3.2).

5.1.4 Hydrogeomorphic drivers of thermal sensitivity

Four hydrogeomorphic variables, including land surface elevation, accumulated duration of subsurface flow reversal, and standard deviation of groundwater and wetland stage, among summary statistics of hydrologic variables (Table 5.1) are found to be significantly correlated with thermal sensitivity (p-value range of 0.003-0.037) (Fig. 5.4). Coefficient correlation ranges 0.26-0.45 across relationships. The highest temperature sites (Fig. 5.2) show greater thermal sensitivity, while cooler sites have less sensitivity. Unlike temperature ranks in Fig. 5.1, thermal sensitivity decreases with increased elevation (Fig. 5.4a). Thermal sensitivity also shows a positive relationship with seasonal variation of wetland stage and groundwater level (Fig. 5.4c, d). Cumulative duration of subsurface flow reversal also affects thermal sensitivity (Fig. 5.4b).

Table 5.1 Summary statistics of hydrologic variables and thermal sensitivity

Site	Perimeter (km)	Elevation (m asl)	Flow reversal (d)	Mean groundwater level (m)	SDGW (m)	SDSW (m)	Sample number of hydrologic measurements	Thermal sensitivity	r ²
GI1	0.05	58	309	0.30	0.38	0.14	390	0.98	0.82
GI2	0.17	87	55	0.70	0.22	0.13	317	0.86	0.79
GI3	0.30	93	5	0.86	0.15	0.13	384	0.64	0.75
GI4	0.51	105	1	1.01	0.16	0.19	384	0.83	0.82
GI5	0.35	99	91	0.74	0.27	0.09	385	0.68	0.67
GI6	0.93	120	34	0.66	0.17	0.11	391	0.60	0.60
GI7	1.15	81	201	0.45	0.25	0.10	385	0.84	0.71
GI8	1.38	126	24	0.63	0.14	0.08	391	0.62	0.63
SC1	1.36	90	50	0.57	0.17	0.09	385	0.61	0.69
SC2	1.99	127	25	0.71	0.15	0.05	397	0.57	0.53
SC3	1.37	138	107	0.62	0.09	0.06	385	0.65	0.61
SC4	1.72	87	0	0.61	0.15	0.14	383	0.62	0.66
SC5	1.23	84	15	0.98	0.20	0.13	320	0.62	0.62
GC1	0.36	97	0	1.14	0.16	0.12	293	0.60	0.70
GC2	1.31	113	0	0.76	0.21	0.13	389	0.85	0.63
GC3	1.33	123	0	0.54	0.10	0.11	383	0.68	0.63
GC4	1.44	76	0	1.73	0.15	0.14	282	0.76	0.73

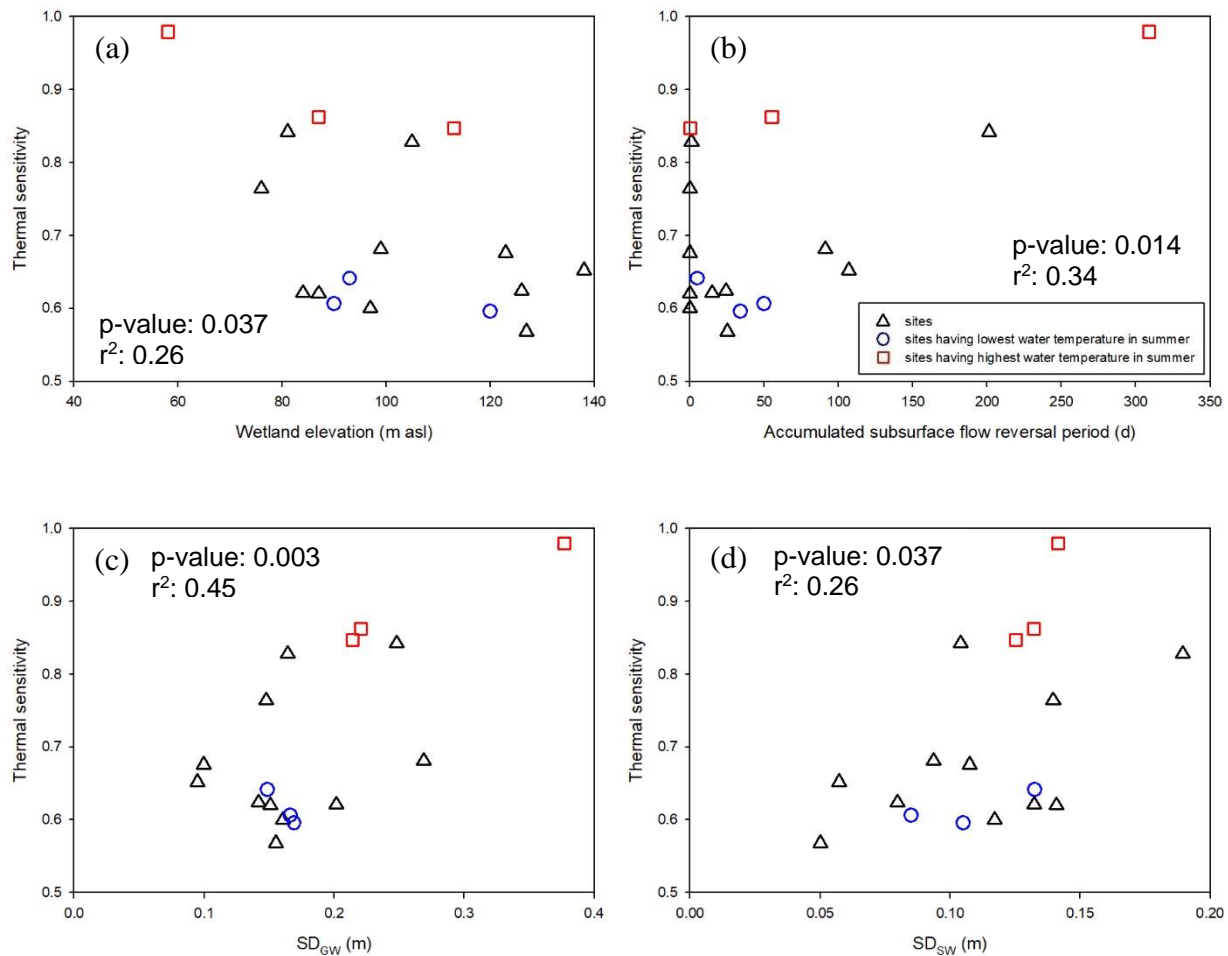


Fig. 5.4 Thermal sensitivity of the wetland sites by (a) elevation, (b) accumulated duration of subsurface flow reversal, (c) standard deviation of groundwater level, and (d) standard deviation of wetland stage

5.2 Discussion

5.2.1 Hydrologic drivers on a thermal regime

Subsurface flow reversal occurred due to different recession rates of wetland stage and the differences in this rate compared to groundwater table. Such flow reversal was commonly

observed from depressional geomorphic settings (Devito et al., 1997; McLaughlin et al., 2014; Winter, 1999). Typical wetland restoration practices often modify local geomorphic settings to impound surface water. This change in the relative contribution of surface water and groundwater to the pool, and the additional mass contained in the pool are expected to alter both site hydrology and thermal regime. The results show that under uniform climate conditions across sites, the thermal regimes of wetlands were similar, and primarily controlled by groundwater due to relatively low volume and velocity of standing water. Groundwater inflow regulated the thermal regimes by warming in winter and cooling in summer (Fig. 5.2). This was reflected in the significant correlation between thermal sensitivity and cumulative subsurface flow reversal period. During summer, evaporative and seepage losses from the pool resulted in greater thermal sensitivity (Fig. 5.4b).

5.2.2 Water temperature trends by site

Spatial temperature regime patterns among sites differed seasonally (Fig. 5.2). Relatively high variability with range of 15-30°C were observed during summer months. Seasonal groundwater influx and associated subsurface temperature regime controlled the thermal regime. Highlighted sites in Fig. 5.2 also represent maximized (blue) and minimized groundwater cooling during summer. Controls of water depth in wetlands were not clearly proven.

A few exceptions of thermal patterns were also applied. For example, stage records and water temperature at GI4 are affected by a spring. Specifically, a spring controlled water temperature to maintain relatively high (4-5°C) throughout the winter months and fairly moderated summer temperature at intermediate ranks during summer (Fig. 5.2). Sites showing relatively low winter temperature (close to 0°C) (i.e., GC3 and GC4) might be attributed to

minimized groundwater warming. This can be drawn that hydrogeomorphic classification can be utilized supplementarily to characterize the thermal regimes of wetlands but hydrologic understanding of the sites is required.

5.2.3 Factors affecting thermal sensitivity

Thermal sensitivity primarily represented how air temperature affects summer water temperature, since most winter water temperature data are excluded from the analysis and spring and fall water temperature does not differ among sites. Although the sample number was relatively small and correlation coefficient ($r^2=0.26-0.45$) was not high, thermal sensitivity showed general trend under same climate and geologic settings.

Elevation of wetlands in this study was negatively correlated with thermal sensitivity: Greater thermal sensitivity was found for lower sites (Fig. 5.4a). This is contrary to prevailing concepts of groundwater supply over elevation what greater groundwater exfiltration is expected at lower elevation. Site elevation did not affect the relative scale of temperature in summer and winter months. Sites having high or low summer temperature did not seem to be primarily driven by elevation in same climate and geologic settings (Fig. 5.2). If the elevation effect to groundwater discharge does not agree with previous findings, hydrologic drivers such as duration of subsurface flow reversal and seasonal variation of wetland stage and groundwater may act as a primary control. Nevertheless, ranks of summer temperature did not correspond to the thermal sensitivity ranks.

Subsurface flow reversal controlled thermal sensitivity as a primary driver. Subsurface flow reversal prevented groundwater cooling to wetlands during a dry period. For sites that experienced subsurface flow reversal within a study period, thermal sensitivity increased by

greater duration of subsurface flow reversal in general (Fig. 5.4b). For wetlands that experienced subsurface flow reversal, thermal sensitivity showed a positive correlation with its duration. Considering that subsurface flow reversal is promoted from different soil composition between wetlands and surrounding uplands during wetland restoration, alteration of geomorphic settings with soil replacement would affect thermal regime of wetlands, although not fully explored in this study. Most sites having very short duration of subsurface flow reversal (less than) were either natural wetlands or restored wetlands in riverine settings. Considering more than two months of temperature and stage data are missing at GI2 from mid-August, one could assume longer duration of subsurface flow reversal closer to the partly linear trend in Fig. 5.4b.

Degree of seasonal fluctuation of wetland stage and groundwater table is another driver on thermal sensitivity associated with duration of subsurface flow reversal. For sites that have intermediate or high summer temperature ranks, higher standard deviation of groundwater table increased thermal sensitivity (Fig. 5.4c). Standard deviation of wetland stage and groundwater table showed a complementary relationship.

5.3 Summary and conclusions

This study presented hydrologic controls on the thermal regime of wetlands. Hydrologic balancing between wetland stage and groundwater table associated with geomorphic settings resulted in characteristic subsurface flow behavior and different thermal responses. Site stage and temperature patterns were largely affected by hydrogeomorphic settings as well as regional climate and geology. Hydrogeomorphic settings are supplemental yet essential resources to characterize site hydrology and thermal functions of wetlands. Wetland restoration practices

need to carefully choose proper hydrogeomorphic settings to promote temperature-sensitive species and biogeochemical purposes.

Subsurface flow reversal was mostly found in late summer due to groundwater depletion. Differences in wetland site temperature during summer was related to subsurface inflow and outflow. Accordingly, thermal sensitivity was primarily determined by summer temperature regime. A range of thermal sensitivity was significantly caused by geographical and hydrologic variables such as site elevation, duration of subsurface flow reversal, and standard deviation of wetland stage and groundwater table. Since main drivers differ by large-scale factors such as climate and geology, additional studies are imperative.

This study may be the first attempt to characterize thermal regime and sensitivity over wetlands. Investigation of such behavior and its controls would contribute to successful wetland restoration.

Chapter 6. Patch scale evapotranspiration of wetland plant species by ground-based infrared thermometry

In this chapter, thermal infrared- (TIR-) based evapotranspiration (ET) estimates are compared to Priestley-Taylor (P-T) method (Section 6.1.1-6.1.2 and 6.2.2). Impacts of atmospheric conditions and landscape context on the TIR-based methods were discussed to determine local controls (Section 6.2.1). Crop coefficients were then estimated for regional use (Section 6.1.3 and 6.2.3).

6.1 Results

The TIR-based estimates of selected plant communities are displayed over course of a day in series to identify how ET varies over the second half of the growing season. The model structure and for the methods presented in Chapter 3.3.3 and 3.3.4 are then compared with a model of potential ET to find structural differences and dependencies of input variables. Model dependencies result in variance from expected behavior during periods when atmospheric conditions violate the validity of encoded model assumptions and assumptions of uniform geomorphology and land cover. To better understand how landscape context affects ET by controlling transport of air parcels, sites are categorized into open (Wetland 1 and 4) and sheltered (Wetland 2 and 3) for analysis.

6.1.1 Seasonal variation of atmosphere and radiation components

Diurnal and seasonal trends of T_s follow those of T_a (Fig. 6.1). From the diurnal curves, T_a is 0-2 hr lagged from T_s curves. For example, daily peak T_s is observed at 14:00 measurement

where daily peak T_a is observed either from 14:00 or 16:00 measurement. This temporal lag is more obvious at Wetland 2 and 3 where the wetland sites are sheltered by surrounding forest (Fig. 6.1b-c).

T_s is greater than T_a for most of the measurement pairs. Exceptions are typically found from the 18:00 measurement by shades from the surrounding forest near sunset (Fig. 6.1a-c) and lower solar azimuth from mid-September (Fig. 6.1d). Partial cloud cover also results in decreased T_s which is even occasionally less than T_a (e.g., 16:00 on 8/1/15 in Fig. 6.1a, 14:00 on 9/4/15 in Fig. 6.1d).

T_s pairs of two species at a same site do not show any consistent relationships (Fig. 6.1a-b). T_s of meadow willow is higher than reed canary grass for most measurements at Wetland 2 (Fig. 6.1b). T_s of cattail is higher than hardstem bulrush for mid-day measurements (10:00-14:00) at Wetland 1 (Fig. 6.1a).

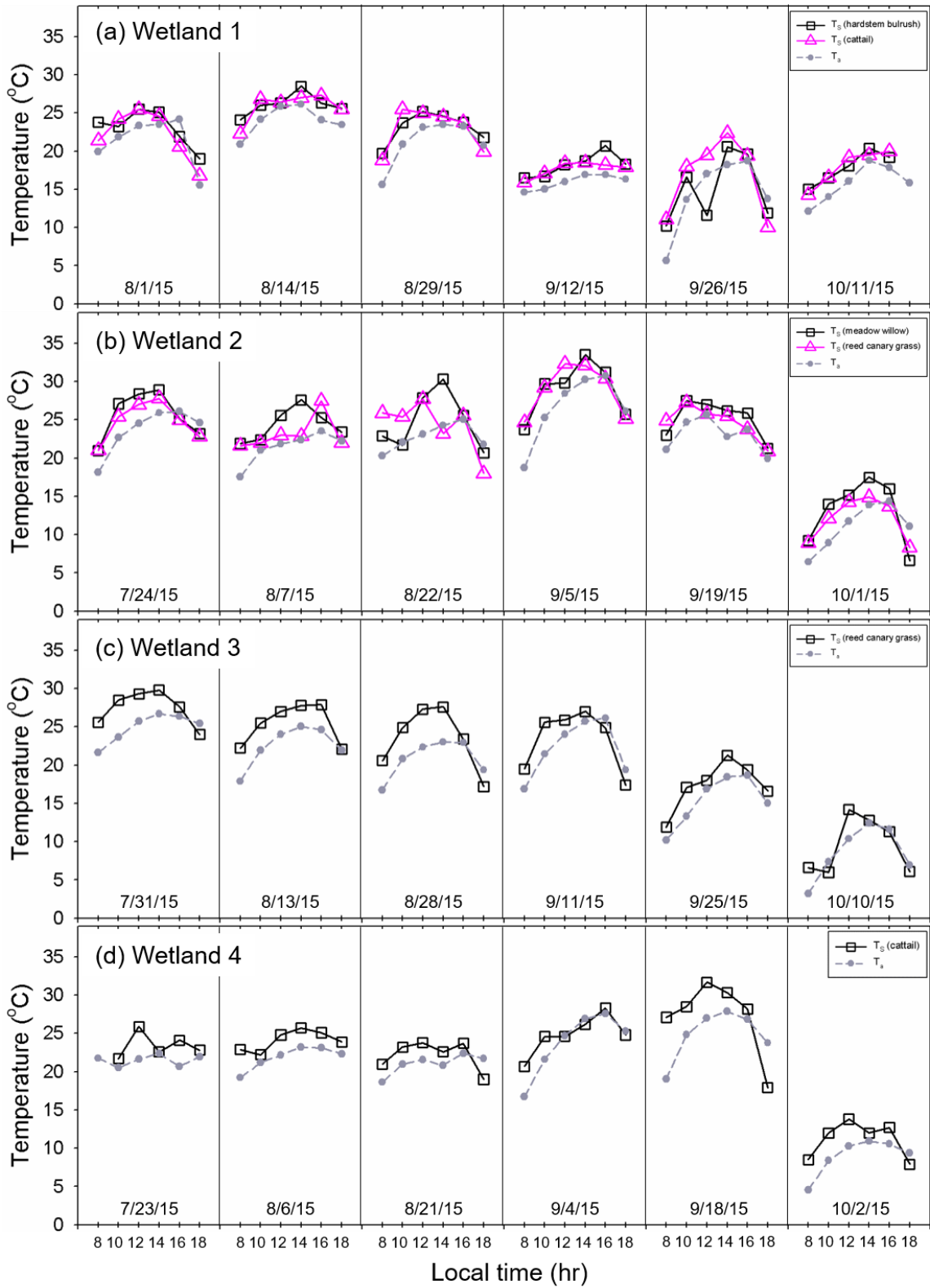


Fig. 6.1 T_a and T_s measurements. T_a and T_s represent hourly average and instantaneous value within an hour frame, respectively. Note that the measurement data were acquired on different days by site.

Vapor pressure deficit (VPD), defined as $e_s - e_a$, and u are characterized largely by surrounding landscape type. Where a wetland is sheltered with surrounding forest (e.g., Wetland 2 and 3), relatively high VPD (0.6-1.6 kPa) and low u (0-2 m s⁻¹) are observed from most measurements (Fig. 6.2b-c). For open landscape (e.g., Wetland 1 and 4), lower VPD (0.4-1.0 kPa) and higher u (2-6 m s⁻¹) than the sheltered wetlands are found for most days (Fig. 6.2a, d).

Diurnal patterns of VPD are similar to those of T_a (Fig. 6.1, 6.2). A daily peak is found from mid-day measurements. VPD on 9/12/15 at Wetland 1 (Fig. 6.2a) is consistently close to 0 due to a rainfall event.

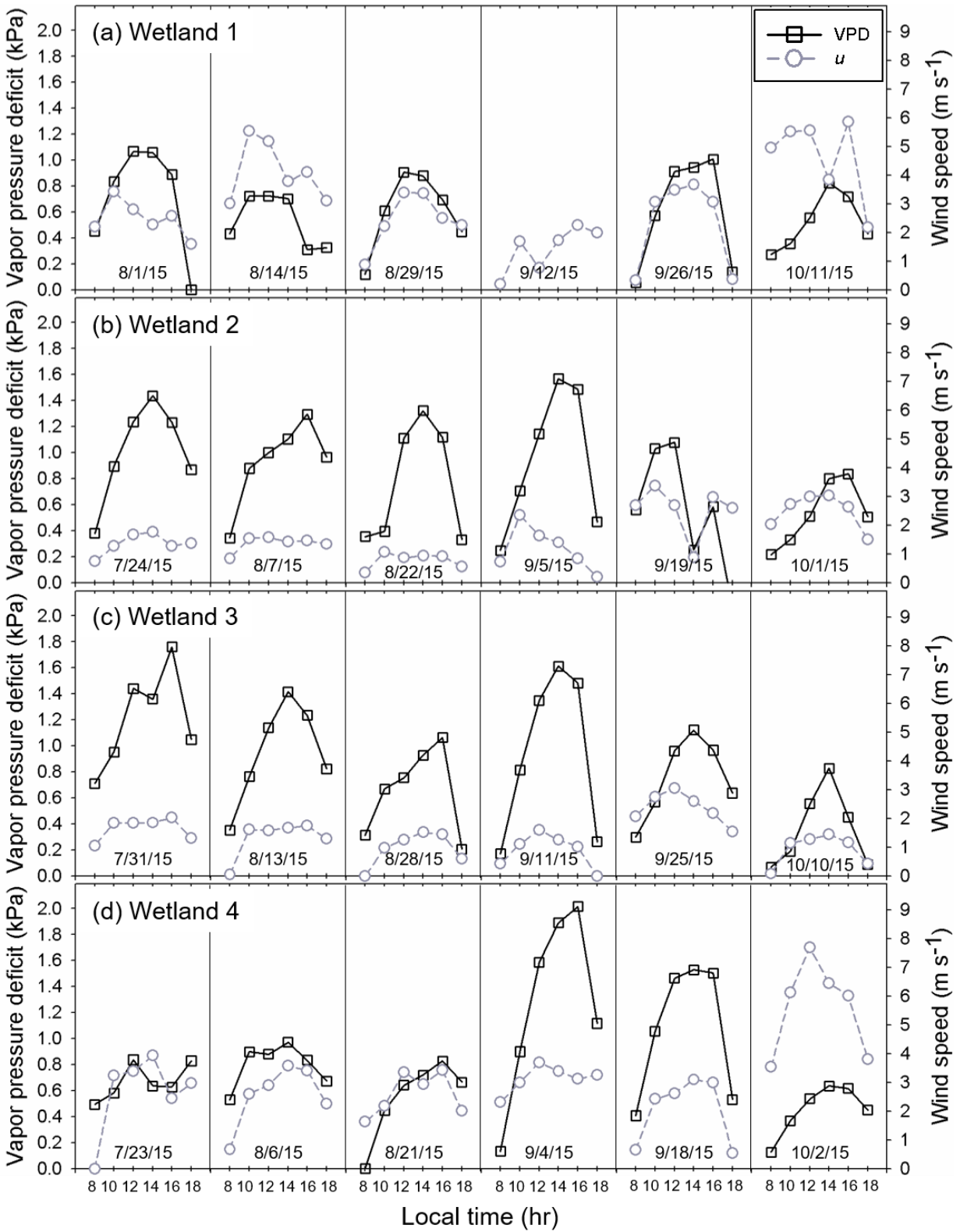


Fig. 6.2 Hourly average VPD and u measurements. Note that VPD on 9/12/15 at Wetland 1 is zero throughout a day due to a rainfall event. VPD at 18:00 on 9/19/15 at Wetland 2 is zero due to a shower.

H estimates by three methods are displayed in Fig. 5. SEB- and β -based *H* ranges are 0-200 W m⁻² while P-T yields a smaller range of 0-100 W m⁻² (Fig. 6.3). SEB estimated much greater *H* than the other methods for October at open landscape (Fig. 6.3a, b, f) when relatively greater *u* was imposed with a range of 2-6 m s⁻¹ at Wetland 1 (Fig. 6.2a) and 3-8 m s⁻¹ at Wetland 4 (Fig. 6.2d).

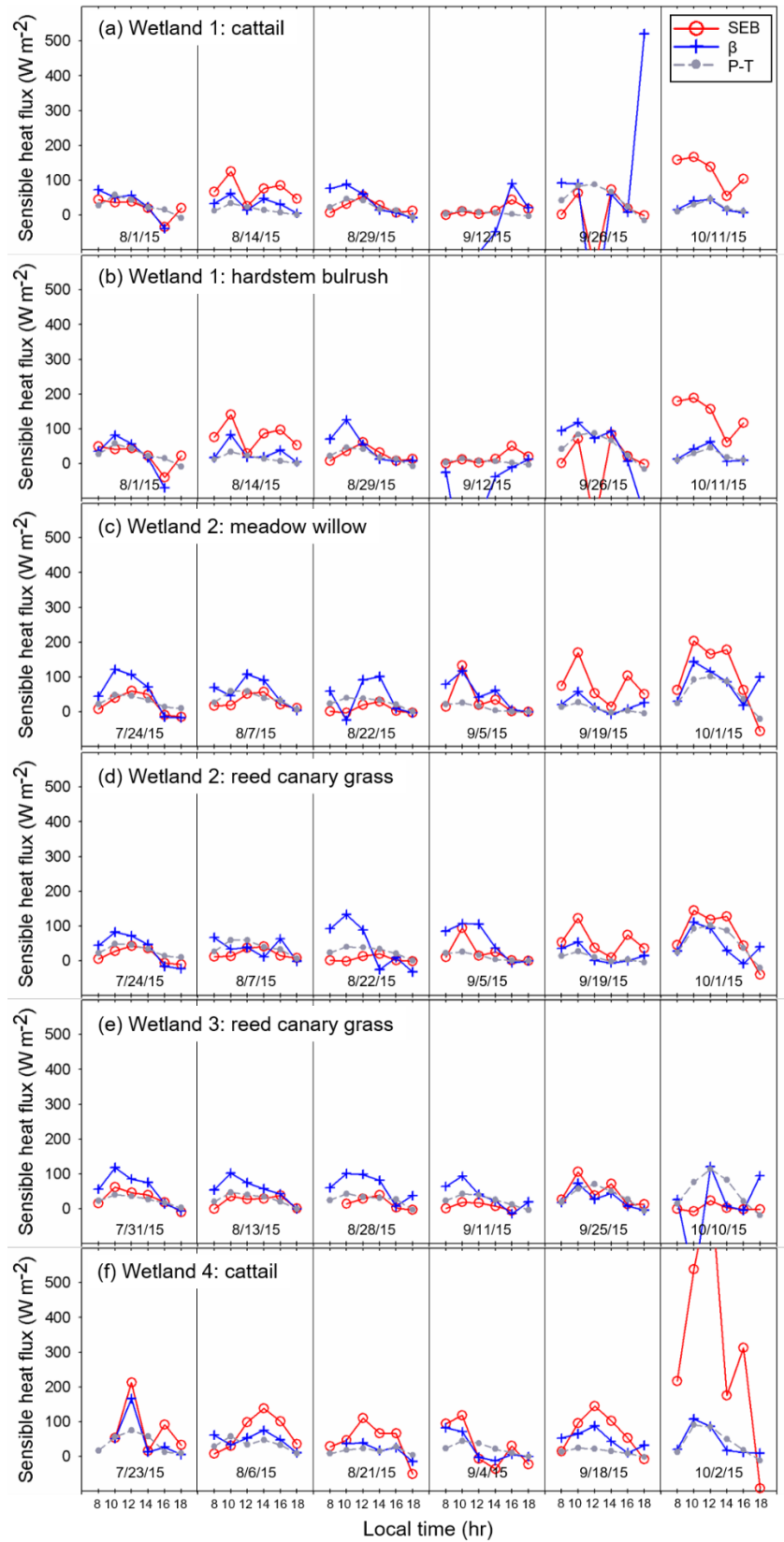


Fig. 6.3 Estimated H from SEB (a red circle), β (a blue cross), and P-T (a gray dot) at six vegetation communities

Like the atmospheric measurements in Fig. 6.1 and 6.2, Diurnal and seasonal trends of the TIR-based ET estimates show similarity in geography and by plant species, yet weather conditions including cloud cover and rainfall events introduce variance from these trends in the daily data. For each study site, the compiled trends in instantaneous ET ($\lambda E(t)$) estimates for clear-sky days approximate expected daily trends in R_n (-100 – 950 W m^{-2}) (Fig. 6.4). Local distortions in the expected daily pattern of $\lambda E(t)$ correspond to periods of partial cloudiness and rain, which diminish R_n . The effect of mid-day rain showers on August 21 and 22 clearly reduces mid-day λE at Wetlands 2 and 4 (Fig. 6.4c, d, f). Additionally, the scale of the $\lambda E(t)$ curve often decreases over the season. However, a smooth seasonal decline in $\lambda E(t)$ is not generalizable, as shown by the values reported for September 4 to 12 during a period of warm clear weather. In addition, Wetlands 1-3 were partly or mostly shaded by the surrounding forest at 18:00 for the last two observation dates due to the low solar azimuth. Further decreases in values of daily $\lambda E(t)$ during late September and October are a response to both declining R_n and plant senescence. ET ranges of the various plant species across sites depended primarily on local weather conditions. For example, in similar geographic settings, ET ranges and seasonal patterns for reed canary grass were similar as shown by Wetland 2 and 3 on all days except late August (Fig. 6.4d-e). However, seasonal behavior of ET varied between sites with similar cover but different site characteristics such as Wetland 1 and 4 on all days (Fig. 6.4a, b, f).

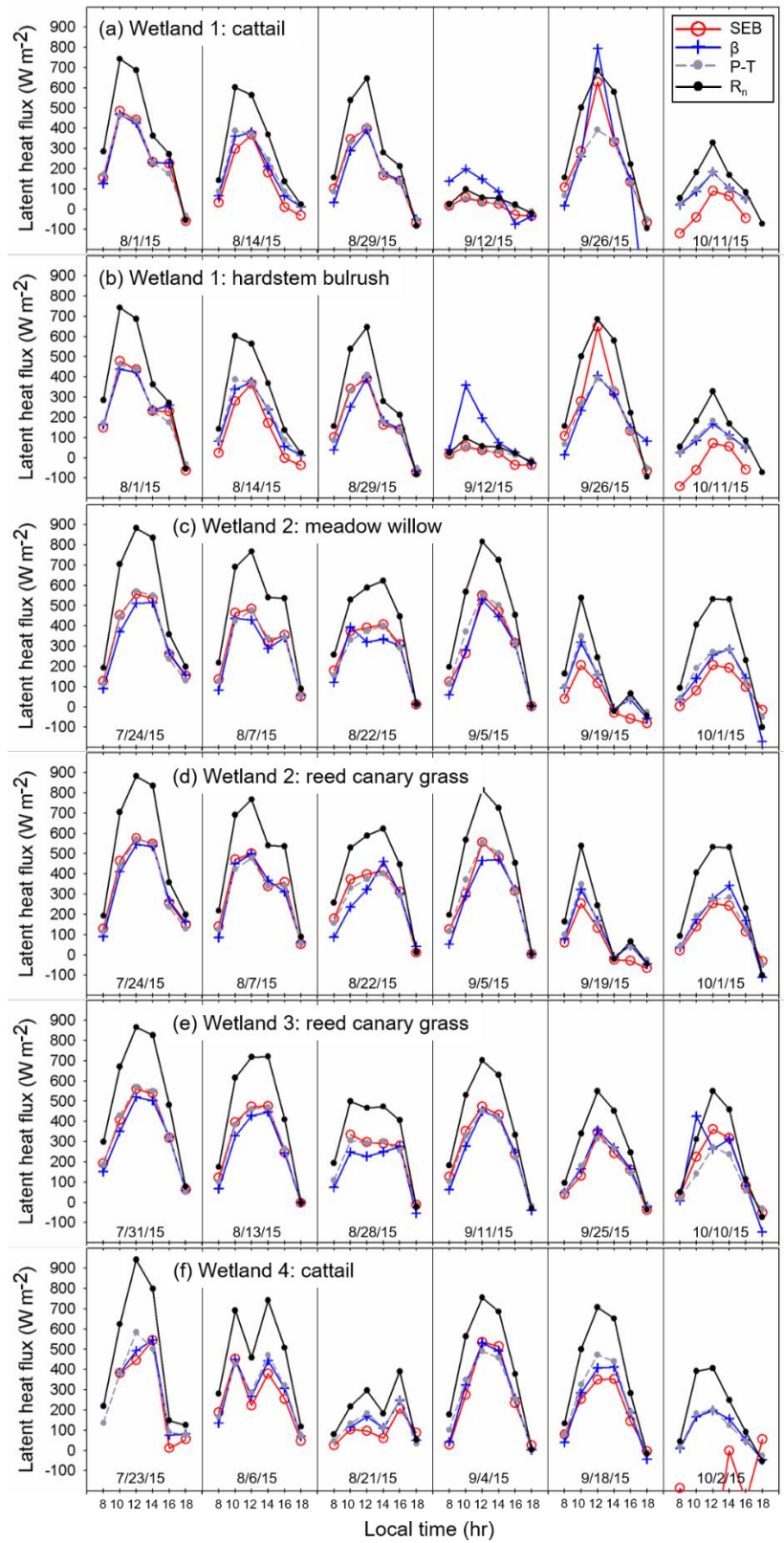


Fig. 6.4 ET estimations from SEB (a red circle), β (a blue cross), and P-T (a gray dot) at six vegetation communities

Sites in open landscapes (Fig. 6.4a, b, f) show less regular daily trends in λE than the sheltered sites (Fig. 6.4c-e). Slight differences in the amplitude of the daily trends in β and SEB between the open landscape and sheltered sites was found. This is attributed to the difference in wind speed (u) between the sites. For the open sites (Wetland 1 and 4) u varied up to 6 m s^{-1} and 8 m s^{-1} , respectively, whereas u at the sheltered sites ranged up to 3.5 m s^{-1} , with typical u below 2 m s^{-1} . The highest wind speeds were observed in October. Whereas the SEB estimates showed similar temporal fluctuation as β , they tended to have lower values late in the growing season and show greater sensitivity to temporary cloudiness. Additionally, the data acquisition rate for the October measurements was constrained by very low air temperatures and observed plant senescence. The last measurement of a day (18:00) usually yields negative R_n near sunset (Fig. 6.4). This is resulted in negative H and λE .

6.1.2 Comparison of TIR-based and P-T methods

Calculations of ET from two TIR-based methods were compared with results from P-T, a traditional weather station-based method, to identify differences in calculated ET in response to different input sources and model derivation structures. The TIR-based methods show good agreement with P-T for all plant species (Fig. 6.5). The coefficient of determination (r^2) ranges 0.83-0.97 for SEB and 0.94-0.98 for β (Table 6.1). Similarly, the regression slope varies 0.94-1.12 for SEB and 0.92-1.01 for β .

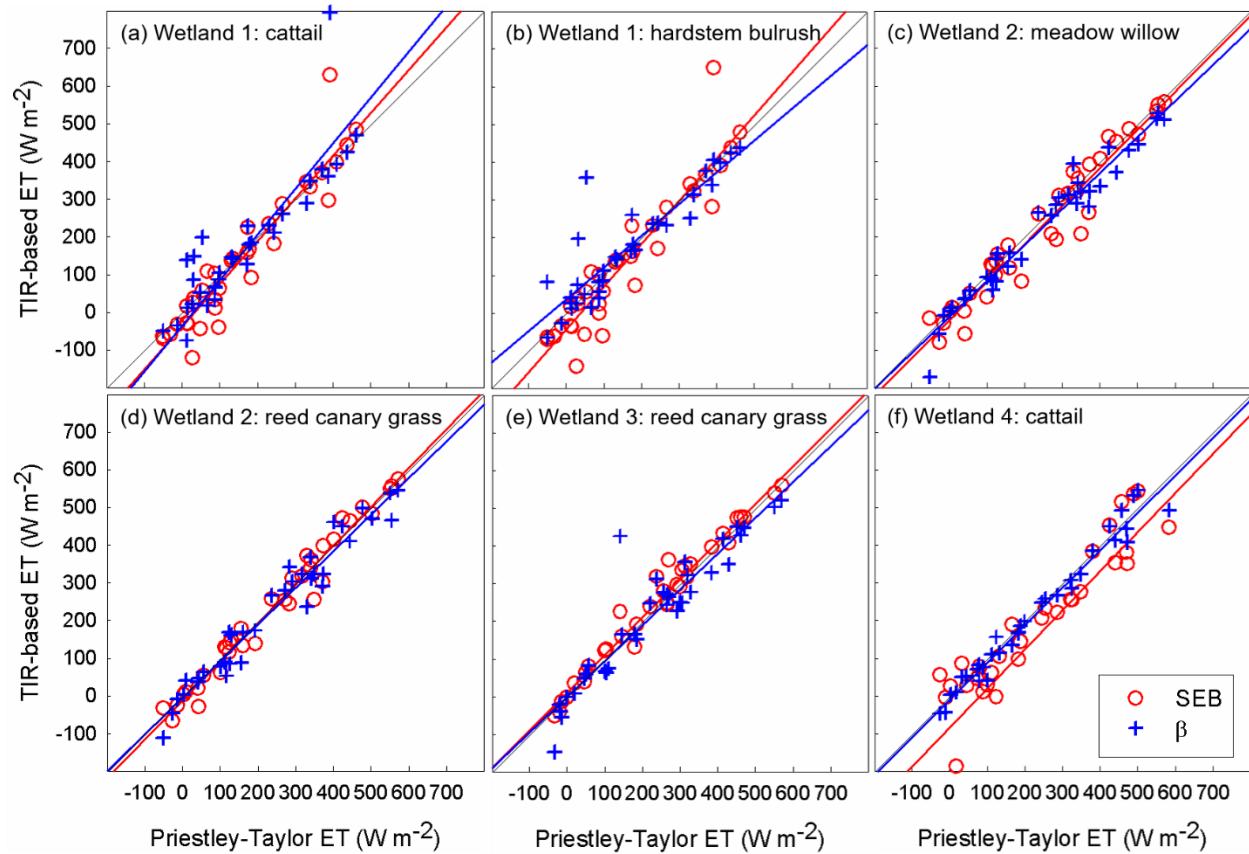


Fig. 6.5 Comparison of the TIR-based methods and P-T at selected vegetation communities. Note that measurement data during rainfall events are excluded.

Table 6.1 Estimation statistics of the TIR-based methods compared to P-T. SEB is the thermal infrared temperature-based surface energy balance method, β is the thermal infrared temperature-based Bowen ratio method, r^2 is the coefficient of determination calculated from a linear regression with P-T, MAD is the mean absolute difference with P-T, and RMSD is root mean squared difference with P-T.

Site	Species	Average canopy height (m)	r^2		Regression slope		MAD ($W m^{-2}$)		RMSD ($W m^{-2}$)	
			SEB	β	SEB	β	SEB	β	SEB	β
Wetland 1	Cattail	2.5	0.83	0.97	1.12	0.97	31.1	19.6	43.8	27.5
	Hardstem bulrush	0.5	0.86	0.98	1.12	1.01	28.1	17.1	38.4	23.4
Wetland 2	Meadow willow	4.0	0.93	0.96	1.02	0.92	34.3	30.8	50.0	39.7
	Reed canary grass	1.2	0.97	0.94	1.03	0.96	23.9	33.2	32.6	41.6
Wetland 3	Reed canary grass	0.9	0.96	0.95	0.96	0.92	24.0	31.4	32.8	38.3
Wetland 4	Cattail	2.5	0.91	0.97	0.94	0.98	53.0	23.2	62.4	31.3

Although canopy height of the plant communities where TIR was measured differed by species and site (Table 6.1), the results from β and P-T were very similar across sites (coefficient of determination (r^2) = 0.94-0.98, mean absolute difference (MAD) = 17.1-33.2 $W m^{-2}$, and root mean squared difference (RMSD) = 23.4-41.6 $W m^{-2}$) (Table 6.1). β varied from 0 to 0.4 for all species and sites, with greater values early (8 am) and late (6 pm) in the day.

SEB showed a slightly greater difference range of 23.9-53.0 $W m^{-2}$ (MAD) and 32.6-62.4 $W m^{-2}$ (RMSD). MAD was greater for SEB than β for all vegetation types except reed canary grass (Table 6.1). The predominantly lower values for SEB than β , relative to P-T, at wetland 4 (Fig. 6.5f) are likely related to interactions between cattail plant structure and u on r_a . Tall emergent species such as cattail (~ 2.5 m) are easily bent by prevailing wind, which may decrease r_a , hence result in greater H .

To better explore the different behavior between TIR-based methods, their sensitivity to changes in u and relative humidity (RH) was assessed. Among six vegetation communities showing similar patterns, differences between the TIR-based and P-T methods are plotted by u over meadow willow at Wetland 2 and RH over hardstem bulrush at Wetland 1 in Fig. 6.6. The

results show little difference in calculated ET between SEB and P-T for u less than 2 m s^{-1} , but distinct differences between the methods for u greater than 2 m s^{-1} . For high u over the course of a day, SEB tended to estimate greater H by decreased r_a , which would finally result in less λE than the other methods. The β method was not systematically influenced by u at any site.

Humidity affected ET estimation slightly, as shown by a comparison between β and P-T (Fig. 6.6). Although increasing RH reduces difference for SEB and slightly increased difference for β , trends are not clear. β , particularly in the proposed method, is essentially determined by vapor pressure deficit (VPD), the difference of saturation and actual vapor pressure from the vertical vapor pressure gradient used to partition available energy into H and λE . Higher RH under potential conditions induces lower VPD or evaporation potential, and thus lower ET. The best agreement between the TIR and P-T models was found at a RH range of 55-70%.

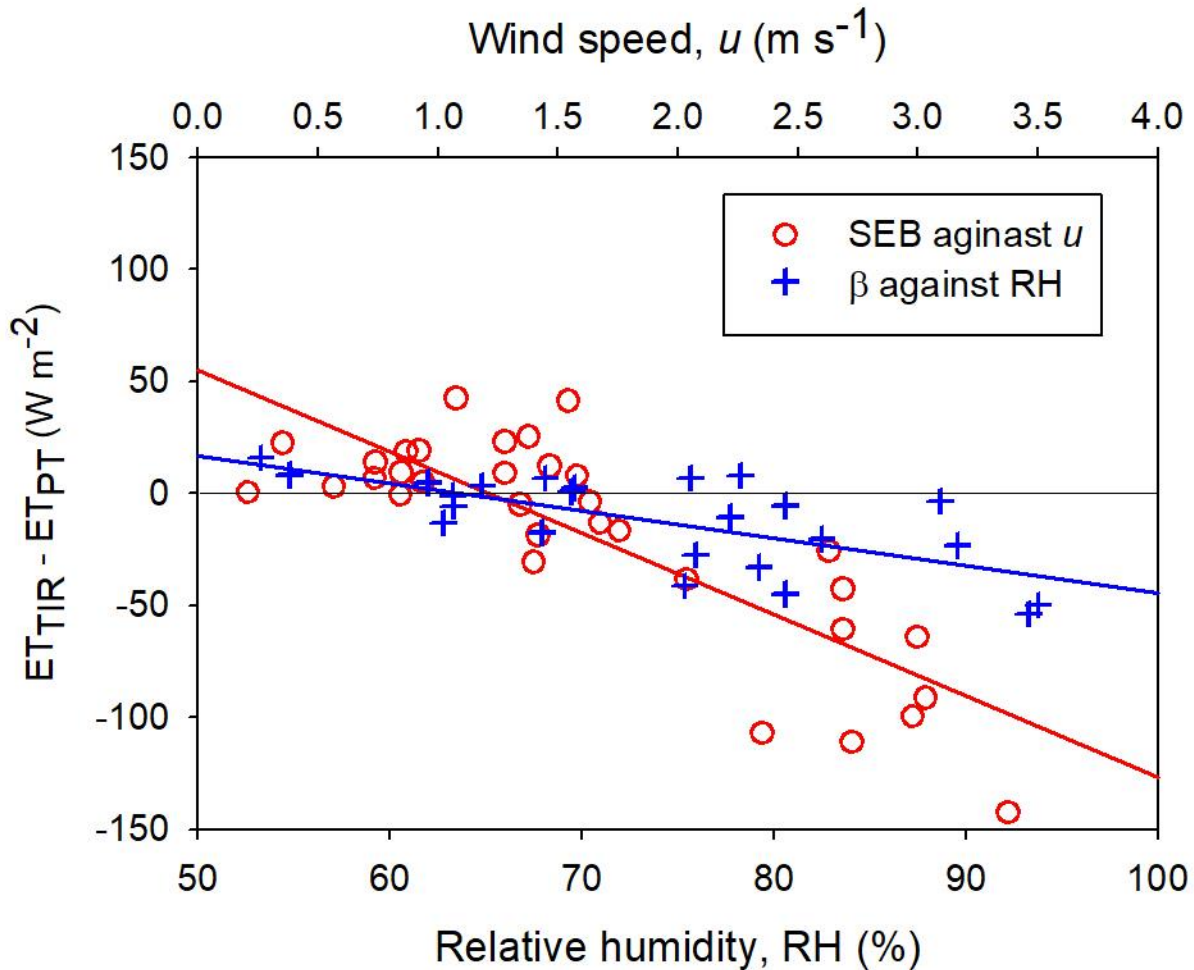


Fig. 6.6 ET difference between the TIR-based methods and P-T by input variables. A red empty circle shows a difference between SEB and P-T plotted against u over meadow willow at Wetland 2. A blue cross shows a difference between β and P-T plotted against RH over hardstem bulrush at Wetland 1.

6.1.3 Estimated crop coefficients of wetland species

K_c ranges are similar within plant species and across sites but differed between the two TIR-based methods (Table 6.2). β -based K_c ranges were 0.85-1.23 for cattail, 0.96-1.19 for meadow willow, 0.98-1.32 for reed canary grass, and 0.84-1.26 for hardstem bulrush. SEB-based K_c generally ranged larger than β -based K_c for all sites and species. Relatively great differences were found for ranges of K_c between SEB and β methods, both within a site, e.g., Wetland 1, and across sites, e.g., cattail.

Table 6.2 Estimated daily crop coefficient (K_c) ranges by two TIR-based methods over wetland vegetation communities

Site	Species	Landscape context	K_c range		Suggested K_c values in other studies
			SEB	β	
Wetland 1	Cattail	Open	0.73-1.43	0.85-1.23	0.3-1.6 (Allen, 1995), 0.76-0.87 (Mao et al., 2002), 2.5-4.2 (Towler, 2004), 2.5 (Beebe et al., 2014)
	Hardstem bulrush	Open	0.81-1.45	0.84-1.26	0.3-1.8 (Allen, 1995), 2.1-3.5 (Towler, 2004)
Wetland 2	Meadow willow	Sheltered	0.65-1.33	0.96-1.19	-
	Reed canary grass	Sheltered	0.82-1.33	0.98-1.32	1.24-1.46 (Mueller et al., 2005)
Wetland 3	Reed canary grass	Sheltered	1.07-1.85	1.05-1.23	Suggested above
Wetland 4	Cattail	Open	0.91-1.10	0.97-1.21	Suggested above

6.2 Discussion

This study aimed to estimate ET over species-level patches of wetland plant cover in a small set of natural and constructed wetlands by a novel approach. To evaluate the approach and understand differences between the TIR-based and traditional meteorological approaches, the influence of model structure and inputs on the estimation of ET was investigated.

6.2.1 Impact of structures and input variables

The differences in structure of the base equations affect model performance in various ways. Therefore, a comparison of differences between the methods may be useful to understand sensitivity of the key variables in the different methods. Although P-T has been found to be reliable for potential ET conditions including wetland environments (Lenters et al., 2011; Mao et al., 2002; Rosenberry et al., 2004), two TIR-based actual ET estimation sets behaved differently due to differences in the model input variables (Fig. 6.6). P-T uses similar atmospheric input variables as two TIR-based methods, but variables such as RH and u are parameterized and not included as functions in the equation. Whereas basic atmospheric variables such as air and

vegetation skin temperature, R_n , u , and RH are required for the P-T and TIR-based methods, the model dependencies on input variables differ: SEB does not require RH , β does not require u , and P-T does not require RH and u .

Unlike other meteorological methods based on physical and empirical estimation of the diffusive vapor flux (i.e., P-T) and physical partitioning of turbulent heat fluxes from the vertical gradient within the atmosphere (i.e., β), r_a inversely contributes to H and then negatively to λE by subtracted from the available energy. On the other hand, difference statistics of the woody meadow willow at Wetland 2 are similar to an intermediate emergent species such as reed canary grass at the same site despite high canopy height (Table 6.1). Shrub species are often resistant to prevailing wind, which results in minimal impact of r_a on H and λE estimations. Similar to other methods using such atmospheric parameters (e.g., Penman-Monteith), SEB depends on proper parameterization of r_a .

Compared to the ratio-based methods, i.e., β and P-T, SEB is more capable of capturing a wind effect for estimating H under low R_n conditions by the physical derivation and a complementary relationship between H and λE from Eq. (2). Despite depending on parameterization of r_a , often referred to as a source of uncertainty, SEB has a great potential to complement existing energy balance models based on high-resolution TIR imagery and readily available atmospheric measurements.

For greater u , which mechanism gets enhanced between transportation of heat and vapor? It was unexpected that u had a negative impact on λE (Fig. 6.6). This was found primarily from SEB whereas β and P-T did not use u . When greater u was imposed, diminished r_a would result in greater H from Eq. (3) and therefore less λE from Eq. (2). Another systematic difference between SEB and β is that the turbulent heat fluxes, H and λE , are partitioned in either

complementary (SEB) or proportional (β) basis. Comparing the data on selected days showing similar VPD and u ranges, relatively small R_n (8/14/15 and 10/11/15 in Fig. 6.4a-b) would cause greater difference in λE with the other models. For sheltered sites (i.e., Wetland 2 and 3), relatively slow supply of an air parcel with a u range of 0-2 m s⁻¹ resulted in greater agreement with the other methods (Fig. 6.4c-e). A prior study indicated that such negative relationship between u and T_a was pointed out to have a counterbalancing effect on reference ET (Liuzzo *et al.*, 2016). In this study, u greater than 2 m s⁻¹ appeared to suppress λE when compared to P-T (Fig. 6.6). Elucidation of a role of u on enhancing heat transfer and/or vaporization needs an attention for reliable energy partitioning.

Sensitivity of u to λE was observed by comparing the SEB estimations at Wetland 4 on 8/21/15 and 10/2/15 (Fig. 6.4f). On these days, diurnal ranges of R_n and VPD were similar where u ranges differ by 1.6-3.4 and 3.5-7.7 m s⁻¹ on 8/21/15 and 10/2/15, respectively (Fig. 6.2d, Fig. 6.4f). All SEB estimates on 10/2/15 showed very low fluxes, including negative values over a day. On both days, however, λE from the other methods resembled each other. VPD marginally affected λE when comparing β and P-T (Fig. 6.6).

Both the proposed methods and P-T require only a limited set of input variables under basic assumptions of atmospheric conditions. The results of this study demonstrate two important points in this regard (Fig. 6.6): (1) When u is greater under diabatic conditions local advection may decrease r_a and hence λE , and (2) the combination of flexible, tall emergent vegetation species with persistent wind is likely to structurally decrease r_a . If this change in r_a is not considered and a static vegetation canopy height is assumed for parameterization, u is shown to be an important variable that differentially affects heat flux estimates by SEB. RH is also found to have a slight impact on energy partitioning in the β method.

6.2.2 Comparison of the TIR-based methods and P-T

The TIR-based methods generally show good agreement (r^2 range of 0.83-0.98 except cattail) with the P-T method for various sites and plant architectures. The ability of the proposed TIR-based methods for direct observation of evapotranspiration from homogeneous and mixed cover surfaces was further considered. Homogeneity of plant distribution should be also considered when compared to an area-based method, like most meteorological methods. Whereas Wetland 3 and 4 have practically uniform vegetative cover by either reed canary grass or cattail, respectively, P-T should successfully reproduce areal ET for these species. However at wetlands 1 and 2, multiple species coexisted as patches (at Wetland 1) or comingled cover (at Wetland 2). In either case P-T would require the heterogeneous cover to be represented as a lumped value, with an intrinsic bias (Fig. 6.5).

Reliability of P-T over wetlands has been tested and discussed in other studies. Wetland ET is generally equated to the potential rate, but the validity of this assumption is challenged by regional and seasonal differences in moisture availability (Mohamed *et al.*, 2012). Nevertheless, the vegetation communities in this study region are generally not water limited, supporting the assumption of equivalence between actual and potential ET. Previous studies found good agreement between P-T calculations and measurements for moisture sufficient conditions (Mao *et al.*, 2002; Rosenberry *et al.*, 2004; Lenters *et al.*, 2011) whereas α was reported as overparameterized in some areas with various moisture conditions (Souch *et al.*, 1996; Bidlake, 2000; Jacobs *et al.*, 2002; Masoner and Stannard, 2010). The output from this method was proven to depend on seasonal and regional changes in land surface (e.g., canopy resistance) and atmosphere (e.g., aerodynamic resistance, advection and humidity) characteristics (Bidlake,

2000; Drexler *et al.*, 2004). Therefore, as the study sites are moisture-sufficient and energy-limited, a comparison with PET provides a good sense for evaluating how actual ET at the vegetation communities behaves over various atmospheric conditions.

P-T partitions λE and H as both always less than the available energy (i.e., $R_n - G$). P-T showed incapability of capturing some extreme cases including advection often defined as $T_s < T_a$ (Tolk *et al.*, 1995). As contemporary energy balance models use P-T for determining the wet surface ET (Fisher *et al.*, 2008; Agam *et al.*, 2010; Yao *et al.*, 2015), cases presented in this study would help better inform for reliable energy partitioning under various atmosphere and land surface conditions.

Comparing T_s of two dominant species, less T_s was found from hardstem bulrush than cattail at Wetland 1 (Fig. 6.1a). This may be due to the resolution of TIR images in part. Hardstem bulrush has relatively low leaf area (maximum leaf area index of 0.81 reported from Williams *et al.*, 2017) than cattail (1.79 from Williams *et al.*, 2017). Considering that the hardstem bulrush community stood on the inundated sediment during a full growing season, relatively low T_s from open water surface might be also resolved into the TIR image. A similar relationship was also found from the meadow willow (maximum LAI for willow shrubs of 4.70 from Brom and Pokorny, 2009) and reed canary grass (2.40 from Williams *et al.*, 2017) at Wetland 2 (Fig. 6.1b). There was less chance for other objects than the leaf surface resolved into TIR image pixels for high LAI species, i.e., meadow willow. Therefore, design of the TIR resolution should be carefully determined for given specification of the measuring instrument and for vegetation species of interest.

Different measurement type may also bring ranging discrepancy between the methods (Allen *et al.*, 1989; Hupet and Vanclooster, 2001). The TIR-based and P-T methods represent

different time scales. The TIR-based methods are based on the instantaneous T_s measurement of the canopy surface. On the other hand, all the other atmosphere and radiation data are hourly averages of multiple instantaneous measurements. When the meteorological variables drastically varied in an hourly lens due to a partial cloud cover and shower (e.g., measurements on 9/19/15 in Fig. 6c-d and on 7/23/15 in Fig. 6.4f), for example, less agreement with P-T was found. If a TIR image was acquired under a shade from temporary cloud, T_s would be lower than its hourly average and even than an hourly average of T_a . As well as the atmospheric observation, frequency of the TIR sensing should be properly designed for better estimation.

6.2.3 Application of the crop coefficient method based on the TIR-based estimates

The use of the crop coefficient method assumes decreasing ET over the period of plant senescence. Measurements for the wetlands in this study demonstrate a general, but inconsistent, decline in λE for most sites from July through October (Fig. 6.4). For this period, decreasing K_c is also anticipated, but trends are similarly inconsistent. Although the study period is classified as a dry period of year and water year 2015 was dry in the study region, actual ET was maintained at near the potential rate by sufficient moisture supply from local water storage (Fig. 6.5). This energy limited regime resulted in K_c values for each species that are high in the ranges reported by previous studies (Table 6.2).

The ranges of K_c values from the two TIR-based methods overlapped value ranges from prior studies (Table 6.2) reasonably well considering that boundary conditions such as climate and local moisture availability varied by studies. Interestingly, the ranges of K_c estimated from this study were smaller than those from prior studies (Table 6.2). The narrow range in K_c may result from the persistent moisture supply from shallow groundwater over the growing season,

and associated low incidence of very dry conditions. As a result, solar insolation and atmospheric conditions are the second order controls on ET. For wetland sites, moisture availability is a primary driver in energy partitioning. Therefore, local moisture conditions should be taken into account especially for areas not subject to inundation or subirrigation. Prior studies revealed importance of seasonal moisture availability (Jacobs et al., 2002) rather than type of wetland (Lott and Hunt, 2001) and seasonal inundation status (Souch et al., 1998; Thompson et al., 1999). This study did not measure ET during early plant growth stages.

Suggested K_c values and ranges are subject to bias from the estimation approach and should be considered carefully. Whereas daily K_c was determined as a regression slope of instantaneous actual ET versus the FAO Penman-Monteith reference ET, values representing monthly (Fermor et al., 2001; Mao et al., 2002) and seasonal (Beebe et al., 2014) time scales were also used if an insufficient number of actual and reference ET pairs prohibited a reliable regression result. Therefore, proper selection of the estimation period is required, particularly if species have different growth duration and stage of plant life cycle. Furthermore, in most previous studies, the y-intercept offset from the linear regression was small but not used for the daily K_c calculation (Beebe et al., 2014; Mao et al., 2002). Consistent application of this approach in wetland restoration projects over a projected period of nationwide implementation and including a variety of species will support systematic regional application of K_c values for wetlands.

The TIR-based ET estimation methods allow handy measurement of vegetation distribution in a various range of spatio-temporal resolution. Once the instruments are calibrated, any other calibration or correction processes are not required. Measurement and estimation processes can be automated with less maintenance, which would be potentially useful for

systematic monitoring of ET at various land surface conditions. In practice, the location of the selected leaf targets and angle of TIR should be carefully determined to reduce error from shading.

6.3 Summary and conclusions

Two infrared temperature-based ET methods were applied over freshwater marshes in northern New York. The observation method adopted in this study has several practical and operational advantages for short-term, field-based evapotranspiration monitoring in remote sites. The portable monitoring system is simple to set up and operate. The TIR-based methods are found to be comparable with the P-T potential ET under most conditions. A slight impact of prevailing wind and plant structure on direct ET estimation was demonstrated. The TIR methods are more sensitive to changes in vegetative characteristics than is P-T.

Although not fully explored here, TIR methods have the potential to detect differences in ET over multiple spatial ranges from centimeters to tens of meters. Additional work more focused on spatial variations may improve understanding of variations in ET rates at both plant and leaf scales.

Finally, estimated crop coefficient ranges agree well with previous studies, and may contribute guidance for plant selection and design of wetland restoration and creation projects.

Chapter 7. Conclusions and recommendations for future work

7.1 Conclusions

Alteration in geomorphic settings from wetland mitigation resulted in abated hydrogeomorphic signals. Most groundwater-fed and some surface water-fed wetlands lost persistent surface connection to downstream waters. More frequent subsurface flow reversal from filling to exfiltration was observed during dry periods. Nevertheless, experimental results demonstrated subsurface connectivity through relationships that represent ecosystem functions of wetlands. Mitigation wetlands showed a similar impact to other wetland types on hydrologic functions such as groundwater regulation and water storage even if geographically isolated. Hydrologic evaluation of wetland mitigation is recommended to consider both hydrogeomorphic settings and alteration of landform as primary controls on ecosystem services.

While site hydrology and thermal functions of wetlands were characterized by hydrogeomorphic settings, wetland mitigation also resulted in modified thermal responses due to subsurface flow reversal. Geographical attributes (i.e., site elevation) and standard deviation of wetland stage and groundwater table also showed significant correlations with thermal sensitivity.

Hydrogeomorphic settings and wetland mitigation showed minimal impact on evapotranspiration (ET) by selected wetland species. Regional humid continental climate allowed wetlands to provide near potential ET conditions for vegetation. Actual ET from thermal infrared temperature-based methods showed good agreement with potential ET estimated by the Priestley-Taylor method except extreme weather conditions such as high u . Nevertheless, the proposed TIR methods showed a great potential to detect changes in vegetative characteristics

than the traditional methods, which guarantees better performance on moisture-stress conditions.

These field-survey oriented studies are expected to benefit regional stakeholders, such as the public service agencies (e.g., United States Department of Agriculture Natural Resources Conservation Service and US Fish and Wildlife Services), non-profit organizations (e.g., Ducks Unlimited) and private land owners, and their partnership on better understanding ecohydrological linkage between regional geomorphic settings and species composition for successful wetland restoration (Benson et al., 2017). Proper evaluation of the system is necessary for sustainability of restored wetlands because they are environmentally fragile yet often excluded from federal protection due to lack of surface water connectivity. Along with nationwide wetland restoration projects and their regional guidebooks on functional assessment, this study would benefit site-wide restoration practices for creating suitable hydrologic and thermal regimes particularly for ecohydrological data-scarce regions.

7.2 Recommendations for future work

Subsurface flow exchange and related hydrologic functions are keys to understand a role of geographically isolated wetlands (GIWs) on ecohydrological pathway. Despite abundance of wetlands on such landform, there have been a limited number of studies conducted to seek for any evidence that relates GIWs and downstream waters at a few regions. Additional case studies at multiple regions will be useful to understand how such hydrologic connections differ from various climate and regional geologic settings. This will ultimately contribute to provide evidence of ecohydrological values for acquiring federal protection back. Such attentions are even more required for restored wetlands, since most studies focus on natural wetlands due to

relatively least disturbance.

Use of thermal sensitivity in various regions will be beneficial to better understand seasonal and regional controls on thermal regimes in wetlands. It can be used as a proxy for characterizing thermal controls and groundwater regulation to wetlands at a regional level. Since thermal sensitivity has hardly been used in wetlands, more instrumentation and related modeling approaches should be applied.

Associated efforts are required to identify contribution of wetland temperature in biological and biogeochemical aspects. It will be useful if thermal sensitivity is compared with biological indices or water quality species. This will reveal a role of thermal sensitivity as linking hydrogeomorphic settings to wetland ecology.

Evaluation of the TIR-based methods will contribute to improve ground-based ET estimation approaches. Although the proposed method is based on physical derivation of H estimation, it has not been validated over various atmospheric and canopy conditions. For the validation purposes, field survey at multiple sites that accommodate sophisticated instrumentation settings such as the eddy covariance towers is essential. This will ultimately contribute to better understand how the TIR-based methods perform under various seasonal, atmospheric, and land surface conditions by comparison with the ground truth.

The proposed TIR-based methods need to be assessed over various climate and land surface conditions to understand how evapotranspiration (ET) is estimated in moisture-limited environment. Accordingly, a hypothesis in this dissertation needs to be extended that ground-based TIR sensing allows accurate estimation of ET over a range of climate and vegetation settings. Since climate varies largely over space, it is necessary to apply this method over multiple climate regimes. In this aspect, field survey at multiple sites with various climate

regimes and vegetation composition is imperative for comparative studies.

Another research opportunity will be to observe how aerodynamic resistance changes by vegetation structure within a dense observation network. Although there have long been numerous efforts for parameterizing the aerodynamic resistance at the canopy cover, most have focused more on atmospheric characteristics (e.g., atmospheric stability) or roughness of the canopy cover as a function of vegetative features (e.g., height) (Allen et al., 1998). Comparison of these vegetation structures will help better understand which conditions accelerate vapor transport.

Investigation of ground-based TIR images in remote sensing perspectives would contribute to estimate ET at multiple spatial scales. Multiple TIR sensors are collecting radiometric temperature of canopy leaf surfaces at different locations in association with the eddy covariance towers. Comparison of the representative point measurement and high-resolution imagery would allow suitable target and monitoring geometry selection. This can be applied to multiple platforms such as satellite, airborne and unmanned aerial vehicle.

All the suggested research opportunities will contribute to clarify how the water and energy balances of various ecosystems change over scale and setting to develop more robust guidelines for watershed management and hydrologic modeling.

References

- Agam, N., Kustas, W.P., Anderson, M.C., Norman, J.M., Colaizzi, P.D., Howell, T.A., Prueger, J.H., Meyers, T.P., Wilson, T.B., 2010. Application of the Priestley–Taylor Approach in a Two-Source Surface Energy Balance Model. *J. Hydrometeorol.*
doi:10.1175/2009JHM1124.1
- Ahrends, H., Haseneder-Lind, R., Schween, J., Crewell, S., Stadler, A., Rascher, U., 2014. Diurnal Dynamics of Wheat Evapotranspiration Derived from Ground-Based Thermal Imagery. *Remote Sens.* 6, 9775–9801. <https://doi.org/10.3390/rs6109775>
- Allen, R.G., 1995. Evapotranspiration and irrigation efficiency. *Am. Consult. Eng. Counc. Color. Color. Div. Water Resour. Meet.*
- Allen, R.G., Hill, R.W., Srikanth, V., 1994. Evapotranspiration parameters for variably-sized wetlands, in: *International Summer Meeting, ASAE and ASCE. Kansas City, MO*, pp. 1–18.
- Allen, R.G., Jensen, M.E., Wright, J.L., Burman, R.D., 1989. Operational Estimates of Reference Evapotranspiration. *Agron. J.* doi:10.2134/agronj1989.00021962008100040019x
- Allen, R.G., Pereira, L.S., Raes, D., Smith, M., 1998. *FAO Irrigation and Drainage Paper No. 56: Crop Evapotranspiration*, Food and Agriculture Organization of the United Nations. Rome, Italy.
- Alves, I., Pereira, L.S., 2000. Non-water-stressed baselines for irrigation scheduling with infrared thermometers: A new approach. *Irrig. Sci.* 19, 101–106.
- Ameli, A.A., Creed, I.F., 2017. Quantifying hydrologic connectivity of wetlands to surface water systems. *Hydrol. Earth Syst. Sci.* 21, 1791–1808. <https://doi.org/10.5194/hess-21-1791-2017>

- Beebe, D.A., Castle, J.W., Molz, F.J., Rodgers, J.H., 2014. Effects of evapotranspiration on treatment performance in constructed wetlands: Experimental studies and modeling. *Ecol. Eng.* 71, 394–400. <https://doi.org/10.1016/j.ecoleng.2014.07.052>
- Benson, C.E., Carberry, B., Langen, T.A., 2017. Public–private partnership wetland restoration programs benefit Species of Greatest Conservation Need and other wetland-associated wildlife. *Wetl. Ecol. Manag.* <https://doi.org/10.1007/s11273-017-9565-8>
- Bidlake, W.R., 2000. Evapotranspiration from a bulrush-dominated wetland in the Klamath Basin, Oregon. *J. Am. Water Resour. Assoc.* 36, 1309–1320.
- Borin, M., Milani, M., Salvato, M., Toscano, A., 2011. Evaluation of *Phragmites australis* (Cav.) Trin. evapotranspiration in Northern and Southern Italy. *Ecol. Eng.* 37, 721–728. <https://doi.org/10.1016/j.ecoleng.2010.05.003>
- Brinson, M.M., 1993. A hydrogeomorphic classification for wetlands. U.S. Army Corps of Engineers, Waterways Experiment Station, Vicksburg, MS.
- Brutsaert, W., 1982. *Evaporation into the Atmosphere: Theory, history and applications*. D. Reidel, Dordrecht, Holland.
- Budelsky, R.A., Galatowitsch, S.M., 1999. Effects of moisture, temperature, and time on seed germination of five wetland *Carices*: Implications for restoration. *Restor. Ecol.* 7, 86–97. <https://doi.org/10.1046/j.1526-100X.1999.07110.x>
- Caissie, D., 2006. The thermal regime of rivers: A review. *Freshw. Biol.* 51, 1389–1406. <https://doi.org/10.1111/j.1365-2427.2006.01597.x>
- Cardenas, M.B., Harvey, J.W., Packman, A.I., Scott, D.T., 2008. Ground-based thermography of fluvial systems at low and high discharge reveals potential complex thermal heterogeneity driven by flow variation and bioroughness. *Hydrol. Process.* 22, 980–986.

<https://doi.org/10.1002/hyp.6932>

- Chang, H., Psaris, M., 2013. Local landscape predictors of maximum stream temperature and thermal sensitivity in the Columbia River Basin, USA. *Sci. Total Environ.* 461–462, 587–600. <https://doi.org/10.1016/j.scitotenv.2013.05.033>
- Cohen, M.J., Creed, I.F., Alexander, L., Basu, N.B., Calhoun, A.J.K., Craft, C., D’Amico, E., DeKeyser, E., Fowler, L., Golden, H.E., Jawitz, J.W., Kalla, P., Kirkman, L.K., Lane, C.R., Lang, M., Leibowitz, S.G., Lewis, D.B., Marton, J., McLaughlin, D.L., Mushet, D.M., Raanan-Kiperwas, H., Rains, M.C., Smith, L., Walls, S.C., 2016. Do geographically isolated wetlands influence landscape functions? *Proc. Natl. Acad. Sci. U. S. A.* 113, 1978–1986. <https://doi.org/10.1073/pnas.1512650113>
- Cole, C.A., Brooks, R.P., 2000. Patterns of wetland hydrology in the ridge and valley province, Pennsylvania, USA. *Wetlands* 20, 438–447.
- Dahl, M., Nilsson, B., Langhoff, J.H., Refsgaard, J.C., 2007. Review of classification systems and new multi-scale typology of groundwater–surface water interaction. *J. Hydrol.* 344, 1–16. <https://doi.org/10.1016/j.jhydrol.2007.06.027>
- Dahl, T.E., 1990. Wetlands losses in the United States, 1780’s to 1980’s, U.S. Department of Interior, Fish and Wildlife Service. Washington, DC.
- Davidson, E.A., Janssens, I.A., 2006. Temperature sensitivity of soil carbon decomposition and feedbacks to climate change. *Nature* 440, 165–173. <https://doi.org/10.1038/nature04514>
- Devito, K.J., Hill, A.R., Roulet, N., 1996. Groundwater-surface water interactions in headwater forested wetlands of the Canadian Shield. *J. Hydrol.* 181, 127–147.
- Devito, K.J., Waddington, J.M., Branfireun, B.A., 1997. Flow reversals in peatlands influenced by local groundwater systems. *Hydrol. Process.* 11, 103–110.

- Dowrick, D.J., Freeman, C., Lock, M.A., Yusoff, F.M., 2015. Using Thermal Sensitivity Analysis to Determine the Impact of Drainage on the Hydrochemistry of a Tropical Peat Soil from Malaysia. *Commun. Soil Sci. Plant Anal.* 46.
<https://doi.org/10.1080/00103624.2015.1069318>
- Drexler, J.Z., Bedford, B.L., DeGaetano, A.T., Siegel, D.I., 1999. Quantification of the water budget and nutrient loading in a small peatland. *J. Am. Water Resour. Assoc.* 35, 753–769.
- Drexler, J.Z., Snyder, R.L., Spano, D., Paw U, K.T., 2004. A review of models and micrometeorological methods used to estimate wetland evapotranspiration. *Hydrol. Process.* 18, 2071–2101. <https://doi.org/10.1002/hyp.1462>
- Ehrenfeld, J.G., Cutway, H.B., Hamilton IV, R., Stander, E., 2003. Hydrologic description of forested wetlands in northeastern New Jersey, USA - An urban/suburban region. *Wetlands* 23, 685–700.
- Ekström, A., Sandblom, E., Blier, P.U., Dupont Cyr, B.-A., Brijs, J., Pichaud, N., 2017. Thermal sensitivity and phenotypic plasticity of cardiac mitochondrial metabolism in European perch, *Perca fluviatilis*. *J. Exp. Biol.* 220, 386–396. <https://doi.org/10.1242/jeb.150698>
- Elliott, J.M., 2000. Pools as refugia for brown trout during two summer droughts: Trout responses to thermal and oxygen stress. *J. Fish Biol.* 56, 938–948.
<https://doi.org/10.1006/jfbi.1999.1220>
- EPA and U.S. Army Corps of Engineers, 2008. Clean Water Act Jurisdiction following the U.S. Supreme Court’s decision in *Rapanos versus United States* and *Carabell versus United States*, U.S. Environmental Protection Agency and Army Corps of Engineers Guidance Memorandum.
- Erwin, K.L., 2009. Wetlands and global climate change: The role of wetland restoration in a

- changing world. *Wetl. Ecol. Manag.* 17, 71–84. <https://doi.org/10.1007/s11273-008-9119-1>
- Evenson, G.R., Golden, H.E., Lane, C.R., D'Amico, E., 2016. An improved representation of geographically isolated wetlands in a watershed-scale hydrologic model. *Hydrol. Process.* 30, 4168–4184. <https://doi.org/10.1002/hyp.10930>
- Evenson, G.R., Golden, H.E., Lane, C.R., D'Amico, E., 2015. Geographically isolated wetlands and watershed hydrology: A modified model analysis. *J. Hydrol.* 529, 240–256. <https://doi.org/10.1016/j.jhydrol.2015.07.039>
- Fermor, P.M., Hedges, P.D., Gilbert, J.C., Gowing, D.J.G., 2001. Reedbed evapotranspiration rates in England. *Hydrol. Process.* 15, 621–631. <https://doi.org/10.1002/hyp.174>
- Fey, S.B., Cottingham, K.L., 2012. Thermal sensitivity predicts the establishment success of nonnative species in a mesocosm warming experiment. *Ecology* 93, 2313–2320. <https://doi.org/10.1890/12-0609.1>
- Fishburn, I.S., Kareiva, P., Gaston, K.J., Armsworth, P.R., 2009. The growth of easements as a conservation tool. *PLoS One* 4, e4996. <https://doi.org/10.1371/journal.pone.0004996>
- Fisher, J.B., Tu, K.P., Baldocchi, D.D., 2008. Global estimates of the land-atmosphere water flux based on monthly AVHRR and ISLSCP-II data, validated at 16 FLUXNET sites. *Remote Sens. Environ.* doi:10.1016/j.rse.2007.06.025
- Fitzgerald, D.F., Price, J.S., Gibson, J.J., 2003. Hillslope-swamp interactions and flow pathways in a hypermaritime rainforest, British Columbia. *Hydrol. Process.* 17, 3005–3022. <https://doi.org/10.1002/hyp.1279>
- Galatowitsch, S.M., van der Valk, A.G., 1996. Characteristics of recently restored wetlands in the prairie pothole region. *Wetlands* 16, 75–83. doi:10.1007/BF03160647
- Gavilán, P., Berengena, J., 2007. Accuracy of the Bowen ratio-energy balance method for

measuring latent heat flux in a semiarid advective environment. *Irrig. Sci.* 25.

<https://doi.org/10.1007/s00271-006-0040-1>

Golden, H.E., Lane, C.R., Amatya, D.M., Bandilla, K.W., Raanan Kiperwas, H., Knightes, C.D.,

Ssegane, H., 2014. Hydrologic connectivity between geographically isolated wetlands and surface water systems: A review of select modeling methods. *Environ. Model. Softw.*

<https://doi.org/10.1016/j.envsoft.2013.12.004>

Golden, H.E., Sander, H.A., Lane, C.R., Zhao, C., Price, K., D'Amico, E., Christensen, J.R.,

2016. Relative effects of geographically isolated wetlands on streamflow: A watershed-scale analysis. *Ecohydrology* 9, 21–38. <https://doi.org/10.1002/eco.1608>

Gwin, S.E., Kentula, M.E., Shaffer, P.W., 1999. Evaluating the effects of wetland regulation

through hydrogeomorphic classification and landscape profiles. *Wetlands* 19, 477–489.

Harris, A., Johnson, J., Horton, K., Garbeil, H., Ramm, H., Pilger, E., Flynn, L., Mougini-Mark,

P., Pirie, D., Donegan, S., Rothery, D., Ripepe, M., Marchetti, E., 2003. Ground-based infrared monitoring provides new tool for remote tracking of volcanic activity. *Eos, Trans. Am. Geophys. Union* 84.

Hayashi, M., Rosenberry, D.O., 2002. Effects of ground water exchange on the hydrology and

ecology of surface water. *Ground Water* 40, 309–316.

Hester, E.T., Doyle, M.W., 2011. Human impacts to river temperature and their effects on

biological processes: A quantitative synthesis. *J. Am. Water Resour. Assoc.* 47, 571–587.

<https://doi.org/10.1111/j.1752-1688.2011.00525.x>

Hruby, T., 2001. Testing the Basic Assumption of the Hydrogeomorphic Approach to

Assessing Wetland Functions. *Environ. Manage.* 27, 749–761.

<https://doi.org/10.1007/s002670010185>

- Hunt, R.J., Strand, M., Walker, J.F., 2006. Measuring groundwater–surface water interaction and its effect on wetland stream benthic productivity, Trout Lake watershed, northern Wisconsin, USA. *J. Hydrol.* 320, 370–384. <https://doi.org/10.1016/j.jhydrol.2005.07.029>
- Hunt, R.J., Walker, J.F., Krabbenhoft, D.P., 1999. Characterizing hydrology and the importance of ground-water discharge in natural and constructed wetlands. *Wetlands* 19, 458–472.
- Hupet, F., Vanclooster, M., 2001. Effect of the sampling frequency of meteorological variables on the estimation of the reference evapotranspiration. *J. Hydrol.* doi:10.1016/S0022-1694(00)00413-3
- Hwang, K., Choi, M., 2013. Seasonal trends of satellite-based evapotranspiration algorithms over a complex ecosystem in East Asia. *Remote Sens. Environ.* 137, 244–263. <https://doi.org/10.1016/j.rse.2013.06.006>
- Inglett, K.S., Inglett, P.W., Reddy, K.R., Osborne, T.Z., 2012. Temperature sensitivity of greenhouse gas production in wetland soils of different vegetation. *Biogeochemistry* 108, 77–90. <https://doi.org/10.1007/s10533-011-9573-3>
- Jacobs, J.M., Mergelsberg, S.L., Lopera, A.F., Myers, D.A., 2002. Evapotranspiration from a wet prairie wetland under drought conditions: Paynes prairie preserve, Florida, USA. *Wetlands* 22, 374–385.
- Jolly, I.D., McEwan, K.L., Holland, K.L., 2008. A review of groundwater-surface water interactions in arid/semi-arid wetlands and the consequences of salinity for wetland ecology. *Ecohydrology* 1, 43–58. <https://doi.org/10.1002/eco.6>
- Jones, H.G., 2004. Application of thermal imaging and infrared sensing in plant physiology and ecophysiology. *Adv. Bot. Res.* 41, 107–163.
- Kalbus, E., Reinstorf, F., Schirmer, M., 2006. Measuring methods for groundwater - surface

- water interactions: A review. *Hydrol. Earth Syst. Sci.*
- Kaya, C.M., 1977. Reproductive Biology of Rainbow and Brown Trout in a Geothermally Heated Stream: The Firehole River of Yellowstone National Park. *Trans. Am. Fish. Soc.* 106, 354–361. [https://doi.org/10.1577/1548-8659\(1977\)106<354:RBORAB>2.0.CO;2](https://doi.org/10.1577/1548-8659(1977)106<354:RBORAB>2.0.CO;2)
- Kelleher, C., Wagener, T., Gooseff, M., McGlynn, B., McGuire, K., Marshall, L., 2012. Investigating controls on the thermal sensitivity of Pennsylvania streams. *Hydrol. Process.* 26, 771–785. <https://doi.org/10.1002/hyp.8186>
- Kiesecker, J.M., Blaustein, A.R., 1997. Population differences in responses of red-legged frogs (*Rana aurora*) to introduced bullfrogs. *Ecology* 78, 1752–1760.
- Kormos, P.R., Marks, D., Pierson, F.B., Williams, C.J., Hardegree, S.P., Havens, S., Hedrick, A., Bates, J.D., Svejcar, T.J., 2017. Ecosystem water availability in juniper versus sagebrush snow-dominated rangelands. *Rangel. Ecol. Manag.* doi:10.1016/j.rama.2016.05.003
- Kraemer, B.M., Chandra, S., Dell, A.I., Dix, M., Kuusisto, E., Livingstone, D.M., Schladow, S.G., Silow, E., Sitoki, L.M., Tamatamah, R., McIntyre, P.B., 2017. Global patterns in lake ecosystem responses to warming based on the temperature dependence of metabolism. *Glob. Chang. Biol.* 23, 1881–1890. <https://doi.org/10.1111/gcb.13459>
- Lafleur, P.M., 1990. Evaporation from wetlands. *Can. Geogr.* 34, 79–88.
- Lane, C.R., Autrey, B.C., Jicha, T., Lehto, L., Elonen, C., Seifert-Monson, L., 2015. Denitrification Potential in Geographically Isolated Wetlands of North Carolina and Florida, USA. *Wetlands* 35, 459–471. <https://doi.org/10.1007/s13157-015-0633-7>
- Lenters, J.D., Cutrell, G.J., Istanbuluoglu, E., Scott, D.T., Herrman, K.S., Irmak, A., Eisenhauer, D.E., 2011. Seasonal energy and water balance of a *Phragmites australis*-dominated wetland in the Republican River basin of south-central Nebraska (USA). *J. Hydrol.* 408, 19–34.

<https://doi.org/10.1016/j.jhydrol.2011.07.010>

- Liuzzo, L., Viola, F., Noto, L. V., 2016. Wind speed and temperature trends impacts on reference evapotranspiration in Southern Italy. *Theor. Appl. Climatol.* doi:10.1007/s00704-014-1342-5
- Lisi, P.J., Schindler, D.E., Cline, T.J., Scheuerell, M.D., Walsh, P.B., 2015. Watershed geomorphology and snowmelt control stream thermal sensitivity to air temperature. *Geophys. Res. Lett.* 42, 3380–3388. <https://doi.org/10.1002/2015GL064083>
- Lott, R.B., Hunt, R.J., 2001. Estimating evapotranspiration in natural and constructed wetlands. *Wetlands* 21, 614–628.
- Maes, W.H., Steppe, K., 2012. Estimating evapotranspiration and drought stress with ground-based thermal remote sensing in agriculture: a review. *J. Exp. Bot.* 63, 4671–712. <https://doi.org/10.1093/jxb/ers165>
- Mao, L.M., Bergman, M.J., Tai, C.C., 2002. Evapotranspiration measurement and estimation of three wetland environments in the Upper St. Johns River Basin, Florida. *J. Am. Water Resour. Assoc.* 38, 1271–1285.
- Marton, J.M., Creed, I.F., Lewis, D.B., Lane, C.R., Basu, N.B., Cohen, M.J., Craft, C.B., 2015. Geographically isolated wetlands are important biogeochemical reactors on the landscape. *Bioscience.* <https://doi.org/10.1093/biosci/biv009>
- Masoner, J.R., Stannard, D.I., 2010. A Comparison of Methods for Estimating Open-Water Evaporation in Small Wetlands. *Wetlands* 30, 513–524. <https://doi.org/10.1007/s13157-010-0041-y>
- McKinney, R.A., Charpentier, M.A., 2009. Extent, properties, and landscape setting of geographically isolated wetlands in urban southern New England watersheds. *Wetl. Ecol.*

- Manag. 17, 331–344. <https://doi.org/10.1007/s11273-008-9110-x>
- McLaughlin, D.L., Cohen, M.J., 2014. Ecosystem specific yield for estimating evapotranspiration and groundwater exchange from diel surface water variation. *Hydrol. Process.* 28, 1495–1506. <https://doi.org/10.1002/hyp.9672>
- McLaughlin, D.L., Cohen, M.J., 2013. Realizing ecosystem services: wetland hydrologic function along a gradient of ecosystem condition. *Ecol. Appl.* 23, 1619–1631. <https://doi.org/10.1890/12-1489.1>
- McLaughlin, D.L., Kaplan, D.A., Cohen, M.J., 2014. A significant nexus: Geographically isolated wetlands influence landscape hydrology. *Water Resour. Res.* 50, 7153–7166. <https://doi.org/10.1002/2013WR015002>
- Min, J.-H., Perkins, D.B., Jawitz, J.W., 2010. Wetland-Groundwater Interactions in Subtropical Depressional Wetlands. *Wetlands* 30, 997–1006. <https://doi.org/10.1007/s13157-010-0043-9>
- Mitsch, W.J., Gosselink, J.G., 2015. *Wetlands*. Wiley, New York, NY.
- Mohamed, Y.A., Bastiaanssen, W.G.M., Savenije, H.H.G., van den Hurk, B.J.J.M., Finlayson, C.M., 2012. Wetland versus open water evaporation: An analysis and literature review. *Phys. Chem. Earth, Parts A/B/C* 47–48, 114–121. <https://doi.org/10.1016/j.pce.2011.08.005>
- Monteith, J.L., 1965. Evaporation and environment. *Symp. Soc. Exp. Biol.* 19.
- Monteith, J.L., Unsworth, M.H., 1990. *Principles of Environmental Physics*, 2nd ed. Edward Arnold, London.
- Morrill, J.C., Bales, R.C., Conklin, M.H., 2005. Estimating stream temperature from air temperature: Implications for future water quality. *J. Environ. Eng.* 131, 139–146. [https://doi.org/10.1061/\(ASCE\)0733-9372\(2005\)131:1\(139\)](https://doi.org/10.1061/(ASCE)0733-9372(2005)131:1(139))

- Mueller, L., Behrendt, A., Schalitz, G., Schindler, U., 2005. Above ground biomass and wue of crops at shallow water tables in a teperate climate.pdf. *Agric. Water Manag.* 75, 117–136.
- Mushet, D.M., Calhoun, A.J.K., Alexander, L.C., Cohen, M.J., DeKeyser, E.S., Fowler, L., Lane, C.R., Lang, M.W., Rains, M.C., Walls, S.C., 2015. Geographically Isolated Wetlands: Rethinking a Misnomer. *Wetlands* 35, 423–431. <https://doi.org/10.1007/s13157-015-0631-9>
- National Research Council, 2001. *Compensating for Wetland Losses Under the Clean Water Act*. Washington, DC.
- Nilsson, K.A., Rains, M.C., Lewis, D.B., Trout, K.E., 2013. Hydrologic characterization of 56 geographically isolated wetlands in west-central Florida using a probabilistic method. *Wetl. Ecol. Manag.* 21, 1–14. <https://doi.org/10.1007/s11273-012-9275-1>
- Park, J., Botter, G., Jawitz, J.W., Rao, P.S.C., 2014. Stochastic modeling of hydrologic variability of geographically isolated wetlands: Effects of hydro-climatic forcing and wetland bathymetry. *Adv. Water Resour.* 69, 38–48. <https://doi.org/10.1016/j.advwatres.2014.03.007>
- Pauliukonis, N., Schneider, R., 2001. Temporal patterns in evapotranspiration from lysimeters with three common wetland plant species in the eastern United States. *Aquat. Bot.* 71, 35–46. [https://doi.org/10.1016/S0304-3770\(01\)00168-1](https://doi.org/10.1016/S0304-3770(01)00168-1)
- Peacock, C.E., Hess, T.M., 2004. Estimating evapotranspiration from a reed bed using the Bowen ratio energy balance method. *Hydrol. Process.* 18, 247–260. <https://doi.org/10.1002/hyp.1373>
- Peel, B.L., Finlayson, B.L., McMahon, T. a., 2007. Updated world map of the Köppen-Geiger climate classification.pdf. *Hydrol. Earth Syst. Sci.* 11, 1633–1644. <https://doi.org/10.5194/hessd-4-439-2007>

- Penman, H.L., 1948. Natural evaporation from open water, bare soil and grass. *Proc. R. Soc. Lond. A. Math. Phys. Sci.* 193.
- Priestley, C.H.B., Taylor, R.J., 1972. On the assessment of surface heat flux and evaporation using large-scale parameters. *Mon. Weather Rev.*
- Rains, M.C., 2011. Water Sources and Hydrodynamics of Closed-Basin Depressions, Cook Inlet Region, Alaska. *Wetlands* 31, 377–387. <https://doi.org/10.1007/s13157-011-0147-x>
- Rains, M.C., Leibowitz, S.G., Cohen, M.J., Creed, I.F., Golden, H.E., Jawitz, J.W., Kalla, P., Lane, C.R., Lang, M.W., McLaughlin, D.L., 2016. Geographically isolated wetlands are part of the hydrological landscape. *Hydrol. Process.* 30, 153–160. <https://doi.org/10.1002/hyp.10610>
- Richter-Boix, A., Katzenberger, M., Duarte, H., Quintela, M., Tejedo, M., Laurila, A., 2015. Local divergence of thermal reaction norms among amphibian populations is affected by pond temperature variation. *Evolution (N. Y.)*. 69, 2210–2226. <https://doi.org/10.1111/evo.12711>
- Rosenberry, D.O., Stannard, D.I., Winter, T.C., Martinez, M.L., 2004. Comparison of 13 equations for determining evapotranspiration from a prairie wetland, Cottonwood Lake area, North Dakota, USA. *Wetlands* 24, 483–497. [https://doi.org/10.1672/0277-5212\(2004\)024\[0483:COEFDE\]2.0.CO;2](https://doi.org/10.1672/0277-5212(2004)024[0483:COEFDE]2.0.CO;2)
- Rosenberry, D.O., Winter, T.C., 1997. Dynamics of water-table fluctuations in an upland between two prairie-pothole wetlands in North Dakota. *J. Hydrol.* 191, 266–289. [https://doi.org/10.1016/S0022-1694\(96\)03050-8](https://doi.org/10.1016/S0022-1694(96)03050-8)
- Roulet, N.T., 1990. Hydrology of a headwater basin wetland: groundwater discharge and wetland maintenance. *Hydrol. Process.*

- Santanello, J.A., Peters-Lidard, C.D., Garcia, M.E., Mocko, D.M., Tischler, M.A., Moran, M.S., Thoma, D.P., 2007. Using remotely-sensed estimates of soil moisture to infer soil texture and hydraulic properties across a semi-arid watershed. *Remote Sens. Environ.* 110, 79–97. <https://doi.org/10.1016/j.rse.2007.02.007>
- Schmugge, T.J., Kustas, W.P., Ritchie, J.C., Jackson, T.J., Rango, A., 2002. Remote sensing in hydrology. *Adv. Water Resour.* 25, 1367–1385. [https://doi.org/10.1016/S0309-1708\(02\)00065-9](https://doi.org/10.1016/S0309-1708(02)00065-9)
- Seabloom, E.W., Van Der Valk, A.G., Moloney, K.A., 1998. The role of water depth and soil temperature in determining initial composition of prairie wetland coenoclines. *Plant Ecol.* 138, 203–216. <https://doi.org/10.1023/A:1009711919757>
- Shaffer, P.W., Kentula, M.E., Gwin, S.E., 1999. Characterization of wetland hydrology using hydrogeomorphic classification. *Wetlands* 19, 490–504.
- Shaw, S.B., 2017. Does an upper limit to river water temperature apply in all places? *Hydrol. Process.* 31, 3729–3739. <https://doi.org/10.1002/hyp.11297>
- Shoemaker, W.B., Huddleston, S., Boudreau, C.L., O'Reilly, A.M., 2008. Sensitivity of wetland saturated hydraulic heads and water budgets to evapotranspiration. *Wetlands* 28, 1040–1047. <https://doi.org/10.1672/08-105.1>
- Siegel, D.I., 1988. The recharge-discharge function of wetlands near Juneau, Alaska: part I. Hydrogeological investigations. *Ground Water* 26, 427–434.
- Smith, R.D., Ammann, A., Bartoldus, C., Brinson, M.M., 1995. An approach for assessing wetland functions using hydrogeomorphic classification, reference wetlands, and functional indices. U.S. Army Corps of Engineers, Waterways Experiment Station, Vicksburg, MS.
- Souch, C., Grimmond, C.S.B., Wolfe, C.P., 1998. Evapotranspiration rates from wetlands with

- different disturbance histories: Indiana Dunes National Lakeshore. *Wetlands* 18, 216–229.
- Souch, C., Wolfe, C.P., Grimmond, C.S.B., 1996. Wetland evaporation and energy partitioning: Indiana Dunes National Lakeshore. *J. Hydrol.* 184, 189–208. [https://doi.org/10.1016/0022-1694\(95\)02989-3](https://doi.org/10.1016/0022-1694(95)02989-3)
- Stander, E.K., Ehrenfeld, J.G., 2009. Rapid assessment of urban wetlands: do hydrogeomorphic classification and reference criteria work? *Environ. Manage.* 43, 725–42. <https://doi.org/10.1007/s00267-008-9211-6>
- Stein, E.D., Mattson, M., Fetscher, A.E., Halama, K.J., 2004. Influence of geologic setting on slope wetland hydrodynamics. *Wetlands* 24, 244–260.
- Stolt, M.H., Genthner, M.H., Daniels, W.L., Groover, V.A., Nagle, S., Haering, K.C., 2000. Comparison of soil and other environmental conditions in constructed and adjacent palustrine reference Wetlands. *Wetlands* 20, 671–683.
- Stryzowska, K.M., Johnson, G., Rivera Mendoza, L., Langen, T.A., Mendoza, L.R., 2016. Species Distribution Modeling of the Threatened Blanding's Turtle's (*Emydoidea blandingii*) Range Edge as a Tool for Conservation Planning. *J. Herpetol.* 50, 366–373. [doi:10.1670/15-089](https://doi.org/10.1670/15-089)
- Telemeco, R.S., Fletcher, B., Levy, O., Riley, A., Rodriguez-Sanchez, Y., Smith, C., Teague, C., Waters, A., Angilletta, M.J., Buckley, L.B., 2017. Lizards fail to plastically adjust nesting behavior or thermal tolerance as needed to buffer populations from climate warming. *Glob. Chang. Biol.* 23, 1075–1084. <https://doi.org/10.1111/gcb.13476>
- Thompson, M.A., Campbell, D.I., Spronken-Smith, R.A., 1999. Evaporation from natural and modified raised peat bogs in New Zealand. *Agric. For. Meteorol.* 95, 85–98. [https://doi.org/10.1016/S0168-1923\(99\)00027-1](https://doi.org/10.1016/S0168-1923(99)00027-1)

- Tiner, R.W., 2003. Geographically isolated wetlands of the United States. *Wetlands* 23, 494–516.
- Todd, R.W., Evett, S.R., Howell, T.A., 2000. The Bowen ratio-energy balance method for estimating latent heat flux of irrigated alfalfa evaluated in a semi-arid, advective environment. *Agric. For. Meteorol.* 103. [https://doi.org/10.1016/S0168-1923\(00\)00139-8](https://doi.org/10.1016/S0168-1923(00)00139-8)
- Tolk, J.A., Howell, T.A., Steiner, J.L., Krieg, D.R., 1995. Aerodynamic characteristics of corn as determined by energy balance techniques. *Agron. J.* 87.
- Torgersen, C.E., Price, D.M., Li, H.W., McIntosh, B.A., 1999. Multiscale thermal refugia and stream habitat associations of chinook salmon in northeastern Oregon. *Ecol. Appl.* 9, 301–319. [https://doi.org/10.1890/1051-0761\(1999\)009\[0301:MTRASH\]2.0.CO;2](https://doi.org/10.1890/1051-0761(1999)009[0301:MTRASH]2.0.CO;2)
- Towler, B.W., 2004. Evapotranspiration crop coefficients for cattail and bulrush. *J. Hydrol. Eng.* 9, 235. [https://doi.org/Doi 10.1061/\(Asce\)1084-0699\(2004\)9:3\(235\)](https://doi.org/Doi%2010.1061/(Asce)1084-0699(2004)9:3(235))
- Triggs, J.M., Kimball, B.A., Pinter, P.J., Wall, G.W., Conley, M.M., Brooks, T.J., LaMorte, R.L., Adam, N.R., Ottman, M.J., Matthias, A.D., Leavitt, S.W., Cerveny, R.S., 2004. Free-air CO₂ enrichment effects on the energy balance and evapotranspiration of sorghum. *Agric. For. Meteorol.* 124, 63–79. <https://doi.org/10.1016/j.agrformet.2004.01.005>
- Voortman, B.R., Bosveld, F.C., Bartholomeus, R.P., Witte, J.P.M., 2016. Spatial extrapolation of lysimeter results using thermal infrared imaging. *J. Hydrol.*
[doi:10.1016/j.jhydrol.2016.09.064](https://doi.org/10.1016/j.jhydrol.2016.09.064)
- Wang, Z., Feyen, J., Van Genuchten, M.T., Nielsen, D.R., 1998. Air entrapment effects on infiltration rate and flow instability. *Water Resour. Res.* 34, 213–222.
- Whittecar, G.R., Daniels, W.L., 1999. Use of hydrogeomorphic concepts to design created wetlands in southeastern Virginia. *Geomorphology* 31, 355–371. [doi:10.1016/S0169-](https://doi.org/10.1016/S0169-)

555X(99)00081-1

- Williams, A.S., Kiniry, J.R., Mushet, D., Smith, L.M., McMurry, S., Attebury, K., Lang, M., McCarty, G.W., Shaffer, J.A., Effland, W.R., Johnson, M.V. V., 2017. Model parameters for representative wetland plant functional groups. *Ecosphere*. doi:10.1002/ecs2.1958
- Winter, T.C., 1999. Relation of streams, lakes, and wetlands to groundwater flow systems. *Hydrogeol. J.* 7, 28–45.
- Winter, T.C., 1995. Recent advances in understanding the interaction of groundwater and surface water. *Rev. Geophys.* 33, 985–994.
- Winter, T.C., Rosenberry, D.O., Buso, D.C., Merk, D.A., 2001. Water source to four U.S. wetlands: Implications for wetland management. *Wetlands* 21, 462–473.
- Woods, S.W., MacDonald, L.H., Westbrook, C.J., 2006. Hydrologic interactions between an alluvial fan and a slope wetland in the central Rocky Mountains, USA. *Wetlands* 26, 230–243.
- Wu, C.L., Shukla, S., 2014. Eddy covariance-based evapotranspiration for a subtropical wetland. *Hydrol. Process.* 28, 5879–5896. <https://doi.org/10.1002/hyp.10075>
- Yao, Y., Liang, S., Li, X., Chen, J., Wang, K., Jia, K., Cheng, J., Jiang, B., Fisher, J.B., Mu, Q., Grünwald, T., Bernhofer, C., Roupsard, O., 2015. A satellite-based hybrid algorithm to determine the Priestley-Taylor parameter for global terrestrial latent heat flux estimation across multiple biomes. *Remote Sens. Environ.* doi:10.1016/j.rse.2015.05.013

Vita

NAME OF AUTHOR: Kyotaek Hwang

PLACE OF BIRTH: Incheon, South Korea

DATE OF BIRTH: January 18, 1984

EDUCATION: Bachelor of Science in Civil and Environmental Engineering, 2009
Hanyang University, Seoul, South Korea

Master of Science in Civil and Environmental Engineering, 2011
Hanyang University, Seoul, South Korea